

Investigating the Relationship between Urban Heat Island (UHI), Sky View Factor (SVF) and different Local Climatic Zones (LCZs): Case study of Kolkata

*Thesis submitted for the partial fulfillment of the requirement
for the degree of
Doctor of Philosophy (Ph.D)*

Santanu Bajani

Index No. D-7/ISLM/5/16

Submitted at the
Faculty of Interdisciplinary Studies, Law & Management
Jadavpur University, Kolkata, India
2023

**Under the guidance of
Prof. Debashish Das**

Department of Architecture, Jadavpur University
Kolkata, India

Every challenging work needs self-efforts as well as guidance of elders especially those who were very close to our heart. My humble effort I dedicate affectionately to the following.

My Father

Late Sri Meghnath Bajani

My Mother

Smt Anima Bajani

My Younger Brother

Sri Krishanu Bajani

My Wife

Smt Sudeshna Bag

My Respected Sir

Prof. Debashish Das

Details of Thesis


- | | |
|---|--|
| 1. Index no. Date of Registration | D-7/ISLM/5/16 dated 18 th January 2016 |
| 2. Title of the thesis | Investigating the Relationship between Urban Heat Island (UHI), Sky View Factor (SVF) and different Local Climatic Zones (LCZs): Case study of Kolkata |
| 3. Name and designation of the supervisor | Dr. Debashish Das
Professor
Department of Architecture
Jadavpur University |
| 4. Email id of supervisor | ddasju@gmail.com |
| 5. List of Publication and Conferences | Attached in Appendix: B |

Statement of Originality

I, Santanu Bajani, registered on 18th January 2016, do hereby declare that this thesis entitled "" contains review of literature and original research work carried out by the undersigned candidate for the partial fulfillment of the doctoral research.

All information in this thesis has been obtained and presented in accordance with existing academic rules and ethical. I declare that as required by these rules and conduct, I have fully cited and provided reference to all materials and results that are not original to this work.

I also declare that I have checked this thesis as per the "Policy on Anti-Plagiarism, Jadavpur University, 2022", and the level of similarity as checked by iThenticate software is less than 10%.


Signature of candidate:
Date:



Certified by Supervisor:
Date:

Professor
Department of Architecture
Jadavpur University
Kolkata-700032

CERTIFICATE FROM THE SUPERVISOR/S

This is to certify that the thesis entitled **"Investigating the Relationship between Urban Heat Island (UHI), Sky View Factor (SVF) and different Local Climatic Zones (LCZs): Case study of Kolkata"** submitted by Shri Santanu Bajani, who got his name registered on 18th January 2016 for the award of Ph.D. (FISLM) degree of Jadavpur University is absolutely based upon his own work under the supervision of Prof. Debashish Das and that neither his/her thesis nor any part of the thesis has been submitted for any degree/diploma or any other academic award anywhere before.



**Professor
Department of Architecture
Jadavpur University
Kolkata-700032**

Signature of the Supervisor and date with Office Seal

Acknowledgement

The author's PhD dissertation is the realization of a lifelong desire that has enhanced both his mind and emotions. Under the watchful direction of Dr. Debashish Das, Professor, Department of Architecture, Jadavpur University, Kolkata, the process of undergoing various lessons of literature in general develops into a reality. He has consistently inspired the author to work toward the noble objective of knowledge progress rather than the modest end of becoming a Doctor of Philosophy.

To thank every one of the well-wishers who helped the author in various ways with this effort would take pages. However, if certain unique contributions are not graciously recognized here, the author will be impudent.

I sincerely appreciate Prof. Suranjan Das, Vice Chancellor of Jadavpur University. Thank you to Dr. Abhra Chanda, Secretary of the Faculty of Interdisciplinary Studies Law and Management at Jadavpur University, as well as to all the professors and staff at the Department of Architecture at Jadavpur University for their insightful comments on how I should conduct my research. My sincere gratitude to Prof. Mainak Ghosh, HOD, Department of Architecture as well as other senior professors Prof. Jayita Guha Niyogi, Prof. Subhrajit Das, Prof. Suchandra Bardhan, Prof Tapas Kumar Bhattayacharya and Prof Sanjib Nag. I am also grateful to Dr Debasree Bhadra, Lady Brabourne College, for her input at different stages of my work. I shall remain thankful to Indian Meteorological Department and The United States Geological Survey for providing different type of data.

I would like to convey my sincere gratitude and appreciation to my topic expert Dr. Biswajit Thakur, Associate Professor of Civil and Environmental Engineering, Meghnad Saha Institute of Technology, Kolkata, India, for his unwavering commitment, ongoing support, invaluable mentoring, and critical examination of my research concepts and the creation of this thesis.

I thank several research scholars who generously helped at various stages to bring my thesis to its current state. Particular mention should be made in this context for Mr. Soumik Sarkar, Ms. Sohini Sen, Ms. Rohini Majumder Chakroborty, Ms. Piu Dutta, and Mr. Chiranjit Biswas.

No words are enough to show my gratefulness to my mother Mrs. Anima Bajani, my younger brother Mr. Krishanu Bajani. I would like to express my earnest gratitude and thankfulness to my relatives Dr. Kaberi Samanta, Dr. Bimalesh Samanta, Mr. Rathindranath Ghosh for their selfless support and constant encouragement all through the period of research work. I express my heartiest gratitude to my wife Ms. Sudeshna Bag who helped me in my research, extending the moral support and co-operation to carry out the research.

I render very special thanks to my late father Mr. Meghnath Bajani for his mental support and inspiration without which the work would not have been possible. I also like to thank my cousin Rajanya, Rupsa and Sankhasubhra because they are constant source of inspiration and co-operation for my work.

During the process of carrying out of this work, all necessary infrastructural facilities have been received from the Department of Architecture, Jadavpur University, Kolkata. The author expresses his heart-felt gratitude for the co-operation, encouragement and amicable attitude of all colleagues at all stages of work. I feel deeply indebted to my friends and colleagues Mr. Subrata Saha, Mr. Venkatesan Balamurugan, Mr. Prabahar Chelldurai for their encouragement and support.

The author regrets if any acknowledgement that is due has been missed out and apologizes for the same.

Santanu Bajani
14/6/24
Santanu Bajani

Abstract

The absence of reliable data describing features of the design and operation of cities at a fine geographical resolution significantly restricts progress in urban climate science. Climate change projections for the next century indicate that Kolkata will experience hotter, wetter weather with more frequent and severe weather events. These changes will be a particular problem in cities, where urban heat islands exacerbate heatwaves.

The spatial study of UHI and SVF for each local climate zone is the main focus of the current research activity. A GIS-based urban characterization was undertaken for Kolkata, mapping urban morphologically types and their surface urban heat islands. According to the findings, adding more green space or installing green roofs on buildings could prevent the increase of urban heat island, that is anticipated in urban cores and high-density residential regions.

The sky view factor (SVF) plays a crucial role in quantifying the solar radiation budget over a surface. Many methods have been developed and evaluated to calculate/estimate SVF but not quantify it uniformly. It is well known that Urban Heat Island (UHI) is caused by the progressive replacement of the natural environment and the increase in urban activities. SVF and UHI depend on the height of obstacles and their surrounding factors as net solar radiation is determined by the same. This research analyses the methods to calculate SVFs including the Fish-eye Photograph method and raster-based shadow casting method using the UMEP tool to determine the sensitivity of SVF and the impact on UHI for different local climate zone. A linear relationship between SVF and UHI intensities was found. This study can be meaningful for climatologists, urban designers, architects and regional or urban planners to assess and develop guidelines to improve the urban environment.

Contents

Acknowledgement	i
Abstract	iii
Contents	iv
List of Figures	vi
List of Tables	viii
List Of Abbreviations And Acronyms	ix
 Chapter 1. INTRODUCTION	 1
1.1 The Background	1
1.2 Necessity of the present study	5
1.3 Study Area	6
1.4 Research Hypothesis	7
1.5 Research Questions	7
1.6 Objectives of the study	8
1.7 Scope of the study	8
1.8 Work Methodology	9
1.9 Chapterization	13
 Chapter 2. REVIEW OF RELEVANT LITERATURE	 16
2.1 Introduction	16
2.2 Urban land use and land cover dynamics study in order to prepare local climate zone map	17
2.3 Urban heat island study in relation with sky view factors	18
2.4 Sky View Factor	19
2.5 Urban Heat Island	22
2.6 Local Climate Zone	25
2.7 Comprehensive analysis of selected literature studies	29
2.8 Research Gap	42
2.9 Chapter summary	43
 Chapter 3. MATERIALS AND METHODS	 46
3.1 Introduction	46
3.2 Research Design Process	48
3.3 Urban Heat Island Estimation	50
3.4 Sky View Factor Analysis	56
3.5 Local Climate Zones	74
3.6 Chapter Summary	79
 Chapter 4. COMPARATIVE ANALYSIS OF LAND-USE LAND-COVER WITH LOCAL CLIMATE ZONE APPROACH FOR URBAN HEAT ISLAND IN KOLKATA	 80
4.1 Introduction	80
4.2 Land use and land cover (LULC) scenario of Kolkata	81
4.3 Local Climate Zones in Kolkata	83

4.4 Comparative Analysis of Land-Use Land-Cover and Local Climate Zone Approach on Formation of Urban Heat Island	89
4.5 Chapter Summary	91
Chapter 5. COMPARATIVE ANALYSIS OF EXISTING AND PROPOSED SKY VIEW FACTOR ANALYSIS IN KOLKATA	94
5.1 Introduction	94
5.2 Sky View Factor Analysis of Kolkata	95
5.3 Chapter Summary	101
Chapter 6. ANALYSIS OF THE RELATIONSHIP BETWEEN THE URBAN HEAT ISLAND AND THE SKY VIEW FACTOR FOR VARIOUS CLIMATE ZONES IN KOLKATA	102
6.1 Introduction	102
6.2 The Relationship between UHI and LCZ	103
6.3 Urban heat Island extraction of Kolkata	104
6.4. The impact of sky view factor on thermal environments in Kolkata ..	106
6.5 The Relationship between SVF and LCZ	108
6.6 Comparative Analysis between SVF, UHI and LCZ	108
6.7 Findings from analysis	115
6.8 Chapter Summary	117
Chapter 7 CONCLUSION AND RECOMMENDATION	120
7.1 Conclusion	120
7.2 Recommendation	132
References	I
Appendix A	XII
Appendix B	XIII

List of Figures

Figure 1.1	Population changes 2014 to 2030	2
Figure 1.2	Former interactive graph of future climate projections based on different human emission pathways	3
Figure 1.3	Vertical atmospheric scales that are associated with horizontal city scales.	4
Figure 1.4	Location of the study area	7
Figure 1.5	Stratified Sampling	11
Figure 1.6	GPS and QGIS Software used for primary data collection	11
Figure 1.7	Details methodological schema of the research	13
Figure 1.8	Outline of chapterization	15
Figure 2.1	Steps wise total number of literature considered for research	16
Figure 2.2	Year wise research trend on Sky View Factor (2009 - 2022)	20
Figure 2.3	Connections between research on Sky View Factor (2009 - 2022)	20
Figure 2.4	Year wise research trend on Urban Heat Island (2009 - 2022)	23
Figure 2.5	Connections between research on Local Climate Zone (1982 - 2019)	25
Figure 2.6	Year wise research trend on Local Climate Zone (2009 - 2022)	26
Figure 2.7	Connections between research on Urban Heat Island mitigation (1984 - 2023)	44
Figure 3.1	Analytical framework showing the workflow approaches used in analyzing correlation between SVF, UHI, and LCZs	48
Figure 3.2	Schematic layout of research process	48
Figure 3.3	Schematic diagram of urban heat island	51
Figure 3.4	Details Workflow of UHI Calculation	52
Figure 3.5	Illustration of SVF concept	56
Figure 3.6	Sky View Factor Calculator software layout	63
Figure 3.7.1	SVF Mapping Tool V1.1 software layout: Input directory path	65
Figure 3.7.2	SVF Mapping Tool V1.1 software layout: Input directory table	65
Figure 3.7.3	SVF Mapping Tool V1.1 software layout: Input directory table	66
Figure 3.7.4	SVF Mapping Tool V1.1 software layout: Feature insert	66
Figure 3.7.5	SVF Mapping Tool V1.1 software layout: Geometry selection	67
Figure 3.7.6	SVF Mapping Tool V1.1 software layout: Height selection	67
Figure 3.7.7	SVF Mapping Tool V1.1 software layout: Calculate step	68
Figure 3.8	UMEP sky view factor calculator software layout	69
Figure 3.9	Local Climate Zone	75
Figure 3.10	<i>The workflow to classify LCZ as per the WUDAPT method</i>	78
Figure 4.1	Land use and land cover map of Kolkata of 2003, 2010 and 2017	82
Figure 4.2	Proportion of LULC class in Kolkata of 2003, 2010 and 2017	82
Figure 4.3	Local Climate Zone Map of Kolkata	84
Figure 4.4	Local climate zone map for the year (a) 2003, (b) 2010, and (c)2017	86
Figure 4.5	Proportion of area of LCZs during the year (a) 2003, (b) 2010 and (c)2017	87
Figure 4.6	Transformation of LCZ in the year 2003, 2010 and 2017	87
Figure 4.7	Shifting of Local Climate Zones 2003 to 2010	88
Figure 4.8	Shifting of Local Climate Zones 2010 to 2017	89
Figure 5.1	Fisheye lens photographs	95

Figure 5.2	Sky View Factor Map was created in QGIS using UMEP plugins	96
Figure 5.3	The spatial resolution of the SRTM DEM	97
Figure 5.4	Python script was used to prepare the Sky View Factor map	98
Figure 5.5	Comparison of SVF values between the SVF calculation methods at 18 locations	99
Figure 5.6	Validation results through Taylor Diagram	99
Figure 6.1	Flow diagram of comparative analysis study	102
Figure 6.2	Boxplot showing the relationship between UHI and LCZ	103
Figure 6.3	Urban Heat Island maps of Kolkata	104
Figure 6.4	Land Surface Temperature Map	105
Figure 6.5	Locations of Urban Heat Island	106
Figure 6.6	Correlation between SVF and UHI	107
Figure 6.7	Mean SVF value on each LCZs	108
Figure 6.8	SVF, UHI, and LCZ comparison	109
Figure 6.9	UHI and SVF comparison at local climate zone 1	110
Figure 6.10	UHI and SVF comparison at local climate zone 2	110
Figure 6.11	UHI and SVF comparison at local climate zone 3	110
Figure 6.12	UHI and SVF comparison at local climate zone 4	111
Figure 6.13	UHI and SVF comparison at local climate zone 5	111
Figure 6.14	UHI and SVF comparison at local climate zone 6	111
Figure 6.15	UHI and SVF comparison at local climate zone 7	112
Figure 6.16	UHI and SVF comparison at local climate zone 8	112
Figure 6.17	UHI and SVF comparison at local climate zone 9	112
Figure 6.18	UHI and SVF comparison at local climate zone 10	113
Figure 6.19	UHI and SVF comparison at local climate zone B	113
Figure 6.20	UHI and SVF comparison at local climate zone C	113
Figure 6.21	UHI and SVF comparison at local climate zone D	114
Figure 6.22	UHI and SVF comparison at local climate zone E	114
Figure 6.23	UHI and SVF comparison at local climate zone F	114
Figure 6.24	UHI and SVF comparison at local climate zone G	115
Figure 6.25	Intensity of heat islands and cool islands on LCZs	116
Figure 6.26	Schematic diagram of city, showing the variation of UHI and SVF over different local climate zones	117
Figure 6.27	Correlation bar between UHI and SVF on different LCZs	118
Figure 7.1	LULC, UHI, and LCZ in Kolkata	122
Figure 7.2	Conceptual framework of the study	123
Figure 7.3	Hight-width ratio of Kolkata streets	124
Figure 7.4	Urban Built Form Canyon Geometry aspects on selected survey points in Kolkata	128
Figure 7.5	3D view of portion of Kolkata	129
Figure 7.6	Corresponding SVF ratios of different urban settings and ideal for reducing the effects of UHI	131

List of Tables

Table 1.1	Details of secondary data source	12
Table 2.1	Comparative summary of selected literature studies	29
Table 3.1	Dataset and software details	49
Table 3.2	Summary of Landsat TM and ETM+ data used to estimate LST	55
Table 3.3	Summary of software used to classify local climate zones of Kolkata	79
Table 4.1	Temporal changes of LULC in Kolkata	82
Table 4.2	LCZs in the Kolkata	83
Table 4.3	LCZ Classification Accuracy Assessment	85
Table 4.4	Proportion of area of LCZs during the year 2003, 2010 and 2017	86
Table 4.5	Transition matrix of Local Climate Zones, between 2003 to 2017	88
Table 4.6	Comparison between class of LULC and LCZ	90
Table 5.1	Sky View Factor Analysis comparison	98
Table 6.1	Minimum, Maximum and Mean temperature of Kolkata	105
Table 6.2	Demonstrates the SVF of Kolkata deviates slightly from Stewart and Oke's suggested range in various LCZ classes	119
Table 7.1	Street width (m), aspect ratio, built form, and street orientation measured at the survey points	127

List Of Abbreviations And Acronyms

ASTER:	Advanced Space borne Thermal Emission and Reflection Radiometer
DEM:	Digital elevation model
DSM:	Digital surface model
ϵ :	Emissivity
GIS:	Geographic information system
IPCC:	Intergovernmental Panel on Climate Change
LCZ:	Local climate zones
LST:	Land Surface Temperature
LULC:	Land Use and Land Cover
NDBI:	Normalized difference built up index
NDVI:	Normalized difference vegetation index
RTE:	Radiative transfer equation
RS:	Remote Sensing
SUHI:	Surface Urban Heat Islands
SVF:	Sky view factor
TIR:	Thermal infrared
UHI:	Urban heat island
UCL:	Urban Canopy Layer
UMEP:	Urban Multi-Scale Environmental Predictor
WUDAPT:	World Urban Database and Access Portal Tools

Chapter 1. INTRODUCTION

1.1 The Background

The number of people living in urban settings outnumbers the rural population, and the trend is increasing. Cities play an important role, especially when it comes to global climate change, given the impact of extreme heat waves on the population. Earth's temperature varies naturally, but human impacts on climate over the past 120 years have reduced the magnitude of natural temperature changes. Natural influences on temperature (El Niño, solar variability, and volcanic aerosols) have varied by about ± 0.2 °C, while human influence has been about 0.8 °C change has contributed to warming since 1889 (Riebeek & Simmon, 2010). Masson-Delmotte et al., (2018) shows that the temperature will likely reach 1.5° C between 2030 – 2052.

Emmanuel (2005) noted that developing nations, particularly those in the tropical zone, have experienced the majority of this recent population expansion. Rapid urbanization leads to changes in land use, urban structure, and urban architecture (Kotharkar & Bagade, 2018). Urban spaces are dominated by functional buildings of various shapes whose thermal, radiative, and aerodynamic properties create unique micro-climates. According to Oke (2006), there are four factors that influence urban climate. These are: (i) urban structure, (ii) urban coverage, (iii) urban building, and (iv) urban metabolism. Urban structures describe the horizontal and vertical dimensions of buildings and the spaces between them, as well as the width and direction of streets. Urban coverage includes the built-up, vegetation, water, bare land, and percentage of built-up or paved area. Urban buildings, on the other hand, include materials for urban construction and natural coverings, and urban metabolism consists of anthropogenic production of heat, water, and pollutants. Not only do we need to distinguish between town and countryside, but we also need to distinguish between different levels of urban density.

Presently, cities are home to more than 50% of the world's population. By 2045, there will be six billion people living in metropolitan areas, a more than twofold increase. In order to provide the necessary services, infrastructure, and affordable housing that expanding populations demand, city planners must move quickly to get ready for development. In the next 20 years, it is anticipated that the population of Indian towns and cities will rise from 282 million to 590 million. It can be said that urbanization is a dynamic process and one of the main anthropic factors of climate change.

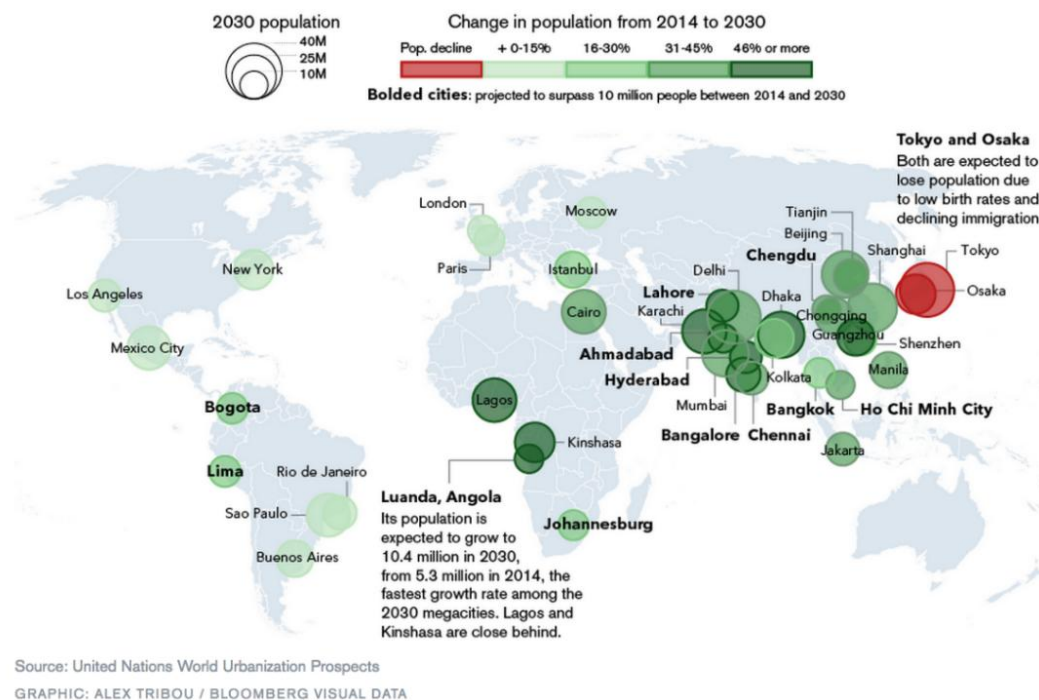


Figure 1.1. Population changes 2014 to 2030

Urban heat island (UHI) is a result of a variety of natural and artificial factors (Memon et al., 2009) and has not been fully explored (Hafner & Kidder, 1999). Urban Heat Islands not only create a temperature higher than average temperature of the adjoining areas but may also lead to further deterioration of the environment causing less rainfall, consequently increasing pollution and suspended solid particulate matters in air. Large cities will be more vulnerable to health risks from heat waves. To lessen the effects of the urban heat island, adaptations must be made in metropolitan areas.

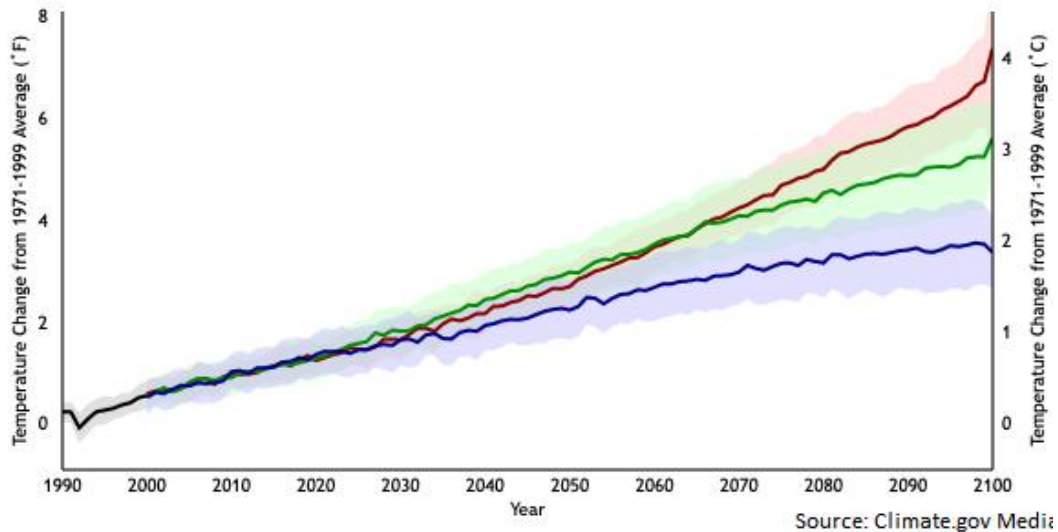


Figure 1.2. Previously available interactive climate estimates based on various human emission routes are shown in this screenshot. The black line on the graph is the average of a series of temperature simulations for the 20th century. The coloured lines on the graph are predicted temperatures for the 21st century based on various emission scenarios. The statistical spread (one standard deviation) supplied by individual model runs is indicated by the shaded areas surrounding each line. (Data processing by Jay Hnilo, CICS-NC, using data courtesy the Coupled Model Inter comparison Project, or CMIP3.)

Various studies have established the relationship between urban morphology and surface temperature (L. Chen et al., 2012; Oke, 1982). The sky view factor (SVF) is significant for describing urban climatology and its spatial changes (de Moraes et al., 2018; Oke, 1973). A restricted view of the sky causes the UHI by increasing net heat storage within buildings (Dirksen et al., 2019). Trees restrict the SVF as well as the outgoing long wave radiation, but do not store much heat (van der Hoeven & Wandl, 2015).

Kolkata is urbanizing, with a population density of more than 24,000 people per km². The city is situated in the tropical climatic region with influences from the south-east monsoon. According to IPCC 2021 report Kolkata has the highest temperature increase among the other global cities with a value of +2.6°C. (IPCC 6th assessment report, 2021). Bajani & Das (2020) shows that the city temperature is around 2°C higher than the surrounding rural areas. Due to the elements that collect and release heat as well as a lack of natural cooling forces like water and vegetation, cities are typically warmer than their surrounding locations.

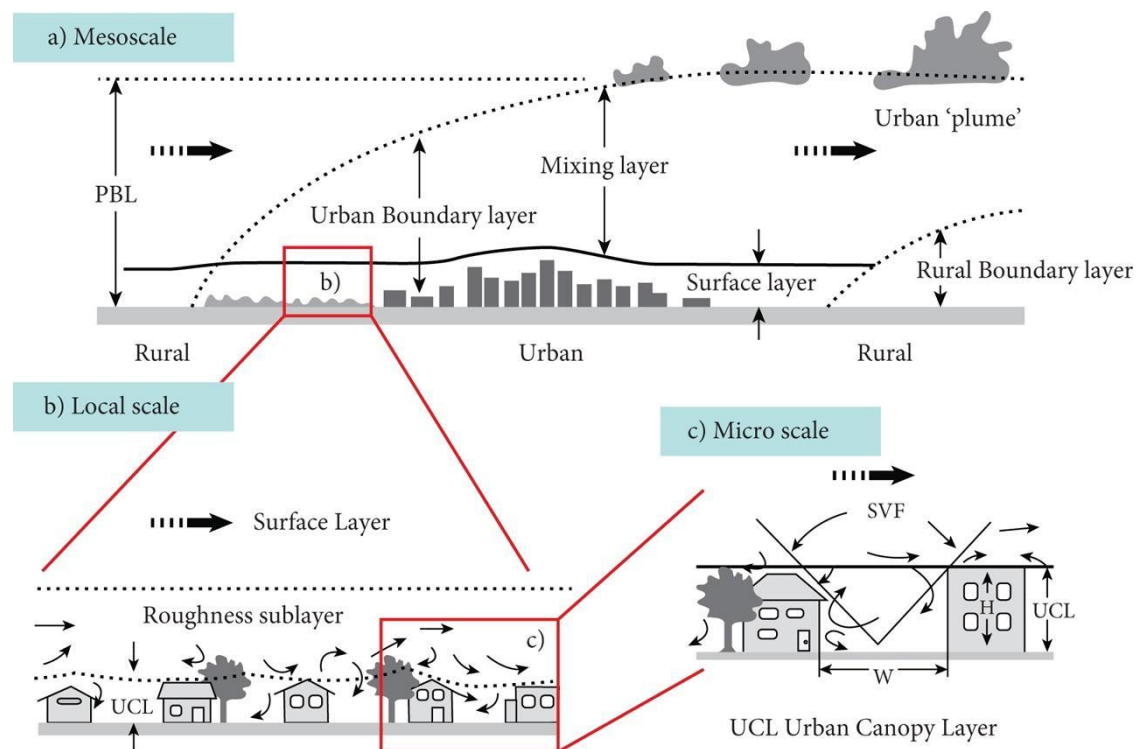


Figure 1.3. Vertical atmospheric scales that are associated with horizontal city scales. The average wind direction is indicated by wide arrows, while turbulent flow is indicated by narrow arrows in (b) and (c). PBL = Planetary Boundary Layer, SVF = Sky View Factor, UBL = Urban Boundary Layer, UCL = Urban Canopy Layer, H = average building height, W = Width of the street. Modified after Oke (1997)

Meso- and micro-scale urban climate studies are also possible. Mesoscale studies focus on the differences in climate between urban and rural areas or on urban heat islands. However, micro-scale urban climatic research focuses on intra-urban micro-climates and their effects on the urban environment (Johansson, 2006). A local climate zone map presents climatic occurrences and issues in maps as a spatial information and assessment tool for merging urban climatic variables and town planning consideration. (Baumuller et al., 1992 and Ren Chao et al., 2010). Remote sensing, even though challenged with the aid of using the spatial and spectral heterogeneity of city environments (Herold et al., 2005; Jensen & Cowen, 1999). It appears to be a suitable source of urban data to support urban climate research (Donnay et al., 2001). The lower sky visibility coefficient, the replacement of ground cover by concrete/asphalt surfaces and the large amount of waste heat emitted from the transport, commercial, residential and industrial sectors create favorable

conditions for warming in the areas urban compared to the surrounding rural areas (Pandey et al., 2012).

1.2 Necessity of the present study

In today's rapidly urbanizing world, the importance of studying the urban climate cannot be overstated. In order to comprehend representative measurement programmes and simulate existing and future cities for any purpose, it is essential to comprehend the scale-dependent character of urban climates. (Grimmond et al., 2015). Cities, with their unique characteristics and complexities, play a crucial role in moderating future global climate change. The materials used in their construction, building and neighborhood design, and residents' behavior all have profound effects on the climate within and beyond a city's boundaries. Furthermore, urban climate studies are essential because the changes in local climate resulting from domestic, commercial, and transport activities within cities can often have a greater magnitude than projected global-scale climate change (Grimmond et al., 2015). Moreover, urban climates have been studied for a long period, resulting in a rich literature with data, concepts, models, and theories that can inform current work. However, there are still important gaps in our understanding of urban atmospheric dynamics, particularly in tropical cities where a large and ever-increasing fraction of the world population resides. Therefore, more attention needs to be directed towards understanding urban atmospheric dynamics in these areas. Detailed research on the thermal behavior of urban surfaces is quite important to reduce the surface heat island effect in urban areas. Thus, investigation of the relationship between urban heat island and sky view factor in different local-climatic zones in a city is now becoming promising work of urban climatology in order to develop a climate resilient city. Additionally, attention should also be directed towards studying towns and small urban areas, as their unique characteristics may have significant impacts on local climate.

1.3 Study Area

The study was chosen for Kolkata. On the left bank of the Hugli River is Kolkata, a tropical metropolis and the state capital of West Bengal. The KMC region spans the longitudes of 88.24°E and 88.46°E and the latitudes of 22.43°N and 22.63°N. It consists of 144 wards that span an area of 200.71 km² with an average elevation of 9 meters, and it is located 154 km north of the Bay of Bengal. Unplanned urban growth in Kolkata, the most significant urban environment in eastern India, has increased the number of impermeable surfaces, making the city more susceptible to heat stress. Consequently, the KMC area was selected for this research's investigation of urban local climate.

With a mean annual temperature of 26.8 ° C and mean monthly temperatures in the range of 19 ° C to 30°C, Kolkata, the "City of Joy," is primarily located in a tropical wet and dry climate. The most sun radiation occurs during the summer months of March through May, and temperatures can approach 40 ° C at this time. The South-West Monsoon, which occurs primarily between the months of June and September, brings the city the majority of its annual rainfall, which amounts to roughly 1,600 mm. From November through February, the region is chilly and dry, with monthly average temperatures between 9 and 11 degrees Celsius. The KMC region had a total population of 44,96,694 people as of the 2011 India Census.

The multifaceted built environment in Kolkata is formed by the multifunctional characteristics of the city and is characterized by diversity. The oldest portion of the KMC region is located in north, central, and south-west Kolkata and is made up of the primarily commercial and industrial Chitpur, Cossipore, Bagbazar, Shyambazar, Barabazar, Esplanade, and Garden Reach sectors. The city expanded to the south and east when the country gained its independence. In places like Tollygunge, Alipore, Ballygunge, Garia, The Eastern Metropolitan Area, and Joka, new buildings and roadways are being built in a comparatively organized manner. The newest urbanized area of the city is the southern periphery. The rural portions of Joka I and Joka II were included in the Kolkata's purview in 2015. The biophysical environment of Kolkata,

which contrasts with the built-up area, is a key factor in determining the local climates.

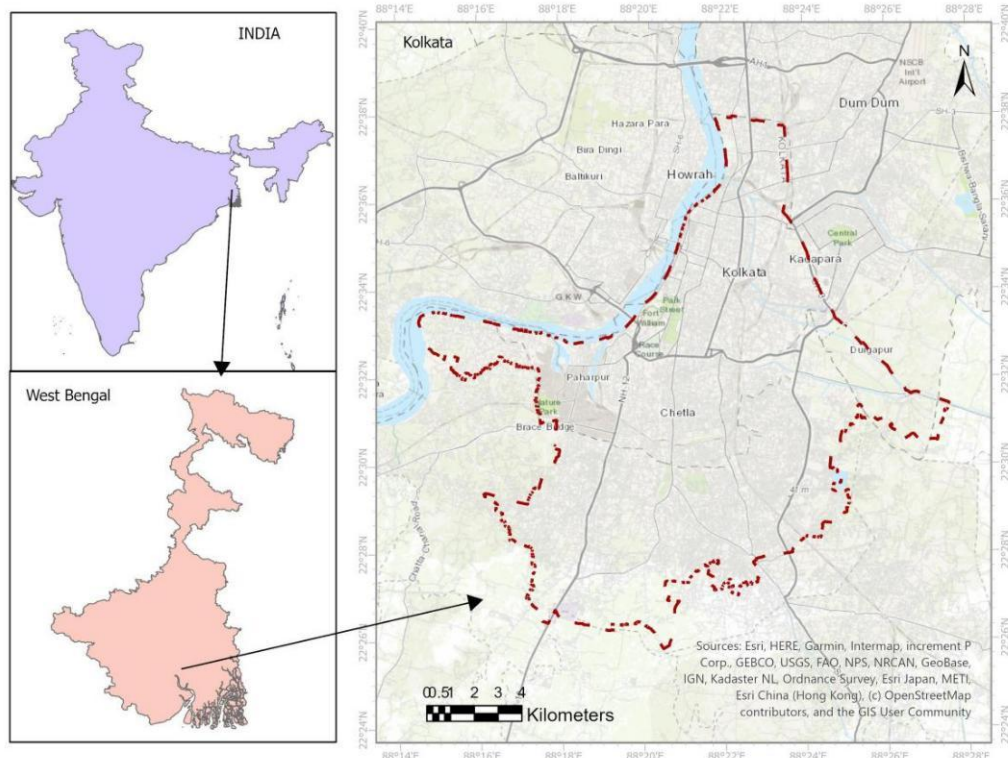


Figure 1.4. Location of the study area (Source: Author)

1.4 Research Hypothesis

Limiting the sky's visibility stores more solar energy, which raises the surface temperature in different urban climatic zones.

1.5 Research Questions

- ? Does different land cover and building volume have an impact on sky view factor?
- ? Is there any relationship between Sky View Factor and different Climatic Zones?
- ? Can we classify the surface urban heat islands with respect to different Sky View Factor for various Local climatic zones?

1.6 Objectives of the study

The objectives of the present study are as follows:

- (1) To study the several facets of SVF and its significance for UHI studies.
- (2) To perform a comparative analysis between the LCZ and LULC approaches in UHI studies.
- (3) Comparative analysis of various SVF calculation method and benefit.
- (4) To analyse the UHI effect in relation to various SVF in different LCZ.
- (5) To suggest and propose suitable SVF ratios for various LCZs to mitigate the effects of UHI.

1.7 Scope of the study

The focus of the current study, "Investigating the Relationship between Urban Heat Island, Sky View Factor for Different Local Climate Zones, A Case Study of Kolkata," is to recognize Kolkata's Local Climate Zones and comprehend the interaction between surface UHI and SVF and how this has an effect on LCZs. The spatial analysis of the urban heat island and the sky view factor are the primary interests of this work. These two variables aid in our comprehension of the ability of urban surfaces to control the surrounding climate over Kolkata. In order to conceptualize the climatic zones of the city, distinct potential local climatic zones have been delineated based on the thermal capacity and reactivity of urban structure, urban cover, and urban fabric.

The scope of this study is broad and includes a number of different areas of research. Some of the key areas of research include:

Understanding the relationship between UHI and SVF: To better understand the relationship between UHI and SVF, and how this relationship varies under different conditions, such as climate, urban form, and land cover.

Developing methods to mitigate UHI: Methods are developing to mitigate UHI, such as through urban design, green infrastructure, and energy efficiency. SVF can be used to inform these mitigation strategies.

Assessing the impacts of UHI: The impacts of UHI on human health, energy demand, and air quality. SVF can be used to assess these impacts at different scales, from individual buildings to entire cities.

In conclusion, the study's scope involves knowing the origins and traits of UHIs, SVFs, and LCZs. designing techniques to lower UHIs and measuring UHIs, SVFs, and LCZs. This research is crucial for reducing the harmful effects that UHIs have on the environment and human health.

1.8 Work Methodology

This study used an exploratory design method to examine how SVF and UHI relate to each other. As per R. K. Yin (2003) exploratory designs are utilized when evaluating interventions that have not been tested or whose effectiveness is unclear. A small amount of research has been conducted to understand the relationship between SVF and UHI in tropical cities. Thus, carrying out an exploratory design will provide a wider perspective on the interaction between sky view factor variations in different urban construction types and urban heat island changes.

1.8.1 General Approach

Urban structure is the one of the most important aspects which influences the land surface temperature and formation of urban heat island due to change in sky view factor and local climate zones. In our study, to meet this goal we followed 4 steps. First phase to evaluate and map the spatial differences of the land surface temperature and urban heat island, the surface temperature was extracted from thermal imagery. This procedure makes it possible to observe the study area's local land surface temperature pattern and urban heat island intensity. In the second

phase, the sky view factor map was prepared to specify the existing SVF scenario. In this step, there were two existing methods, i.e. - Photograph method by using fish-eye lens and RS & GIS method by using 'Sky View Factor Calculator' and UMEP tools of QGIS software is used to evaluate the SVF in study area. In this step a new python-based approach was introduced to extract SVF map from DEM. In the third phase, the LCZ classification approach is used to specify the existing LCZ classes. The LCZ map was generated based on the method mentioned by WUDAPT (World Urban Database and Access Portal Tools). Random forest classifier system is used to extract LCZ map of Kolkata. In the final section, we used statistical methods to find the correlation between surface urban heat island and Sky View Factor for various Local Climate Zones.

1.8.2 Data Collection

1.8.2.1 Primary Data Collection

Primary data are the original datasets that are collected for particular research goals and utilized to address research questions (Hox & Boeijs, 2005). Primary data for this study were collected over the span of 5 year-long field works in 2017-2021. Before starting this approach, several preparations were made. For the purpose of gathering data, a base map was prepared. Local temperature data was collected as reference point for accuracy assessment of UHIs. The land surface maps were prepared from thermal satellite image, the ground surface temperature values were collected during the Landsat descending acquisitions time between 10:00 and 10:25 am over the region. A crucial element in providing accurate information about the surface temperature in the research area was the comparison of ground temperature with Landsat acquisition. Around 50,000 building data were gathered in order to extract SVF maps over the selected region within Kolkata. Road width and building height are the major findings in the steps to extract the height-width ratio. Sky view photographs were taken from various locations to calculate SVF. Signature files from various land cover types associated with climate zones are categorized in google earth and verified in field. In total 500 sampling points of various built-up and land cover types were collected to check the accuracy of LCZs. Random stratified sampling

method is applied in order to define LCZ classes. In stratified random sampling, each class is given a certain amount of sample points based on its size or relevance (McCoy, 2005). By using this technique, an unfair distribution of points among the classified category would be avoided.

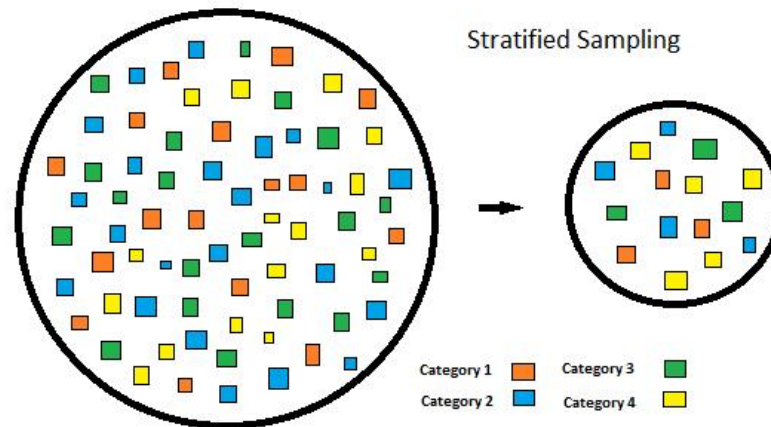


Figure 1.5. Stratified Sampling (Source: Author)

Garmin eTrex-10 GPS and android based Q-Field software were used to collect these observation points. Nikon D-650 DSLR camera with Nikon 10.5mm f/2.8G Fisheye ED AF DX Fisheye Nikkon Autofocus Lens was used to capture sky photos. Two colleagues assisted in the collection of the primary data during this phase. Local experts were interviewed to discuss the early findings regarding the trend in surface temperature caused by high rise and growing building density in Kolkata. The purpose of the interview was to learn more about and pinpoint Kolkata's surface temperature features. This approach is thought to be efficient since it provides a thorough understanding of surface temperature and its features in the studied area.

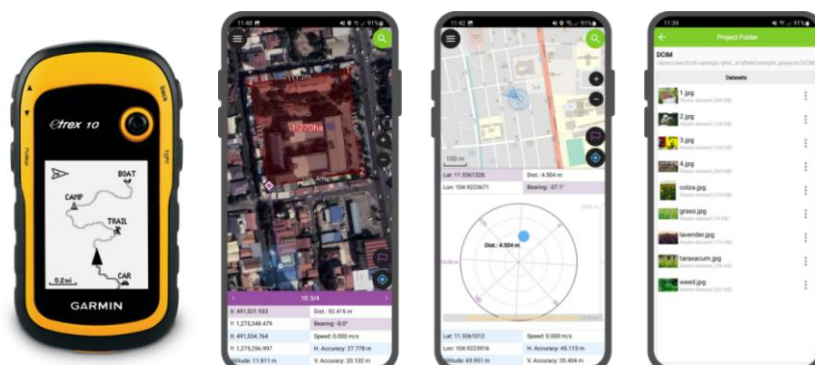


Figure 1.6. GPS and QGIS Software used for primary data collection (Source: www.google.com)

1.8.2.2 Secondary Data Collection

Regarding secondary data collection, two categories of imagery were used to evaluate urban structure types and land surface temperatures. Landsat TM5 and Landsat 8 OLI TIRS were chosen. The thermal band is found in band 6 of Landsat TM5, however there are two thermal bands on Landsat 8 OLI/TIRS, band 10 and band 11. Both the imageries have been resampled to a resolution of 30 meters. Google earth pro and Landsat 8 images were used to extract detailed information on urban structure types. Building footprints were extracted from Open Street Map data. Table 1.1 provides the details about the dataset used during the study.

Table 1.1. Details of secondary data source

No	Data	Format	Data Source	Data Collection
1	Landsat 5	Raster	USGS https://earthexplorer.usgs.gov/	Download
2	Landsat 8	Raster	USGS https://earthexplorer.usgs.gov/	Download
3	Google Earth Pro	Raster	Google https://earth.google.com/web/	Online
4	Land cover	Vector	ESRI https://livingatlas.arcgis.com/landcover/	Survey
5	Administrative Boundaries	Vector	Kolkata Municipal Corporation https://www.kmcgov.in/KMCPortal/jsp/KMCMMap.jsp	Survey
6	Building Footprint	Vector	Open Street Map https://www.openstreetmap.org/	Download

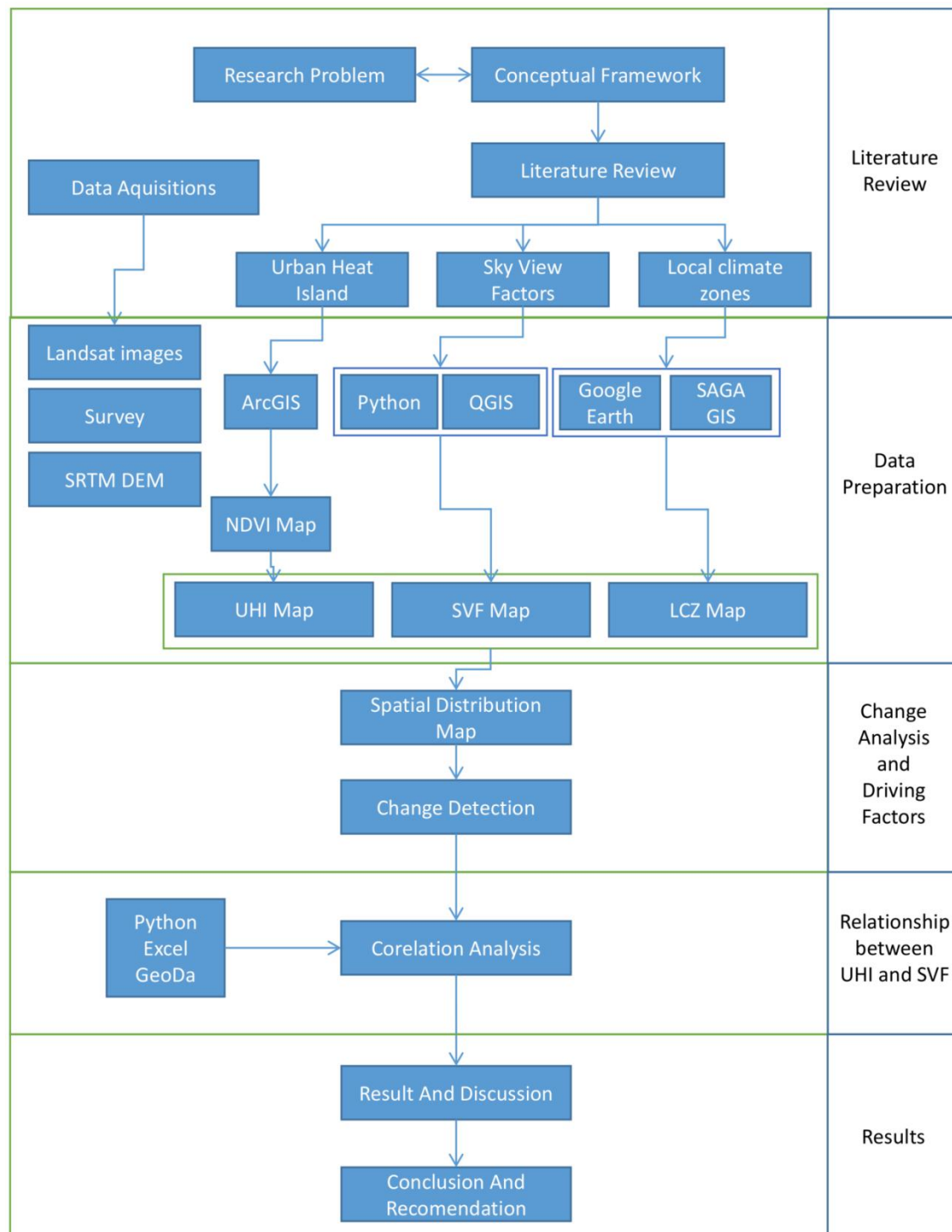


Figure 1.7. Details methodological schema of the research (Source: Author)

1.9 Chapterization

Localized climate changes are the most well-known consequences of changes in land use and land cover driven on by urbanization (Bajani & Das, 2020). Numerous analyses, including those involving acoustics, thermodynamics, ventilation, and solar

radiation, are affected by the sky view factor (Cheng 2010). In order to explore the SVF phenomenon more carefully, incorporating both speculative models and actual locations that display various sorts of obstruction, it is important to understand the fundamental principles and linkages underlying the numerous variables concerned. The thesis includes the climatic study of Kolkata. The whole thesis is structured into 7 different chapters.

The study background, need for the study, brief description of the study area, probable objectives, scope of the work, and work methodology are all covered in **Chapter 1**.

Chapter 2 starts with literature study on various aspects of urban morphology, Local Climate Zones, Urban Heat Island, and Sky View Factor.

Chapter 3 explains all the materials and methods which have been used for primary data collection, processing of data and also limitations faced.

Chapter 4 illustrates the concepts of land cover and local climate zone concept with an emphasis on each study's significance, scalability, and relevance.

Chapter 5 is one of the most important chapter of the thesis, as it analyses various methods for Sky View Factor calculations in urban areas, their pros and cons, and based on that a new approach to calculate the SVF is also proposed and validated for its accuracy with other techniques. In this chapter the SVF data and analysis for the study area is also presented.

In **Chapter 6**, an in-depth analysis was conducted to explore the intricate relationship between the urban heat island effect and the sky view factor across various local climate zones in Kolkata. Due to constraints in data availability, a specialized Sky View Factor map was meticulously crafted for a specific area within Kolkata, enabling a comprehensive analysis to be carried out within the defined limits. The assessment of spatial, temporal, and longitudinal trends pertaining to the Urban Heat Island

phenomenon in the Kolkata region, spanning from the years 2000 to 2020, was meticulously executed using a comprehensive dataset comprising Landsat TM, ETM+, and TIRS thermal data. By delving into the severity and extent of the Urban Heat Island effect and Sky View Factor characteristics in Kolkata, this chapter sheds light on the multifaceted nature of these phenomena. Furthermore, advanced satellite image categorization algorithms were employed to scrutinize the evolving state of Local Climate Zones (LCZs) in Kolkata, presenting a detailed examination of the changing landscape dynamics.

The conclusions and future directions are the focus of **Chapter 7**. Local climatic zones are identified using urban morphology data, and their characteristics are enumerated using UHI and SVF values. The superimposition of all factors provides a detailed perspective of Kolkata's metropolitan climate.

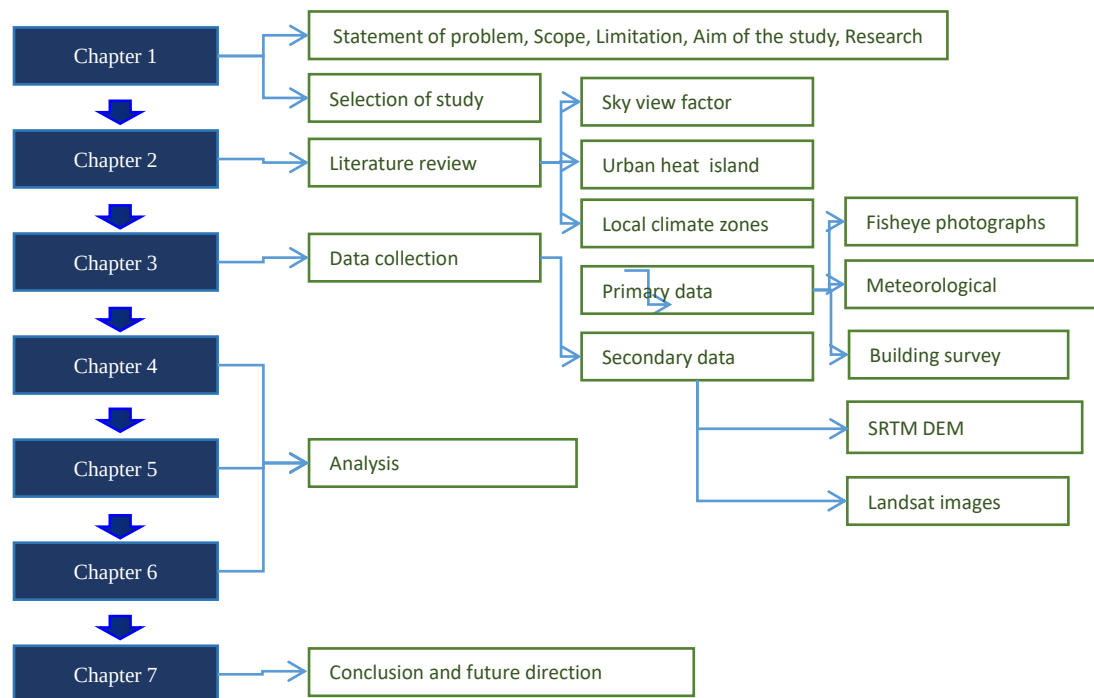


Figure 1.8. Outline of chapterization (Source: Author)

Chapter 2. REVIEW OF RELEVANT LITERATURE

2.1 Introduction

The selection process of the reviewed articles is significant since it takes into account the reviews' importance to present a broad picture on the chosen research problems, its methodological approaches, the direction of research, and the problems and points for improvement highlighted. The publications were initially examined to determine which ones applied research in UHI, SVF, LCZ, and LULC investigations. The data from the chosen papers was then organized, recognized, and filtered while taking the titles, abstracts, and methodology into consideration. Following the identification and filtering of the resultant data, the use of descriptive statistics, the plotting of analytical graphs, and a class discussion, the outcomes were reviewed.

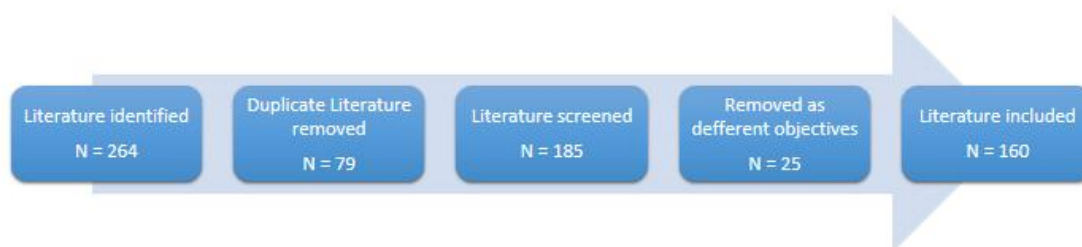


Figure 2.1. Steps wise total number of literature considered for research (Source: Author)

The relationship between urban heat island (UHI) and sky view factor (SVF) has been extensively studied in urban climate research. The SVF is a measure of the proportion of the sky visible from a particular location, and it plays a crucial role in regulating long-wave radiative heat loss in urban canyons (Oke, 1981). The SVF is considered a significant factor in UHI studies and has been shown to have a negative relationship with daytime intra-urban temperature differences (Shi et al., 2021).

Several studies have investigated the impact of canyon geometry, including the aspect ratio and SVF, on the intensity of the UHI. It has been established that because the SVF controls long-wave radiative heat loss, it is a significant factor in the production of nocturnal UHI (Oke, 1981). The SVF has also been shown to have a significant correlation with UHI intensity and building density (Zhang et al., 2022). In

high-rise, high-density urban areas, the SVF analysis of street canyons has implications for daytime intra-urban air temperature differentials (Chen et al., 2010).

Studies examining the impacts of urban physical settings on the duration of high air temperature provide additional evidence for the association between SVF and UHI. There has been evidence that longer periods of high air temperature are caused by increases in commercial and traffic areas, which can affect SVF (Choi et al., 2018). Furthermore, due to radiation trapping effects, high-albedo materials can lessen the benefits of high SVF (Choi et al., 2018).

It should be noted that the relationship between UHI and SVF is influenced by other factors as well. For example, the impact factors of UHI are complex, and the selection of sample grids may introduce uncertainty (Shi et al., 2021). Energy consumption per capita and thermal admittance differences are additional factors that can affect UHI intensity (Roth, 2007).

In conclusion, the relationship between UHI and SVF is well-established in urban climate research. The SVF, as a measure of canyon geometry, plays a crucial role in regulating long-wave radiative heat loss and has a significant correlation with UHI intensity. However, the relationship is influenced by other factors, such as energy consumption per capita and thermal admittance differences. Understanding the relationship between UHI and SVF is important for mitigating the adverse effects of UHI and improving urban thermal environments.

2.2 Urban land use and land cover dynamics study in order to prepare local climate zone map

Urban land use and land cover dynamics refer to the changes in the way land is used and the physical characteristics of the land in urban areas. These changes have significant impacts on the environment, society, and the economy. The interaction between human activities and the local biophysical circumstances determines the paths and rate of change, which vary over time and space. Urban environments are

affected over the long run by changes in spatio-temporal land use and land cover. According to McCloy (1995), land use refers to the purpose for which a piece of land is used, whereas land cover refers to the characteristics of the surface. It has always been the subject of scholarly study and social and economic discussions since land use growth involves high economic risk and profitability, massive consumption of arable land, and significant adverse externalities on environmental sustainability (Bourne, 1996; Peiser, 1989).

2.3 Urban heat island study in relation with sky view factors

The urban heat island (UHI) is a type of heat buildup phenomenon that occurs in urban areas as a result of habitation and urban development (Yang et al., 2016). It is widely agreed upon as being the most prominent aspect of the urban climate. Urban ecological systems' material and energy flow, as well as their structure and functions, will undoubtedly be impacted by the rise in land surface temperature brought on by the UHI effect. Numerous ecological and environmental consequences, including those on soil qualities, atmospheric conditions, biological habits, material cycles, energy metabolism, and resident health, will result from this, as would urban climates and hydrological conditions.

The UHI phenomenon has received a great deal of attention as a major indicator of the impact of urban settings on the local climate. Furthermore, while fewer studies are focusing on tropical regions than on mid-latitude western urban areas (Oke, 1982), there is relatively well-developed literature on urban heating in sub-tropical regions. Recently, studies have used a variety of approaches to evaluate the urban heat island, including surface energy balance modeling (Tso, 1996; Tso et al., 1990), satellite images and remote sensing, weather station and temperature sensor field monitoring (Elsayed, 2012), and numerical modeling (Morris et al., 2017). The primary drivers of the urban heat island have been identified as various anthropogenic factors, including changes in land use/land cover, an increase in built-up areas, and a decrease in green areas.

Sky view factor (SVF) is an important factor in describing urban climatology at scales below 100m (Dirksen et al., 2019). It serves as a stand-in for net radiation and is reliant on the surrounding obstructions' height (Dirksen et al., 2019). A rasterized point cloud height dataset with six to ten points per square metre is used to compute SVF. Several studies have investigated the relationship between SVF and urban heat island (UHI) (Baghaeipoor and Nasrollahi, 2019; Cheung et al., 2016; Svensson, 2004; Unger, 2008).

Model experiments have shown that the canyon geometry or SVF in central areas is a relevant variable in producing a nocturnal UHI (Svensson, 2004). A study has reviewed the methods of SVF determination and intra-urban surface geometry-air temperature relationship (Unger, 2008). Baghaeipoor and Nasrollahi (2019) discovered in another investigation that there is an inverse relationship at night and a direct relationship between SVF and air temperature during the day. The study also confirmed the relationship between SVF and air temperature by comparing the average geometry and air temperature variations (Baghaeipoor and Nasrollahi, 2019). Furthermore, the study discovered that on the hottest day, there was an air temperature differential of roughly 2–7°C, and on the coldest day, there was a difference of 1–4°C (Baghaeipoor & Nasrollahi, 2019).

SVF was employed in a Greater Manchester, UK study as a measure of how much sky is visible from the ground in an urban location (Cheung et al., 2016). The study found that SVF was correlated with UHI (Cheung et al., 2016).

2.4 Sky View Factor

The Sky View Factor (SVF) is a significant urban climatology parameter that characterizes the amount of visible sky from a given location at the ground level. It plays a crucial role in various fields, such as urban planning, climate studies, and energy-efficient building design. Understanding SVF is essential for evaluating urban local climates, predicting temperature variations, and enhancing thermal comfort. This literature review aims to present a comprehensive analysis of the research

conducted on the Sky View Factor, discussing its importance, measurement techniques, applications, and the influence it has on urban environments. Figure 2.2. shows a positive trend in Sky View Factor studies. Figure 2.3 explains the relationship and connections in the research on the sky view factor.

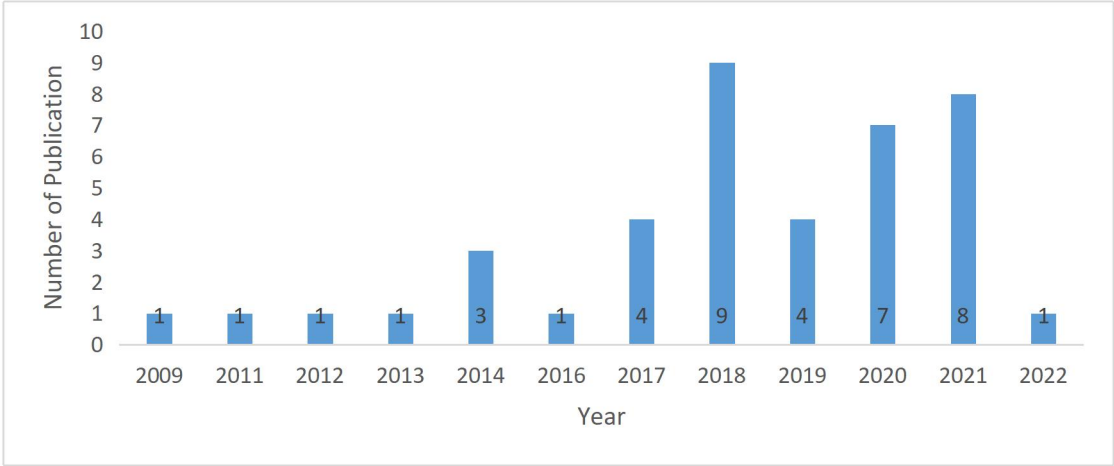


Figure 2.2. Year wise research trend on Sky View Factor (2009 - 2022) (Source: Author)

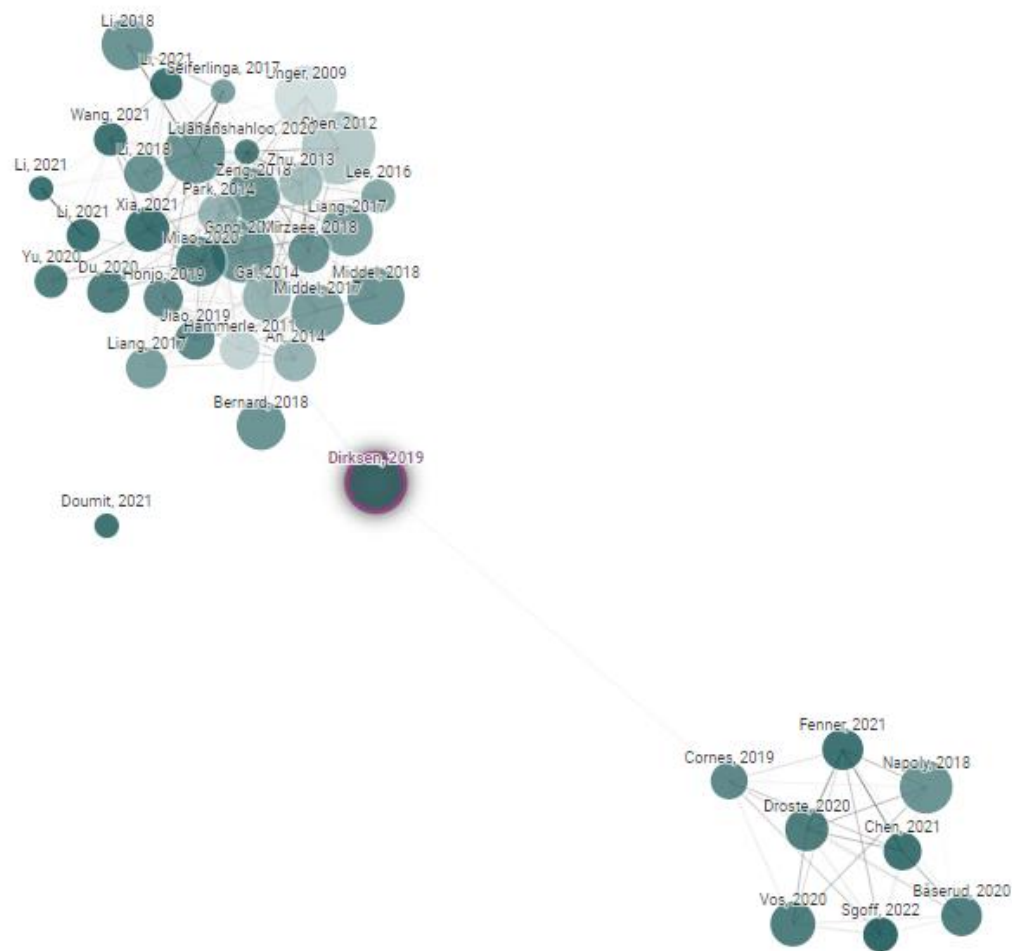


Figure 2.3. Connections between research on Sky View Factor (2009 - 2022) (Source: <https://www.connectedpapers.com/>)

Stewart, I.D., & Oke, T.R. (2012) introduces the concept of Local Climate Zones (LCZ) and their significance in understanding urban microclimates. It discusses how SVF is a key parameter for classifying LCZs, as it influences temperature variations and thermal comfort in cities.

Järvi, L., & Grimmond, C.S.B. (2011) investigates that different tree types of influence SVF and subsequent microclimates. It demonstrates that deciduous trees tend to have a significant impact on SVF due to their seasonal variations in leaf cover, affecting urban cooling.

Ali-Toudert, F., & Mayer, H. (2007) shows the street canyons' impact on SVF and thermal comfort. It shows that the orientation and aspect ratio of street canyons have a direct influence on SVF, with specific implications for hot and dry climates.

Kleerekoper, L., van Esch, M., & Salcedo, T.B. (2012) explores strategies to mitigate the Urban Heat Island (UHI) effect through urban planning and design. It emphasizes the importance of increasing SVF in dense urban areas to enhance ventilation and reduce heat stress.

Shashua-Bar, L., & Hoffman, M.E. (2000) proposes an empirical model to predict the thermal performance of urban streets based on vegetation cover and SVF. It highlights the cooling effect of vegetation and its interaction with SVF in shaping microclimates.

Coutts, A.M., Tapper, N.J., & Beringer, J. (2007) investigates the relationship between urban density, SVF, and the surface energy balance in Melbourne. It emphasizes the need for balanced urban planning to maintain appropriate SVF for thermal comfort.

Diaz, J., & Planells, A. (1996) analyzes the impact of urban morphology on the nocturnal Urban Heat Island (UHI) in Valencia, Spain, with a focus on SVF. It highlights the correlation between UHI intensity and SVF in different urban configurations.

Ali-Toudert, F., & Mayer, H. (2006) investigates the influence of street canyon geometry on SVF and its thermal behavior. It provides valuable insights into how various canyon configurations affect SVF and, subsequently, outdoor thermal conditions.

Jiang, B., & Liu, Y. (2015) evaluates the impact of tree shade on outdoor thermal comfort in a subtropical megacity, considering the spatial distribution of trees and SVF. It emphasizes the need for incorporating greenery strategically to improve thermal conditions.

Mayer, H. (1993) emphasizes the joint consideration of SVF and wall temperatures in urban canyons for a comprehensive understanding of microclimates. It highlights SVF's role in influencing air and wall temperature variations.

The Sky View Factor (SVF) is a critical parameter in understanding urban microclimates and designing climate-responsive urban environments. This literature review has highlighted ten significant research studies on SVF, showcasing its diverse applications in urban planning, climate studies, and building design. From the impact of vegetation and street canyon geometry to the role of SVF in mitigating the Urban Heat Island (UHI) effect, these studies collectively emphasize the importance of SVF in creating sustainable and comfortable urban spaces. Future research in this field should focus on integrating SVF analysis into urban planning strategies and exploring innovative ways to enhance urban cooling and thermal comfort.

2.5 Urban Heat Island

The phenomenon known as urban Heat Island (UHI) is well-documented and is attributed to the higher temperatures experienced in metropolitan areas relative to their rural surrounds. This literature review examines the current state of research on UHI, exploring its causes, impacts on urban environments, human health, and ecosystems, and highlighting effective mitigation strategies. Some literature was analyzed to provide an in-depth understanding of UHI and potential solutions. Figure

2.4 explains the current research trend in the field of urban heat island research and demonstrates that UHI research has been selected as a topic of study due to its significance to the environment and planet.

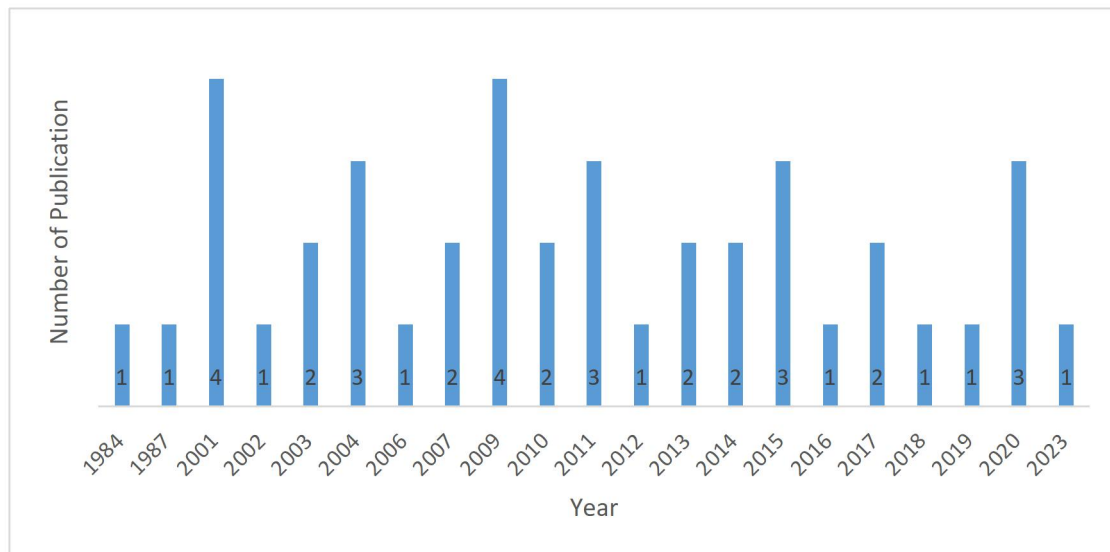


Figure 2.4 Year wise research trend on Urban Heat Island (2009 - 2022) (Source: Author)

Oke, T.R. (2017) in his *Boundary Layer Climates*, discusses that the foundational work explores the principles and mechanisms that lead to UHI formation, including land-use changes, anthropogenic heat, and urban geometry. It delves into the role of local meteorological factors in creating and intensifying UHI effects.

Santamouris, M. (Ed.) (2016) in his book *Urban Heat Island: Mitigation and Adaptation* presents a comprehensive overview of UHI mitigation and adaptation strategies. It includes case studies on green roofs, cool pavements, urban greenery, and the use of reflective materials, outlining their effectiveness in combating UHI effects.

Stone Jr, B., Vargo, J., & Liu, P. (2015) in their study discusses spatial variations in temperature and UHI impacts on public perceptions of climate change, providing insights into how these disparities can influence climate change beliefs and policy decisions.

Li, X., Zhou, W., Ouyang, Z., & Xu, W. (2019) investigates that UHI can affect regional climate patterns, including precipitation, temperature, and atmospheric circulation, which has significant implications for urban planning and climate change adaptation.

Chow, W. T. L., Roth, M., & Salamanca, F. (2015) quantifies the energy consumption impact of UHI on cooling and heating needs, highlighting the importance of urban planning strategies to reduce energy demand.

Chen, L., Ng, E., An, X., Ren, C., Lee, M., & Wang, X. (2020) assesses the UHI effect and its energy impact in high-density cities, suggesting feasible strategies to enhance urban resilience and energy efficiency.

Tan, J., Zheng, Y., Tang, X., Guo, C., Li, L., & Song, G. (2020) examining the relationship between UHI and air quality, this study reveals how UHI exacerbates air pollution and poses health risks to urban residents.

Yang, J., Yuan, Y., & Tang, M. (2019) compares the UHI mitigation strategies adopted in Shanghai, Hong Kong, and Tokyo, providing valuable insights into effective measures for different urban contexts.

Escobedo, F. J., Kroeger, T., & Wagner, J. E. (2011) explores how urban forests can help alleviate UHI effects and mitigate pollution, enhancing the understanding of green infrastructure's role in UHI mitigation.

Li, D., Bou-Zeid, E., & Oppenheimer, M. (2019) assesses the influence of UHI on climate change, examining the broader implications for global warming and highlighting the necessity of UHI mitigation in climate adaptation strategies.

Urban Heat Island is a complex phenomenon that affects numerous aspects of urban life, including public health, energy consumption, air quality, and regional climate patterns. Through analyzing these ten research references, this literature review has provided a thorough understanding of the causes, impacts, and potential solutions to

UHI. Implementing effective mitigation strategies, such as green infrastructure, cool pavements, and urban planning interventions, can help create more sustainable and resilient cities in the face of a changing climate. Further research is essential to refine and develop innovative approaches to combat the adverse effects of UHI and promote sustainable urban development.

2.6 Local Climate Zone

In recent years, the rapid growth of urbanization has led to significant changes in local climate patterns, creating what is known as the Urban Heat Island (UHI) effect. Local Climate Zones (LCZs) have emerged as a valuable tool for understanding the complex microclimates within urban areas, helping urban planners and policymakers develop strategies to mitigate the adverse impacts of climate change on cities. This literature review aims to explore the concept of Local Climate Zones, their classification systems, methodologies for their characterization, and their implications for sustainable urban development.

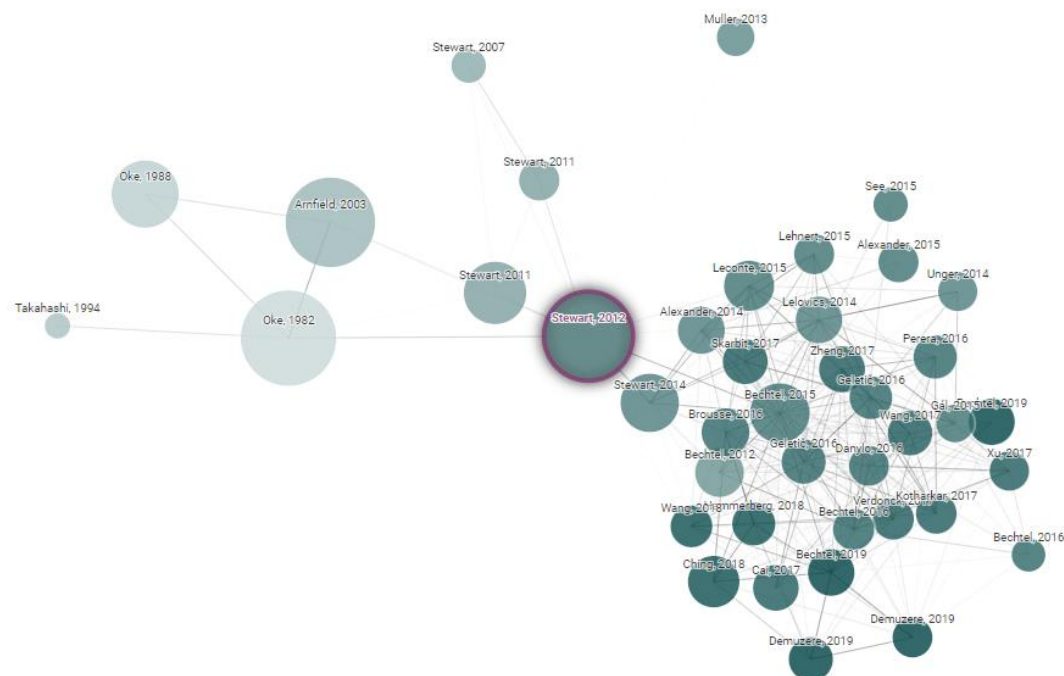


Figure 2.5 Connections between research on Local Climate Zone (1982 - 2019)
(Source: <https://www.connectedpapers.com/>)

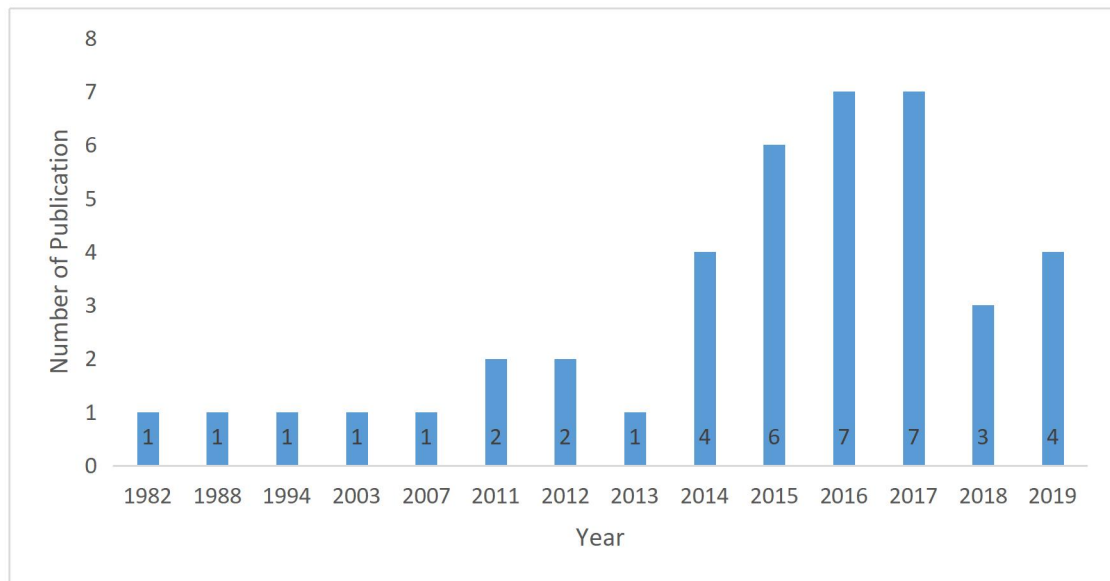


Figure 2.6 Year wise research trend on Local Climate Zone (2009 - 2022) (Source: Author)

Figures 2.5 and 2.6 vividly depict the ongoing growth and evolution of the research trend within the realm of local climatic zone studies. An in-depth analysis of these figures reveals a compelling narrative that underscores the increasing importance and impact of LCZ research on both the environment and the planet as a whole. The graphical representations not only capture the expanding scope of this field but also serve as a testament to the intrinsic value that LCZ research brings to the forefront of scientific inquiry. It is evident from these illustrations that the selection of LCZ as a focal study topic has been driven by its profound significance in shedding light on crucial environmental issues and enhancing our understanding of planetary processes. As we delve deeper into the data presented in Figures 2.5 and 2.6, it becomes apparent that the trajectory of LCZ research is intertwined with the broader narrative of environmental sustainability and global awareness. These visual representations serve as powerful tools for highlighting the intricate interplay between research, knowledge dissemination, and environmental stewardship in the context of local climatic zone studies.

Stewart, I. D., & Oke, T. R. (2012) introduces the Local Climate Zones scheme as a classification system for urban areas, which aids in understanding the surface properties that drive local climate patterns. The authors present a comprehensive

overview of various LCZ categories and their impact on temperature variations within cities.

Bechtel, B., Alexander, P. J., Böhner, J., Ching, J., Conrad, O., Feddema, J., ... & Stewart, I. (2015) outlines the development of a global LCZ database, presenting a harmonized approach for mapping and characterizing LCZs across diverse urban environments worldwide. The paper highlights the importance of LCZs in supporting climate-related research and urban planning on a global scale.

Coutts, A. M., Beringer, J., Tapper, N. J., & Loughnan, M. (2013) explores the relationship between urban microclimates, energy consumption, and the built environment. The authors emphasize the role of LCZs in influencing local energy demand and discuss the potential for sustainable urban planning strategies to mitigate the UHI effect.

De Ridder, K., Bechtel, B., Russo, A., & Fonte, C. C. (2019) investigates the impact of different LCZs on heat stress in various urban configurations. By analyzing multiple case studies, the researchers provide valuable insights into how urban planners can optimize city layouts to enhance thermal comfort and reduce heat stress.

Ward, H. C., Kotthaus, S., Järvi, L., & Grimmond, C. S. (2016) focuses on the Surface Urban Energy and Water Balance Scheme (SUEWS), which is an urban climate model heavily reliant on LCZ classifications. The authors showcase the efficacy of SUEWS in simulating energy and water balance components within urban areas, providing valuable information for sustainable urban planning.

Salamanca, F., Martilli, A., & Tewari, M. (2017) presents an overview of numerical models used to simulate temperature and wind fields in urban areas. The authors discuss how the incorporation of LCZs in these models helps improve their accuracy, facilitating better urban climate predictions.

Masson, V. (2006) proposes a physically based scheme for simulating the urban energy budget in atmospheric models, incorporating LCZ information. The study emphasizes the importance of considering urban morphology and surface characteristics in climate models to enhance their representation of urban climates.

Middel, A., Häb, K., & Brazel, A. J. (2017) shows the urban form and design impact on local climate conditions. By utilizing LCZ classifications, the study provides valuable insights for sustainable urban design that minimizes heat exposure and improves overall urban livability.

Marconcini, M., Syrbe, R. U., & Lehmann, S. (2018) evaluates the local climate zones and their relationship with land surface temperature patterns in Leipzig, Germany. The findings reveal how different LCZs influence temperature variations within the city and offer guidance for targeted urban interventions.

Katzschner, L., Bechtel, B., Foley, M., De Ridder, K., & Schawe, R. (2020) assesses the cooling potential of urban green spaces using LCZs and ENVI-met simulations. The study highlights the significance of green spaces in moderating local climate conditions, contributing to sustainable urban planning efforts.

Local Climate Zones have emerged as a crucial tool in understanding urban microclimates and the potential impacts of climate change on cities. This literature review has explored the development of LCZ classification schemes, their applications in climate modeling and urban planning, and their implications for sustainable city development. The integration of LCZs into urban planning strategies can aid in mitigating the Urban Heat Island effect, enhancing urban livability, and promoting climate-resilient cities. As research in this field continues to evolve, further investigations into the intricate relationship between LCZs and urban microclimates are warranted to foster informed decision-making and sustainable urban development practices.

2.7 Comprehensive analysis of selected literature studies

A comparative summary of a few works of literature studies is discussed in table 2.1.

Table 2.1. Comparative summary of selected literature studies

Paper title	Abstract summary	Authors	Year	Outcomes measured
Connection between urban heat island and sky view factor approximated by a software tool on a 3D urban database	If the chosen scale is suitable, surface geometry plays a major role in defining the temperature distribution.	J. Unger	2009	<ul style="list-style-type: none"> •Sky View Factor (SVF) •Intra Urban Surface Geometry Air Temperature Relationship •Temperature Distribution
On relationships between heat island and sky view factor in the cities of Tama River basin, Japan	SVF is a very useful indicator of the effect of urbanization on heat island intensity.	Shuji Yamashita, Kiyoshi Sekine, Masahiro Shoda, Kohji Yamashita, Yoshio Hara	1986	<ul style="list-style-type: none"> •Heat Island Intensity •City Size •Horizontal Distributions of Dry And Wet Bulb Temperature •Wind Speed •Wind Direction •Sky View Factor
Sky view factor analysis of street canyons and its implications for daytime intra-urban air temperature differentials in high-rise, high-density urban areas of Hong Kong: a GIS-based simulation approach	The spatial average of sky view factor values has a close negative relationship with daytime intra-urban temperature differences in urban Hong Kong.	Liang Chen, E. Ng, Xipo An, C. Ren, M. Lee, U. Wang, Zhengjun He	2012	<ul style="list-style-type: none"> •Daytime intra urban air temperature differences

Influence of sky temperature distribution on sky view factor and its applications in urban heat island	The proposed effective sky view factor is sensitive to the sky temperature distribution and cloud cover fraction.	Shanyou Zhu, H. Guan, J. Bennett, R. Clay, C. Ewenz, S. Benger, A. Maghrabi, A. Millington	2013	<ul style="list-style-type: none"> •Sky View Factor •Effective SVF •Urban Heat Island Intensity Variance
Mitigating urban heat island effects in high-density cities based on sky view factor and urban morphological understanding: a study of Hong Kong	Urban planners could efficiently boost sky view factor to decrease urban heat island effect (UHI) in high-density urban settings without sacrificing the land's development efficacy by carefully managing the site coverage ratio and building height.	C. Yuan, Liang Chen	2011	<ul style="list-style-type: none"> •Sky View Factor (SVF) •Urban Heat Island (UHI) •Air Temperature •Site Coverage Ratio •Building Height
Sky view factor calculations and its application in urban heat island studies	At scales smaller than 100 metres, the sky view factor is crucial to understanding urban climatology.	M. Dirksen, Reinder Ronda, N. E. Theeuwes, G. A. Pagani	2019	<ul style="list-style-type: none"> •Sky View Factor (SVF) •Diurnal Maximum Urban Heat Island (UHI)
Urban heat island analysis of Greater Manchester, UK using sky view factor analysis	Sky view factors can be computed by the analysis of images captured with a fisheye lens on a camera.	Hkw Cheung, D. Coles, GJ Levermore	2016	<ul style="list-style-type: none"> •Sky View Factor Values •Urban Heat Island Intensities
Sky view factor and sunshine factor of urban geometry for urban heat island and	Indicators of the intensity of the urban heat island are the sky view factor and	Kwan-ho Lee, G. Levermore	2018	<ul style="list-style-type: none"> •Sky View Factor (SVF) •Sunshine Factor (SF)

renewable energy	sunshine factor of urban geometry.			
Assessing the relationship between sky view factor and land surface temperature to the spatial resolution	A trustworthy study requires a digital database that can accurately depict urban elements at an appropriate spatial scale.	M. Scarano, F. Mancini	2017	<ul style="list-style-type: none"> •Land Surface Temperature (LST) •Sky View Factor (SVF)
Quantification of the effect of thermal indices and sky view factor on park attendance	The lower the area-averaged sky view factor, the higher the park utilization.	Tzu Ping Lin, Kang-Ting Tsai, Ruey Lung Hwang, Andreas Matzarakis	2012	<ul style="list-style-type: none"> •Number Of People Visiting an Outdoor Space •Park Utilization
The role of sky view factor and urban street greenery in human thermal comfort and heat stress in a desert climate	The effect of the Sky View Factor on the E-W streets was more significant than in N-S streets.	Armaghan Ahmadi Venhari, Martin Tenpierik, Mohammad Taleghani	2019	<ul style="list-style-type: none"> •Physiological Equivalent Temperature (PET) Values •Meteorological Parameters
Evaluating The Effects of High rise building On Urban Heat Island by Sky View Factor: A case study of Narmak neighborhood, Tehran	The intensity of heat island impacts in the study area will decrease in the detailed plan scenario.	H. R. Rad, Mojtaba Rafieiana	2015	<ul style="list-style-type: none"> •Sky View Factor (SVF)
Effects of Foliage and Sky View Factor on the Urban Thermal Environment	0.27-0.35 foliage view factor = 8.2-9.0°C PET difference.	Atsushi Toriyama, N. Monji, Y. Aono, K. Hamotani	2001	<ul style="list-style-type: none"> •Mean Radiation Temperature (MRT) •Physiologically Equivalent Temperature (PET)

Influence of sky view factor on outdoor thermal environment and physiological equivalent temperature	The extent of shading contributes to variations in thermal perception distribution.	Xiaodong He, Shiguang Miao, Shuanghe Shen, Ju Li, Benzhi Zhang, Ziyue Zhang, Xiujie Chen	2014	<ul style="list-style-type: none"> •Outdoor Thermal Conditions •Physiological Equivalent Temperature (Pet) •Thermal Perception Distribution •Hot Discomfort in Summer •Cold Discomfort in Winter •Comfort Periods in Outdoor Spaces
A New Technique for Predicting the Sky-View Factor for Urban Heat Island Assessment	A geometric parameter is the best predictor of sky-view factor.	R. Shaker, T. Drezner	2010	<ul style="list-style-type: none"> •Sky View Factor (SVF)
Effect of Sky View Factor on Outdoor Temperature and Comfort in Montreal	A low sky view factor could mitigate the urban heat island effect by decreasing urban temperatures and increasing outdoor thermal comfort in urban areas.	WangYupeng, AkbariHashem	2014	<ul style="list-style-type: none"> •Air Temperature (Ta) •Mean Radiant Temperature (MRT) •Human Weighted Mean Radiant Temperature
The impact of sky view factor on thermal environments in urban parks in a subtropical coastal city of Australia	The sky view factor has positive impacts on both park cooling intensity and mean radiant temperature in parks in subtropical coastal cities.	Jian Zhang, Zhonghua Gou, Yi Lu, Pingying Lin	2019	<ul style="list-style-type: none"> •Cooling Intensity (Temperature Difference Between Measured Parks and a Nearby Weather Station) •Mean Radiant Temperature (MRT, a Thermal Comfort

				Index Considering Objects Surrounding the Body)
Analysis of the urban surface thermal condition based on sky-view factor and vegetation cover	Areas with high sensible heat and land surface temperature had higher sky-view factor and less vegetation.	Mojolaoluwa Toluwalase Daramola, Ifeoluwa A. Balogun	2019	<ul style="list-style-type: none"> •Surface Heat Flux •Land Surface Temperature
Correlating the Sky View Factor with the Pedestrian Thermal Environment in a Hot Arid University Campus Plaza	The Sky View Factor had a significant direct impact on mean radiant temperature, PET, and UTCI in summer.	Randa Osama Shata, A. Mahmoud, M. Fahmy	2021	<ul style="list-style-type: none"> •Mean Radiant Temperature •Physiological Equivalent Temperature (PET) •Universal Thermal Comfort Index •Microclimatic Variables •Meteorological Parameters
Cooling the cities – A review of reflective and green roof mitigation technologies to fight heat island and improve comfort in urban environments	Cool roofs may reduce the average ambient temperature between 0.3 and 3 K.	M. Santamouris	2014	<ul style="list-style-type: none"> •Average Ambient Temperature •Peak Ambient Temperature
The Effect of Sky View Factor on Air temperature in High-rise Urban Residential Environments	The Sky View Factor may often be a desirable criterion in densely populated areas.	Golnar Baghaeipour, N. Nasrollahi	2019	<ul style="list-style-type: none"> •Sky View Factor •Air Temperature

A Graphical Method for the Sky View Factor Calculation in the Urban Heat Island Studies	The local sky view factor is important for understanding the temperature dynamics on urban sites.	I. G. Santos, Henrique Gazzola de Lima	2003	<ul style="list-style-type: none"> •Sky View Factor •Temperature Change Inside City Structures •Local Capacity of The Urban Fabric in Losing Heat by Radiation Exchange to The Sky at Night •Temperature Dynamics on The Urban Sites
Urban design factors influencing heat island intensity in high-rise high-density environments of Hong Kong	Key factors for reducing urban heat island effect include sky view, surface albedo, altitude, vegetation above 1m, building height ratio, location quotient, and proximity to the sea.	R. Giridharan, Stephen S.Y. Lau, S. Ganesan, Baruch Givoni	2007	<ul style="list-style-type: none"> •Urban Heat Island Intensity
Effects of urban morphology on shading for pedestrians: sky view factor (SVF) as an indicator of solar access	In urban morphology, the sky view factor may serve as a solar access indicator.	Badia Masoud, Isabel Crespo Cabillo, Helena Coch Roura, B. Beckers	2019	<ul style="list-style-type: none"> •Sky View Factor •Direct Solar Radiation
Sky view factor calculations and its application in urban heat island studies	At scales smaller than 100 m, the sky view factor is crucial to understanding urban climatology.	M. Dirksena, R. J. Rondab, N. E. Theeuwesc, G. A. Pagania		<ul style="list-style-type: none"> •Sky View Factor •Diurnal Maximum Urban Heat Island

Cool surfaces and shade trees to reduce energy use and improve air quality in urban areas	Hot cities use more energy and create more smog.	Hashem Akbari, Melvin Pomerantz, Haider Taha	2001	<ul style="list-style-type: none"> •Urban Temperatures •Electricity Demand •Smog Formation •National Energy Use in Air Conditioning •Energy Use Cost Savings •Urban Air Quality
The city and urban heat islands: A review of strategies to mitigate adverse effects	Sun and city activities raise temperatures in cities.	Eulalia Jadraque Gago, J. Roldan, Rosalía Pacheco-Torres, Javier Ordóñez	2013	<ul style="list-style-type: none"> •City Temperatures •Energy Consumption •Co2 Emissions into The Atmosphere
The necessity of using Sky View Factor in urban planning: A case study of Narmak neighborhood, Tehran	Sky view factor drops to 0.08-0.69 in detailed plan.	M. Rafieian, H. R. Rad, Ayyoob Sharifi	2014	<ul style="list-style-type: none"> •Sky View Factor
Simulation of surface urban heat islands under 'ideal' conditions at night part 2: Diagnosis of causation	The effects of the urban greenhouse and surface emissivity are relatively minor causes of urban heat islands.	Timothy R. Oke, G. T. Johnson, Douw G. Steyn, I. D. Watson	1991	<ul style="list-style-type: none"> •Thermal Regime of Urban and Rural Surfaces •Heat Storage Release •Street shape affects radiation. •Impact of Thermal Properties on Heat Storage Release. •Effects Of the Urban 'Greenhouse' •Surface Emissivity

Daytime urban heat island effect in high-rise and high-density residential developments in Hong Kong	The urban heat island effect is in the order of 1.5 °C within an estate.	R. Giridharan, S. Ganesan, Stephen Siu Yu Lau	2004	<ul style="list-style-type: none"> •Outdoor Micro Level Daytime Heat Island Effect •Energy Efficient Designs •Surface Albedo •Sky View Factor •Height-to-Floor Ratio for Buildings. •Cross Ventilation
Observations of the Urban Heat Island Effect in New York City	Urban heat island intensity is highest near the surface but drops to zero at 300m during strong urban elevated inversion layers in the morning.	R. Bornstein	1968	<ul style="list-style-type: none"> •Atmospheric temperature in lowest 700m. •Urban Surface Temperature Inversions •Elevated Inversion Layers •City heat island (city temperature excess). •Rural Temperatures
The Effect of Sky View Factor on the Thermic Ambiances: Case of Batna City	The sky view factor and the H/L ratio are among the elements that influence most of the urban ambiances during the period of thermal stress.	Chetara Aicha, Benabbas Moussadek, Djaghroui Djamila	2022	<ul style="list-style-type: none"> •Air Temperature. •Relative Humidity. •Wind Velocity. •Outdoor Thermal Comfort Rating Using the Pmv Thermal Index (Predicted Mean Vote)
How factors of land use/land cover, building configuration, and adjacent heat sources	Impervious surface and tree canopy percentages explain 68% of extreme heat	Paul Coseo, Larissa Larsen	2014	<ul style="list-style-type: none"> •Air Temperature

and sinks explain Urban Heat Islands in Chicago	event air temperature variation at 2 a.m.			
Application of high-resolution thermal infrared remote sensing and GIS to assess the urban heat island effect	The thermal signatures of urban land cover types between day and night were selected for use in this analysis.	C. Lo, D. Quattrochi, J. Luvall	1997	<ul style="list-style-type: none"> •Thermal changes in urban land cover types day/night. •Land cover irradiance affects vegetation amount. •Normalized Difference Vegetation Index •Mean Radiance Values •Standard Deviations
Satellite-derived urban heat islands from three coastal cities and the utilization of such data in urban climatology	Heat island intensities are largest in the daytime and in the warm season.	M. Roth, T. Oke, W. Emery	1989	<ul style="list-style-type: none"> •Surface Radiant Temperature Heat Islands •Heat Island Intensities •Day Time Intra Urban Thermal Patterns •Nocturnal Heat Island Intensities •Correlation Of the Surface Radiant Temperature Distribution with Land Use
Sky view factors estimation using a 3d-gis extension	The less visibility a surface has to the sky, the slower its cooling	L. Souza, D. Rodrigues, J. Mendes	2003	<ul style="list-style-type: none"> •Sky View Factor

	ability.			
Canyon geometry, street temperatures and urban heat island in malmö, sweden	Street layout and distribution impact city's surface temperature pattern, known as 'heat island'.	L. Barring, J. Mattsson, S. Lindqvist	1985	<ul style="list-style-type: none"> •Street Surface Temperature Pattern of The City •Surface Heat Island
Urban heat island development affected by urban surface factors	The mean maximum urban heat island intensity reaches more than 2.6°C in the city centre.	J. Unger, Z. Bottyán, Z. Sümeghy, Á. Gulyás	2000	<ul style="list-style-type: none"> •Spatial Distribution Of Mean Maximum Urban Heat Island Intensity. •Effects Of Urban Surface Parameters on the UHI.
Calculation of Ground View Factor as an Index for Urban Thermal Environment Optimization	More site information may be described by the percentage of the ground that is visible from a certain point.	Zaoshi Jiang, Wei You, Wowo Ding	2017	<ul style="list-style-type: none"> •Ground View Factor •Sky View Factor
Sky-View Factor Estimation: A Case Study of Athens, Georgia	In Athens, Georgia, the residential and downtown areas nearest the urban core had the lowest sky-view factor values.	Neil Debbage	2013	<ul style="list-style-type: none"> •Sky View Factor Values
Urban heat islands and landscape heterogeneity: linking spatiotemporal variations in surface temperatures to land-cover and socioeconomic patterns	The urban core was generally warmer than the rest of the area.	Alexander Buyantuyev, Jianguo Wu	2009	<ul style="list-style-type: none"> •Surface Urban Heat Island Characteristics •Spatio-temporal Variation of Surface Temperatures

The Influence of Height/width Ratio on Urban Heat Island in Hot-arid Climates	The intensity of the Urban Heat Island phenomenon increases with the decrease of H/W ratio.	Mohammed A. Bakarman, Jae D. Chang	2015	<ul style="list-style-type: none"> •Ambient Air Temperatures Inside The Canyon •Ambient Air Temperatures At The Roof Level •Surface Temperature Of Walls •Surface Temperature Of Roofs •Surface Temperature Of Streets
Urban heat island intensity in London: An investigation of the impact of physical characteristics on changes in outdoor air temperature during summer	The most significant meteorological factors and geographic features that impact variations in the outside air temperature in London are partly cloudy days and metropolitan regions, respectively.	Maria Kolokotroni, R. Giridharan	2008	•Changes In Outdoor Air Temperature
Quantifying the influence of land-use and surface characteristics on spatial variability in the urban heat island	It was discovered that weekdays had warmer air than weekend air above important thoroughfares.	Melissa Hart, David J. Sailor	2009	•Summertime ~2 M Air Temperature
The influence of land use on the urban heat island in Singapore	The land usage will influence urban temperature in	Steve Kardinal Jusuf, Nyuk Hien Wong,	2007	<ul style="list-style-type: none"> •Ambient Temperature •Surface

	Singapore.	Emlyn Hagen, Roni Anggoro, Yan Hong		Temperature
Urban heat island and wind flow characteristics of a tropical city	The most effective geometry for urban geometry modifications was step up configuration.	Priyadarsini Rajagopalan, Kee Chuan Lim, Elmira Jamei	2014	<ul style="list-style-type: none"> •Heat Island Intensity •Wind Flow Characteristics
Analysis of the urban heat island effects on building energy consumption	We assess and talk about how UHI mitigation techniques affect the energy requirements of buildings.	Susanna Magli, Chiara Lodi, Luca Lombroso, Alberto Muscio, Sergio Teggi	2015	<ul style="list-style-type: none"> •Heating Energy Needs of An Existing University Building •Cooling Energy Needs of An Existing University Building
Urban heat island: Aerodynamics or imperviousness?	City heat is stronger where urban areas don't cool down well.	Dan Li, Weilin Liao, A. Rigden, Xiaoping Liu, Dagang Wang, S. Malyshev, E. Shevliakova	2019	<ul style="list-style-type: none"> •Daytime Urban Heat Islands (Uhis) •Spatial Variability of Daytime Uhi Intensity •The efficiency with which heat is convected from the surface of the land to the lower atmosphere in urban and rural areas •Capacity Of Urban And Rural Areas To Evaporate Water
Energy Saving Potentials and Air Quality Benefits of Urban Heat Island Mitigation	The cooling energy savings in the U.S. from cool surfaces and shade trees are estimated to be \$5	H. Akbari	2005	<ul style="list-style-type: none"> •Urban Air Temperature •Urban Peak Electric Demand For a/C Use •Population

	billion per year.			Weighted Smog Concentrations In Urban Areas •Cooling Energy Cost Savings
Influences of urban spatial form on urban heat island effects at the community level in China	High land surface temperature values were concentrated in central and eastern areas of Ganjingzi District, Dalian.	Andong Guo, Jun Yang, Xiangming Xiao, Jianhong Xia (Cecilia), Cui Jin, Xueming Li	2020	•Land Surface Temperature
Is everyone hot in the city? Spatial pattern of land surface temperatures, land cover and neighborhood socioeconomic characteristics in Baltimore, MD.	Block groups with high rates of poverty, poor income, low levels of education, a higher proportion of senior residents, more members of racial or ethnic minorities, and a higher risk of crime had statistically higher land surface temperatures.	Ganlin Huang, Weiqi Zhou, M L Cadenasso	2011	•Land Surface Temperature
Urban heat island	The symptoms of diurnal heating begin to appear by mid-morning in summer.	Hongsuk H. Kim	1992	•Urban Heating •Heat From Urban Surfaces •Temperature
Effects of vegetation, urban density, building height, and atmospheric conditions on local temperatures and thermal comfort	Ground and roof-mounted vegetation reduces the demand for air conditioning indoors, moderates summer temperatures, and enhances outdoor	Katia Perini, Adriano Magliocco	2014	•Potential Temperature •Mean Radiant Temperature •Predicted Mean Vote

	comfort.			
Assessment of the urban heat island effect through the use of satellite data	Research on the correlation between air temperature and remotely sensed surface temperature will be necessary for a comprehensive understanding of the elevated urban surface temperature.	J. C. Price	1979	<ul style="list-style-type: none"> •Urban Surface Heating Extent •Urban Surface Heating Intensity
Interaction of Urban Heat Island Effects and Land–Sea Breezes during a New York City Heat Event	Comparing the most advanced urban parameterization scheme with surface observation data shows which one is the most accurate.	T. Bauer	2020	<ul style="list-style-type: none"> •Urban Surface Air Temperatures •Rural Temperatures •Daytime Skin Temperatures
A review of studies involving the effect of land cover and land use on the urban heat island phenomenon, assessed by means of the MUKLIMO model	When there are more urban green spaces and fewer impermeable surfaces across all land cover and land use classes, the urban heat island effect is reduced.	J. Feranec, M. Kopecká, Daniel Szatmári, Juraj Holec, P. Šťastný, R. Pazúr, Hana Bobálová	2019	<ul style="list-style-type: none"> •Temperature Of Air •Temperature Of Ground Surface •Thermal And Other Climatic Characteristics

2.8 Research Gap

The LCZ concept must be used to urban climate research in order to examine how urban morphology factors—primarily the Sky View Factor—affect surface urban heat island studies in the global south.

Kolkata, being a metropolitan city, and urbanizing very rapidly is witnessing a major change in warming conditions. Research on comparative analysis is required to determine the relationship between the sky view factor, the urban heat island effect and the different local climate zone in Kolkata with regard to the surrounding climate zones.

2.9 Chapter summary

The concept of local climate zone (Bechtel et al. 2015) was created to precisely quantify the relationship between urban morphology and the UHI phenomena because the conventional approach merely employs "rural" and "urban" to define UHI with little regard to the diversity of the urban morphology. Researchers mostly concentrate on two facets of studies concerning the LCZ system (Shi et al., 2019). The first is the LCZ mapping research for one city or a study region, which uses satellite images or GIS techniques to form LCZ as a clear way to visualize urban morphology (Danylo et al., 2016; Geletič & Lehnert, 2016; Verdonck et al., 2017; Zheng et al., 2018). The second is LCZs' thermal characteristics. Using screen-height temperature recorded by sensors placed in various LCZs, Stewart et al., Cardoso and Amorim, and Yang et al. analysed the heat island magnitude ($\Delta\text{TLCZ XY}$) as an example of the second approach. Leconte et al., Kotharkar and Bagade, and Alexander and Mills compared the air temperature change in LCZs using mobile measurements. LCZ is recognized as a good option for UHI study due to its clear delineation of the urban landscape and classification hierarchy (Shi et al., 2019). Furthermore, one of the frequent UHI research is SUHI, and the LCZ is a reasonable method for differentiating LST from SUHI at the local scale. For instance, Bechtel et al. investigated the differences in the thermal environments of LCZs in one or more cities using LST derived from remote sensor photos. The LCZ has been utilised in another study to quantify SUHI. Nevertheless, the bulk of the previously stated studies focused on the degree of urban heat island effect (SUHI) and the thermal efficiency of low-lying areas (LCZs); only a small number of them addressed the essential components of urban design that influence SUHI in various LCZs.

The urban design elements that affect UHI, such as canyon radiative geometry, the thermal qualities of a building's material, anthropogenic heat emission, and turbulent transmission, have been reviewed by Oke et al., and Santamouris. The quantity of vegetation and people were identified as factors that affected the creation of SUHI. Only a small percentage of them, though, were using the LCZ method. According to Nassar et al. (2016), the height of roughness elements, building height variations, sky view factor, and proximity to the ocean were the main factors influencing the zonal SUHI. Accompanied by numerous limitations on sample size and spatial resolution. Because LST and many urban design elements can now be quickly and simply recovered using GIS and remotely sensed retrieval algorithms, the regression models of SUHI could address these limitations.

There are few studies using the LCZ paradigm to examine how urban design variables affect SUHI. The goal of this study is to use a large sample of LCZs, a remotely sensed retrieval method, and GIS tools to discover the important urban design aspects that affect the SUHI intensity in Kolkata, a high-density metropolis.

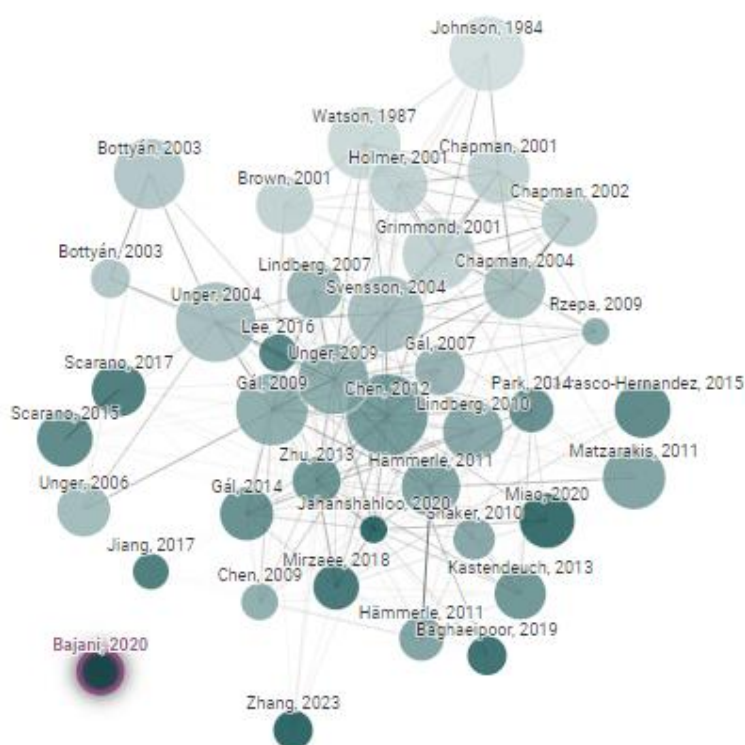


Figure 2.7 Connections between research on Urban Heat Island mitigation (1984 - 2023)
(Source: <https://www.connectedpapers.com/>)

In Figure 2.7, a detailed visualization illustrates the intricate connections found within the research papers pertaining to the urban heat island phenomenon. The analysis delves into the relationships established within the field, shedding light on the various interconnections and influences on UHI prediction models. Specifically, a novel UHI prediction model tailored for different Local Climate Zones (LCZs) in Kolkata has been proposed, highlighting the significance of considering the city's specific characteristics. This model integrates key factors such as Sky View Factor (SVF), which plays a crucial role in understanding and predicting urban heat island intensities across different urban contexts. The proposed model not only offers insights into the urban temperature dynamics but also showcases the importance of accounting for variations in land use and land cover within the city. By bridging the gap between theoretical frameworks and practical applications, this research contributes valuable knowledge to the field of urban climate studies, offering a comprehensive approach to assessing and mitigating urban heat island effects.

Furthermore, LCZs and SUHI prediction models were suggested for Kolkata, a high-density city. The current study's conclusions could be helpful for urban designs and regeneration in high-density cities because it would provide a mechanism for effectively gathering information regarding SUHI at the local scale and the corresponding urban design elements in cities in the significantly urbanized zones. The sky view aspect is not sufficiently addressed in the Southeast Asian context. There are few works of literature from temperate climates. Many researchers used land use and land cover mapping methods to categorize urban areas, but categorization based on local climate zone is a widely used concept in urban climate studies.

Chapter 3. MATERIALS AND METHODS

3.1 Introduction

The Methodology chapter serves as the cornerstone of any rigorous academic research, providing a comprehensive outline of the strategies and procedures adopted to address the research objectives and answer the research questions. This chapter delves into the systematic and organized approach used to design, conduct, and analyze the study, ensuring the reliability and validity of the findings. By outlining the research methods, data collection techniques, and analytical tools, the Methodology chapter establishes the credibility and robustness of the research outcomes, paving the way for valuable contributions to the existing body of knowledge.

The thesis explores the relationship between SVF and UHI in different local climate zones and attempts to delve into its intricacies to gain a deeper understanding of its complexities. The Methodology chapter plays a fundamental role in guiding the investigation and aligning it with the research objectives. It acts as a blueprint that facilitates a clear and logical progression of the research process, enabling the reader to grasp the researcher's decision-making rationale.

The structure of this chapter is designed to present a comprehensive and transparent account of the research design, encompassing the overall research approach, the rationale behind the chosen methodology, data collection techniques, data analysis procedures, and any ethical considerations involved in the research process. By meticulously documenting each step taken, we aim to enhance the reproducibility and transparency of the study, ultimately contributing to the overall credibility and reliability of the research.

Furthermore, this chapter acknowledges the existence of various research paradigms and philosophies, emphasizing the appropriateness and alignment of the selected

methodology with the nature of the research question and its objectives. The chapter also acknowledges potential limitations and discusses strategies employed to mitigate them, ensuring that the study's outcomes remain grounded and defensible.

The Methodology chapter acts as a bridge between the theoretical framework and the empirical investigation, translating abstract concepts and hypotheses into tangible actions and measurable data. Through careful planning and execution, this research seeks to yield insights that are both valid and generalizable, thus contributing to the advancement of knowledge in the field.

In summary, this chapter not only showcases the rigor of the research but also highlights the researcher's ability to make well-informed decisions that have direct implications for the study's outcomes. It is an invitation for the reader to journey alongside the researcher in understanding the intricacies of the research process and appreciating the significance of the findings that lie ahead.

In the subsequent sections, we will provide a detailed account of the research design, elucidate the data collection methods utilized, elucidate the analytical techniques applied, and discuss any ethical considerations. Through this, we aim to offer transparency and clarity that will enable readers and future researchers to build upon this study's foundations and expand the frontiers of knowledge in this domain.

The results of several studies have varied in their strengths. Therefore, it is crucial to combine different approaches in order to generate knowledge that is more insightful and thorough than what would be produced by each approach alone (Denzin & Lincoln, 2005; Morgan, 1998). The combination of methods and the inclusion of data from multiple sources of evidence increase the validity of a study. This research methodology implementation framework's goal is to illustrate the connections between Kolkata's SVF, UHI, and LCZs. The strategies discussed here complement the methodological framework created in the beginning chapter of this work.

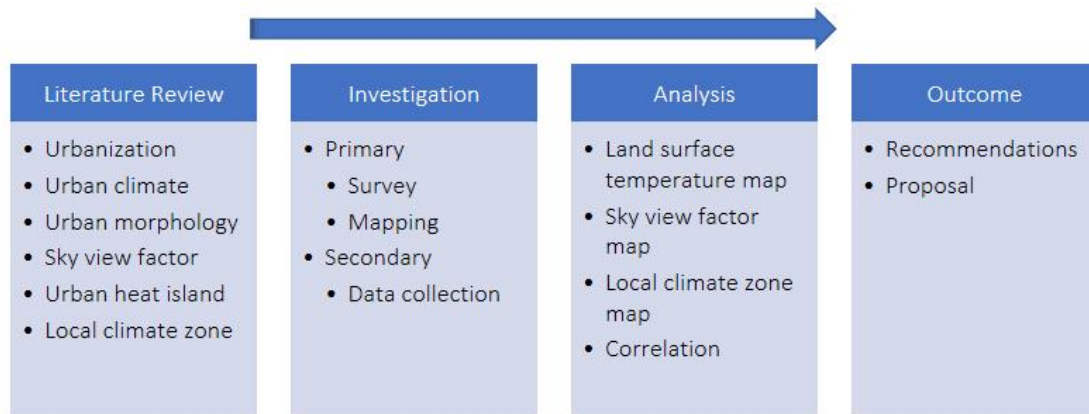


Figure 3.1. Analytical framework showing the workflow approaches used in analyzing correlation between SVF, UHI, and LCZs (Source: Author)

3.2 Research Design Process

This research technique design makes use of a variety of approaches. This chapter's goal is to construct the research approach methodology using a variety of research approaches. In-depth explanations of the research's overall structure and the data collection techniques are provided in this part. There are three primary sections to it. The thesis design is highlighted in the first section. The second section talks about how to acquire data in both qualitative and quantitative ways. The overall research framework is illustrated in the final section. This section's goal is to describe the methodology used throughout the study periods.

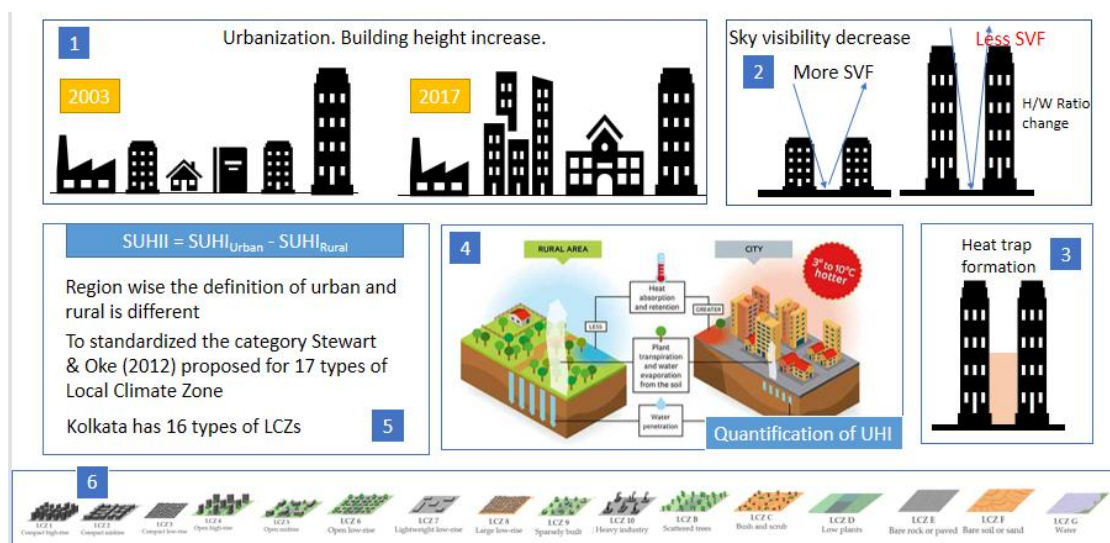


Figure 3.2. Schematic layout of research process. (1) Building density and height increase with time. (2) Sky visibility decreases with the increase of building limits. (3) Heat trap

formation. (4) Temperature difference between rural and urban. (5) Surface urban heat island index requirement. (6) Local climate zones of Kolkata. (Source: Author)

Figure 3.2 shows the thesis's conceptual organization. The built form changes in the first layout throughout time. The second arrangement shows how the sky view factor decreases as building height rises. The heat is focused between the building canyons, according to the third pattern. The surface temperature differences between rural and urban areas are described in the fourth arrangement. The fifth arrangement shows the concept of the surface urban heat island, while the sixth pattern displays the regional climate zones.

Table 3.1. Dataset and software details

	Software/Material Used	Input Data	output data format	Data Source/Collection
SVF	DSLR with Fisheye lens			Institutional Survey
	Sky View Factor Calculator	Fisheye lens photo	Vector	Institutional Survey
	SVF Mapping Tool V1.1	Building footprint	Vector	Institutional Survey
	Python Script	DSM	Raster	Download SRTM DEM and Institutional Survey
	Urban Multi-scale Environmental Predictor (UMEP) Tool	DSM	Raster	Download SRTM DEM and Institutional Survey
UHI	ArcGIS Pro	Landsat 8 Image	Raster	Download from USGS website
LCZ	Google Earth			
	SAGA GIS	Landsat 8 Image and signature file	Raster	Institutional Survey and Download from USGS website

Table 3.1 showing the data set and instruments used during the research work. Sky view factor is calculated in four different ways. Sky view factor calculator software is used to calculate SVF using Fisheye lens. Apart from photographic method, RS & GIS method is used to calculate Sky view factor. SVF mapping tool V1.1 uses vector building footprint data set in shape file format to calculate SVF on a point location. Multiple point shape file is supported by this software. Urban multi scale environmental predictor tool uses DSM to extract continuous SVF value. Aside from this Python script is used to extract SVF using DSM. The python-based output is a continuous map. Building footprints were digitized using google earth pro and building elevations were surveyed using laser height meter. SRTM DEM data was downloaded and used as input of DSM along with building footprints. Using AcrGIS Pro, urban heat islands are extracted. Landsat imageries were processed to separate heat islands. Local Climate Zones are divided into groups using the approach provided by UMEP. To define signatures for this, Google Earth Pro software is used. Then, SAGA GIS software was used to import all of those signatures, and Landsat 8 imagery was used to categorize the imagery. A ground survey was done to verify the signatures.

3.3 Urban Heat Island Estimation

The study of urban heat islands (UHI) is regarded as a crucial component of urban climate research. Urban shape and function frequently alter the urban atmosphere and raise the surrounding area's ambient temperature (T. R. Oke, 2006). Shortwave solar radiation and long-wave terrestrial heat are trapped, resulting in the storage of greater sensible heat in urban canyons and interior environments, which causes the UHI phenomenon (Memon et al., 2009; T. R. Oke, 1982). However, the intensity of UHI grows due to the declining rate of evapotranspiration potential caused by a lack of vegetation and urban water bodies (Lee & Levermore, 2019). The net difference in land surface temperature (LST) between urban and suburban areas is known as the Surface Urban Heat Island (SUHI), and it may be detected remotely using a sensor that uses the thermal infrared part of the electromagnetic spectrum.

It is referred to as a non-atmospheric urban heat island and describes the urban surfaces' comparatively greater temperature compared to rural areas. In SUHI, there are some locations that are noticeably hotter than the nearby heated urban surfaces. These locations could be considered urban hot spots. These are very significant locations that release an excessive amount of terrestrial thermal radiation into the lower atmosphere, raising the temperature of the surrounding air. Identification of these heat islands is therefore a crucial factor to take into account in micro-climatic research. These thermal hot-spots, which are the primary sources of terrestrial heat emission in urban areas, are referred to as Urban Thermal Potential (UTP) zones and are an essential component of the creation of an urban climate map (UCMap) for the purpose of spatial city planning. Different materials make up the earth's surface, which complicates efforts to estimate land surface temperatures (Qin & Karnieli, 1999). Land Surface Temperature (LST) is one of the most significant variables in the physical processes of surface energy and water balance at all scales, and LST contributes to UHI, according to Brunzell & Gillies (2003) and Kustas & Anderson (2009). Surface Urban Heat Island (SUHI) is taken into consideration for the study since it has the most direct impact on city climate and human health.

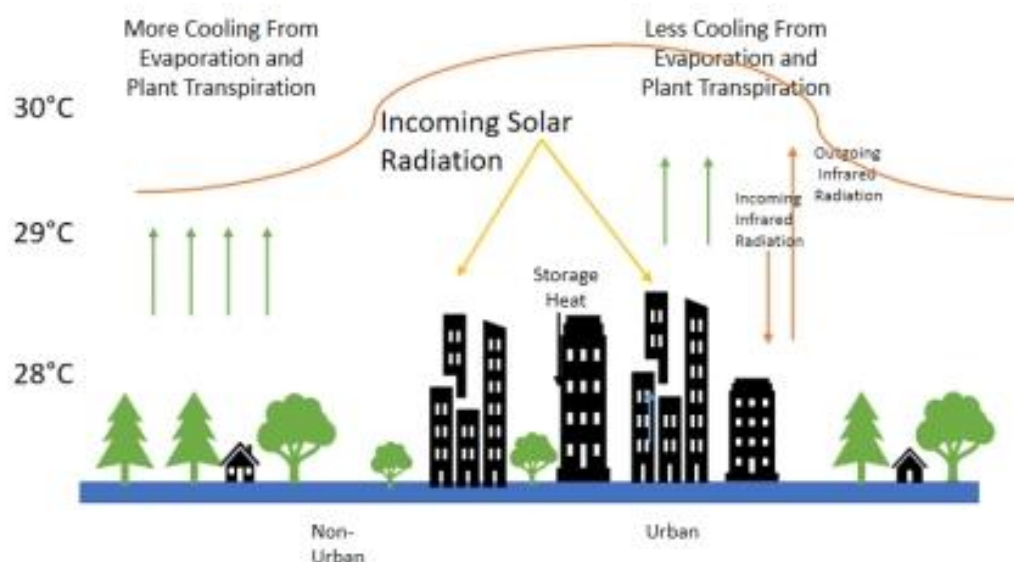


Figure 3.3. Schematic diagram of urban heat island. (Source: Author)

3.3.1 Workflow of Urban Heat Island extraction using Landsat images

The flowchart for the research process is shown in Figure 3.4. Two steps in the analysis procedure are the UHI estimation using the thermal infrared sensor and operational land image band coefficients extracted from the metadata file. Images were processed, and data was analyzed, using Esri® ArcGIS Pro software. The United States Geological Survey (USGS) made the Landsat data and a step-by-step explanation of how UHI was calculated available.

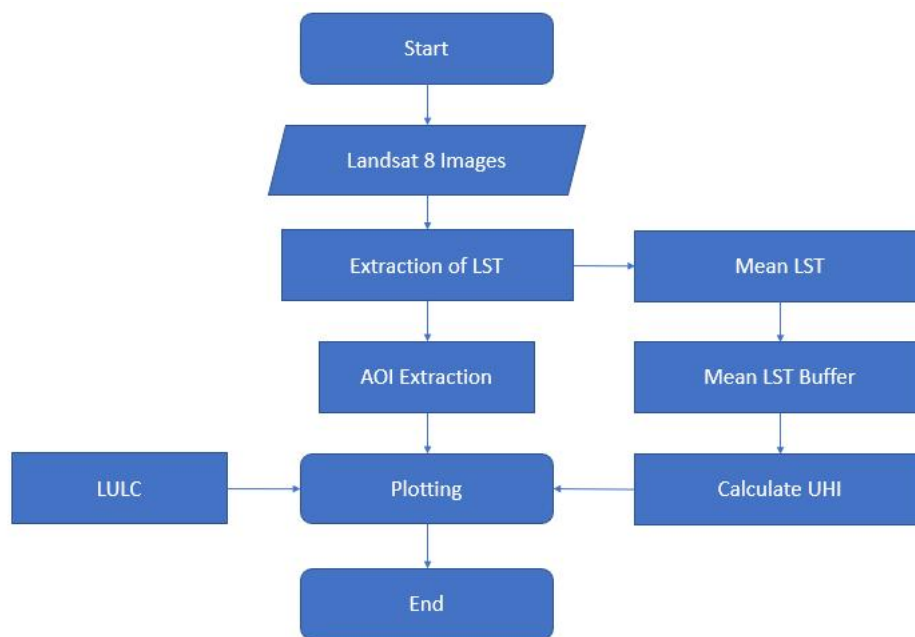


Figure 3.4. Details Workflow of UHI Calculation. (Source: Author)

a) Retrieving Top-Of-Atmosphere (TOA)

Using the radiance rescaling coefficients provided for each band in the metadata file, the Landsat thermal band/s data are transformed to TOA ($L\lambda$) spectral radiance. The algorithm is as follows:

$$L\lambda = MLQ_{cal} + AL$$

ML = Band specific multiplicative re-scaling factor

Q_{cal} = Band

AL = Band specific additive re-scaling factor

b) TOA to Brightness Temperature conversion

The principle behind thermal remote sensing is the existence of a strong positive correlation between the radiant flux amounts emitted by an object and its actual kinetic temperature. As a result, the radiant temperature of an item can be easily determined using radiometers that are located far away. The algorithm to convert TOA to Brightness Temperature (BT) is as follows:

$$BT = (K2 / (\ln (K1 / L \lambda) + 1)) - 273.15$$

K1 = Band-specific thermal conversion is constant from the metadata (K1_CONSTANT_BAND_x, where x is the thermal band number).

K2 = Band-specific thermal conversion is constant from the metadata (K2_CONSTANT_BAND_x, where x is the thermal band number).

c) Calculate the NDVI

NDVI calculation is important to find out the Proportion of Vegetation (P_v), which is highly related to the NDVI, and emissivity (ε). The algorithm to calculate NDVI is as follows:

$$NDVI = (Band\ 5 - Band\ 4) / (Band\ 5 + Band\ 4)$$

d) Determine the proportion of vegetation (P_v)

P_v is defined as the proportion of the total vegetation area to the vertical projection area of vegetation (which includes leaves, stalks, and branches) on the ground (Neinavaz et al., 2020). The proportion of vegetation is important to identify the emissivity of bare soil and vegetation. The algorithm to calculate P_v is as follows:

$$P_v = ((NDVI - NDVI_{min}) / (NDVI_{max} - NDVI_{min}))^2$$

e) Land Surface Emissivity Calculation (LSE)

Accurate values of LST can depend on well-characterized land surface emissivity (Jimenez-Munoz et al., 2012), which is a variance of 0.01 units and denotes a temperature inaccuracy of 0.5K. Surface composition (chemical and physical) and surface roughness can both have an impact on spectral emissivity (Snyder et al., 1998). In these studies, the emissivity map was elaborated by using the NDVI thresholds method, which in turn reflects an eye-catching comparison to have a reference method that is mainly based on the TISI indices (Becker & Li, 1990).

The algorithm is,

$$\text{LSE (e)} = 0.004 * \text{Pv} + 0.986$$

Pv = Potential Vegetation

f) Calculate the Land Surface Temperature

To finish the operation, use the LST equation to get the surface temperature map.

The algorithm to calculate LST is as follows:

$$\text{LST} = \text{BT} / (1 + w * (\text{BT} / \text{P}) * \ln(e))$$

BT= Brightness Temperature.

w = wavelength of emitted radiance.

p = $h * c / s$ ($1.438 * 10^{-2}$ m K) [14380]

h = Planck's constant ($6.626 * 10^{-34}$ Js)

s = Boltzmann constant ($1.38 * 10^{-23}$ J/K)

c = Velocity of light ($2.998 * 10^8$ m/sl)

e = Emissivity

g) Identify Urban Heat Islands

The land surface temperature pattern shows the concentration of UHI above or below mean LST based on the diurnal LST distribution maps. Standard score or Z-score had been calculated and mapped to determine the anomaly in UHI distribution.

The peak thermal zone or urban heat islands were calculated from the Z-score map where the value of Z-score was equal to or greater than 1.5°C.

3.3.2 Dataset used to estimate Urban Heat Island of Kolkata

United States Geological Survey (USGS) archived Landsat TM and ETM+ images have been downloaded. Nearly all of the images had no noise. The details of the images used to estimate LST are as follows.

Table 3.2. Summary of Landsat TM and ETM+ data used to estimate LST

Scene Id	Sensor	Date of Acquisition (YYYY-MM-DD)	Path & Row	Used Bands	Spatial Resolution (m)
LT05_L1TP_138044_20031118_20161203_01_T1	TM	2003-11-18	138 & 044	TM (Band No. 6)	120m
LT05_L1TP_138044_20101105_20161012_01_T1	TM	2010-11-05	138 & 044	TM (Band No. 6)	120m
LC08_L1TP_138044_20201124_20171206_01_T1	TIRS	2020-11-24	138 & 044	TIRS (Band No. 10 and 11)	100m

The Landsat TM and ETM+ pictures underwent radiometric calibrations and atmospheric adjustments utilizing the image-based dark-object subtraction (DOS) technique. Cubic convolution (CC) resampling was employed together with geometric correction (Projection: UTM-45N, Datum & Ellipsoid: WGS 1984) for all the images. After resampling, the spatial resolution (pixel size) of every band—including the thermal band—was 30 meters, and the root mean square (RMSE) error was less than 1 pixel.

3.4 Sky View Factor Analysis

Urbanization results in a drastic shift in the land's cover (Stewart, 2011) . Urban growth speeds up development but destroys natural habitats, which causes higher temperatures than would otherwise occur. Open space has been diluted by a complex urban layout. From the surface, the sky became less and less visible. The sky view factor shows the proportion of the sky that can be seen from a particular location (Holmer et al., 2000) . SVF values, which represent blocked and open areas, are dimensionless and range from 0 to 1 (Oke, 1988) . Urban regions face unique challenges when it comes to climate change. The site surface temperature and radiation fluxes, which have an effect on thermal comfort, have been concerned by this study. Over the past few decades, various approaches of determining SVF have been researched. These works were centered on the creation of mathematical methods for SVF calculation employing geometric equations based on the height and width of the urban canyon. Sky view factor is a measurement of how much of the sky is obscured by the surroundings at a particular position. In this study, the SVF was calculated using photographic and Geographical Information System (GIS) tools, and the accuracy and relationships between the chosen methods were examined.

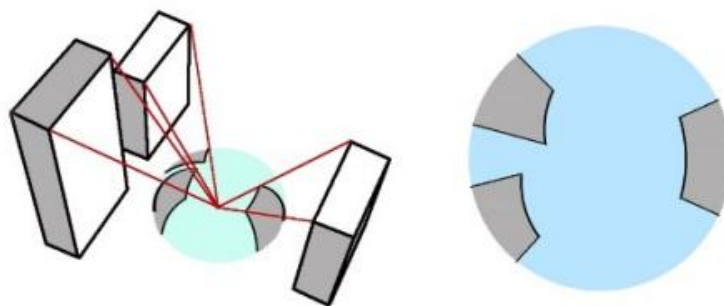


Figure 3.5. Illustration of SVF concept (Source: Author)

3.4.1 Methods to estimate Sky View Factor

There have been many methods developed to determine the sky view factor, each having advantages and disadvantages of its own, but ultimately no method can be deemed to be effective. SVF measurement and calculation in urban climate studies

has a long history (Johnson & Watson, 1984). Therefore, it continues to be regarded as extensive research in the subject of urban studies. The techniques can be divided into four groups: software methods, GPS methods, photographic approaches, and analytical models.

- Analytical Method
- Plane projection
- Random shadow casting
- Luminance simulation
- Photographic Method
- Fish-eye Photograph
- GPS Method
- Remote Sensing and GIS Techniques
- 3D Building Dataset
- SVF Mapping Tool V1.1
- SVF Calculator by UMEP
- Python Script

a) Analytical methods

Geometrical methods are another name for analytical techniques. SVF is calculated using a geometric and radiation exchange model of urban canyons. By examining the portion of the radiation flux exiting a surface element that is available and reaches the visible sky, Johnson & Watson (1984) determined the SVF for a general situation.

$$SVF = \frac{1}{\pi R^2} \int_{S_v} \cos \phi dS$$

Where,

S is the section representing the visible sky

ϕ is the angle from S to the zenith

R is the radius of the hemispheric radiating environment

The analytical methods offer a conceptual framework for determining SVF for a particular point in different urban structures. They are perfectly suited for depicting parametric analysis and algorithm testing.

b) Photographic methods

The hemispheric environment is projected onto a circular plane using site pictures taken with the use of a fish-eye lens. The photos are subjected to extra processing in order to define the skyline. The appropriate transformations are then used to establish the relationship between the obstructed and unblocked sections of the sky. Video pictures are used by Steyn et al., (1986) to analyze SVF. After being digitized, the video image is next inspected to distinguish between "sky" and "non-sky" pixels. The individual view factors for all "sky" pixels are added up to create a composite sky view factor for the image. Anderson (1964) was the first to take into account the view factor issue using a photographic computation to estimate sunshine distribution methods; nevertheless, the true importance of SVF in urban study was only discovered in the 1980s.

The photographic method, which can accommodate structures of all sizes and odd shapes, is particularly well suited for measuring SVF in real-world situations. In this scenario, it is possible to get precise SVF without risk of inaccuracy from alternative methodologies because the photos also contain information about the vegetation (Brown et al., 2001; T. GÁL, M. RZEPA, 2007). However, this method is typically time-consuming because it necessitates the development and processing of photographs. Furthermore, because this technique requires a consistently clouded sky and problems with image processing emerge from direct sunlight or various cloud kinds, there aren't many opportunities for surveys using this method (CHAPMAN & THORNES, 2003). Additionally, the spatial information for the analyzed points is either completely missing or needs to be kept in other databases. These limitations make photography technologies unsuitable for large-scale area investigation. The most common way to determine SVF is to capture a 180-degree fisheye picture. SVF can be calculated using digital models of the environment (Bruse & Fleer, 1998; Teller & Azar, 2001). This calculation takes into account each angle that makes up the

hemispheric environment, together with the corresponding azimuth angle and elevation angle β (relative to the generated shadow).

$$SVF=1-i\sum\sin^2i(ai360^\circ)$$

c) GPS Methods

Using real-time data input, the GPS methodology (Chapman et al., 2002) was employed to measure SVF; this is in contrast to the approaches discussed for photography, which rely mostly on direct SVF calculation. The bare minimum of satellite visibility information was acquired with a GPS receiver. A regression equation for the prediction of SVF was developed by taking into consideration the number of visible satellites, precision dilution, and satellite signal intensity (Zeng et al., 2010). The study demonstrated that the approach worked well in urban settings but was less explicative in suburban settings. When looking for signals in rural areas, a lot of noise can be produced. The variance in tree covering in these places is probably to blame for this. Chapman & Thornes (2004) improved the prototype method to obtain instant SVF calculation. For simultaneous but approximate SVF in real-time, the GPS has been separated from the fish-eye lens, which captures and processes on a common mobile platform. Using the total of signal-to-noise ratios, the number of visible satellites, and the number of monitored satellites, an artificial neural network was trained to predict SVF. At a processing rate of one second, the system could account for more than 69% of SVF changes in metropolitan environments.

The following are only a few benefits of using GPS techniques over traditional ones. The techniques still have limitations, though, which restrict the uses they may be put to. The approaches are inadequate for circumstances when precision is essential since they are inherently imprecise. Second, it is impossible to create a universal equation because the prediction equation is dependent on the GPS device being utilized. Third, the technique only functions well in cities.

d) Software Methods

The representation of urban geometry can now be done "virtually" because to developments in digital mapping and land surveying technology, as well as growing computer power. Software techniques include building databases, frequently using GIS to create 3-D models, and modelling the urban environment in the computer's memory. Applications are developed to simulate SVF in the rebuilt setting. Depending on the types of databases being used, there are two fundamental software method approaches: the raster method and the vector method.

The vector database compresses the buildings into flat-roofed blocks that are represented by polygons. A rotation angle uniformly divides the hemispheric radiating environment into slices. The strategy then seeks out the one structure that has the greatest elevation angle along a particular rotation angle. According to Oke (1987) analysis, the sky section blocked by this building is regarded as a slice of the basin. By combining the view factors for each basin slice in each direction, SVF can then be calculated (Gál & Unger, 2014). The accuracy of this method depends on the rotation angle and searching radius; a smaller rotation angle and a larger radius result in more accurate SVF estimates.

Another often used technique for figuring out SVF is raster-based. Surface topography and terrain data are often stored in raster format in a digital elevation model (DEM) database. A "shadow casting" approach developed by Ratti & Richens (1999) using high-resolution DEM data is used to calculate the shadow patterns of buildings. Further improvements have been made to this SVF computation technique, and Lindberg (2007) has verified that it produces results that are satisfactory. Compared to the raster-based approach, the vector approach requires a lot more time (Hämmerle et al., 2011b). The resolution of the database affects how long the procedure takes; higher resolution results in more accurate output. The software methods' ability to generate databases is a crucial element. On the other hand, they offer simple techniques for computing continuous SVF over large areas, which could be the starting point for additional research.

Later, a few models for calculating SVF were created. A unique distribution of sky view factors that characterise a city's centre or its whole area is called a continuous sky view factor, and some models even compute it (Gál et al., 2009). According to Souza et al. (2003), the majority of models are primarily digital elevation models (DEM), which permit flat roofs and simple-shaped buildings. Several prototypes allow modeling on non-flat roofs and trees since they are based on the concept of barriers. In a few prototypes, the concept of barriers is used to depict non-flat roofs and trees as well (Hämmerle et al., 2011a).

A Python-based script was created to assess from a digital surface model (DSM) on any platform with an Integrated Development Environment in order to get beyond the shortcomings of the current SVF computation methodologies. In order to maintain the optimum image quality, the script outputs a continuous sky view factor map in raster format (preferably tiff). A DSM is required as input.

3.4.2 Sky View Factor calculation with the existing and proposed approach of Kolkata

a) Sky View Factor Calculation using Fisheye Lens

Sky View Factor (SVF) is a crucial metric in urban and environmental studies that quantifies the portion of the sky visible from a specific location on the ground. It is widely used in urban planning, climate studies, and ecological research to assess factors like urban heat islands, micro-climates, and habitat suitability.

The fish-eye lens has a wider angle than a regular lens, roughly 180 degrees. The methods utilized to take images of the scene on-site that circle the hemispheric area. After that, the photos are analyzed using a variety of methods to identify the skyline and compute the relationship between the blocked and unblocked areas of the image. The most used techniques are the equiangular projection techniques, which Steyn created in 1980. To estimate SVF, he split the projected image into many concentric annuli, where the annular sections represented the sky.

$$SVF = \frac{1}{2n} \sum_{i=1}^n \sin[\pi(i-1/2)/2n] \cos[\pi(i-1/2)/2n] \alpha_i \theta_{sky}$$

$$= \frac{1}{2n} \sum_{i=1}^n \sin \theta_i - \frac{1}{22n} \cos \theta_i - \frac{1}{22n} \theta_i$$

θ is referred to as the annulus index and α_i is referred to as the angular width of the sky in the i^{th} annulus where n is given as the number of annuli. Later, in 1984, Johnson & Watson created a modified variation of Steyn's technique.

$$SVF = 12\pi \sin^2 \theta \sum_{i=1}^n \sin[\pi(2i-1)/2n] \alpha_i \theta_{sky} = 12\pi \sin^2 \theta \sum_{i=1}^n \sin[\pi(2i-1)/2n] \theta_i$$

indicating that, for sufficiently big n , Steyn had approached $\sin[\pi/(2n)]$ by $\pi/(2n)$. Blennow (1995) further refined the photography approach by extending the projection to equiangular scenarios based on their theoretical concepts and employing more sophisticated hardware and software (Brown et al., 2001; Chapman et al., 2001; Hämmerle et al., 2011a).

SVF is easily obtainable from structures of various sizes and asymmetrical shapes. Using this technique, barriers such as vegetation can be located. This method, nevertheless, typically requires a lot of time. Additionally, since this method requires a consistently cloudy sky and problems with image processing emerge from direct sunlight or various cloud kinds, there aren't many opportunities for surveys utilizing it (CHAPMAN & THORNES, 2003). Additionally, spatial data is lacking. Due to these restrictions, the approach cannot be used for large-area analysis.

Traditionally, SVF has been calculated using hemispherical photography, where a camera with a fish-eye lens captures the entire sky dome above a specific location. The fish-eye lens provides a wide-angle view, allowing the camera to capture the sky from horizon to zenith.



Procedure for SVF Calculation using Fisheye Lens:

1. Equipment Setup: Set up the camera with the fish-eye lens on a sturdy tripod at the desired location. Ensure that the camera is level and pointing directly upwards.

For this study Nikon DSLR D60 camera with NIKKOR 16 mm f/2.8D fisheye lens was used to capture images.

2. Camera Settings: Adjust the camera settings for proper exposure. It is recommended to use manual mode with a low ISO setting, a small aperture (high f-stop number), and a relatively fast shutter speed to avoid overexposure and reduce motion blur.

3. Capture Images: Take a series of pictures capturing the entire sky dome by rotating the camera horizontally. It is essential to have overlapping images to ensure complete coverage.

4. Image Processing: Transfer the images to a computer and use specialized software for image stitching. There are various software tools available that can automatically stitch the overlapping images into a single high-resolution hemispherical image. Sky View Factor Calculator software, developed by Johnson & Watson (1984) is used to process all images.

5. Hemispherical Image Analysis: Analyze the stitched hemispherical image to calculate the SVF. This can be done using image processing software or dedicated SVF analysis tools. The software will process the image to distinguish between sky pixels and obstruction pixels (e.g., buildings, trees, etc.).

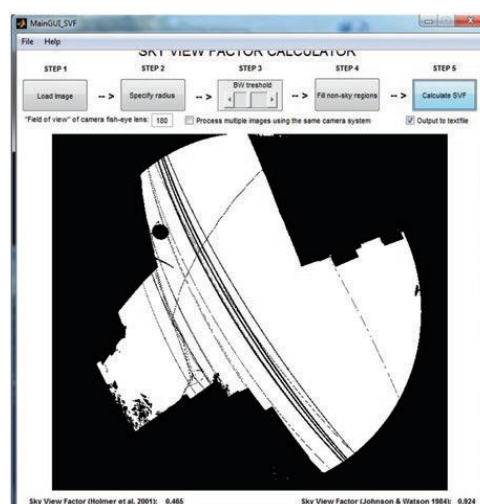


Figure 3.6 Sky View Factor Calculator software layout (Source: Johnson & Watson)

6. Calculation of SVF: Once the image processing is complete, the software will calculate the SVF as the ratio of the number of sky pixels to the total number of pixels in the image. SVF is expressed as a decimal or a percentage.

7. Interpretation: The SVF value provides insights into the openness of the location's surroundings. High SVF values indicate more open areas with a greater view of the sky, while low SVF values suggest more obstructed areas with limited sky visibility.

b) SVF calculation using Remote Sensing and GIS data

Remote sensing and Geographical Information Systems (GIS) are now widely used to comprehend and analyze SVF. Both spatial and non-spatial analyses are possible with the technology. The use of geographic information systems speeds up computations and cuts down on research time. In particular, the digital elevation model (DEM) is a raster format that shows 3D data on a 2D digital surface (Ratti & Richens, 2004) . Urban morphologies are represented more simply with DEM. It is seen "as a tool to facilitate numerous sorts of analysis, not only as a repository of knowledge (Falcidieno, 1994) ." Due to its tight link with GIS systems, DEM has really found its most extensive applications in geographic studies (Lin & Oguchi, 2006; Ruiz-Arias et al., 2009; Tarekegn et al., 2010) . To examine the SVF values, GIS software such as ArcGIS, ArcView, MapInfo, ENVI, QGIS, Saga, etc. can be utilized. Utilize GIS spatial analysis tools to calculate the SVF based on the available DEM, building height, and land cover data. The calculation involves analyzing the proportion of visible sky for each location in the study area.

GIS tools were used in the initial step to generate the database. The building map was created using Landsat and Google Earth pictures so that each structure's precise location could be ascertained. In order to conduct this research, two essential tools have been used. The first was created by (Lindberg et al., 2018) and was called the "Urban Multi-scale Environmental Predictor" (UMEP) Modules of QGIS. The building footprints are rasterized from vector to SVF analysis because the algorithm is based

on raster input. The second, called SVF Mapping Tool V1.1, was created in the shapefile (.shp) format by Gál and Unger (2014) and is based on vector input.

The method of Gál and Unger (2014) is followed to calculate SVF of Kolkata. The details steps describe below:

The inputDirectory.txt file defines where the input and output files should be stored.

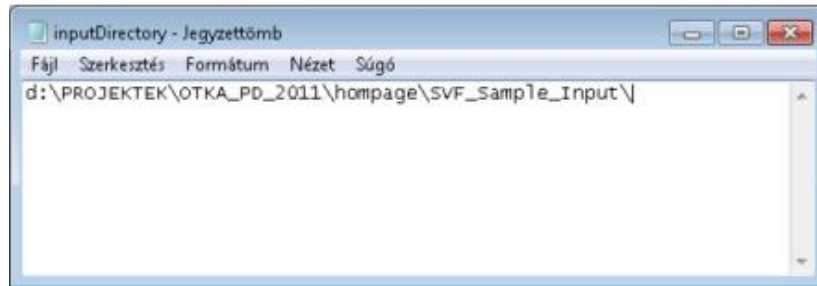


Figure 3.7.1. SVF Mapping Tool V1.1 software layout: Input directory path (Source: <http://urban-path.hu/>)

With the inputDirectory.txt modified, SVFCalc.jar can be used to launch the programme.

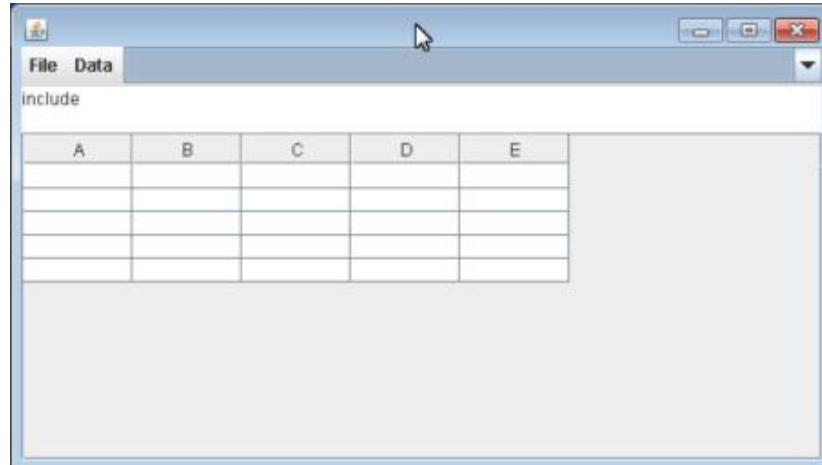


Figure 3.7.2. SVF Mapping Tool V1.1 software layout: Input directory table (Source: <http://urban-path.hu/>)

First the input files have to be defined

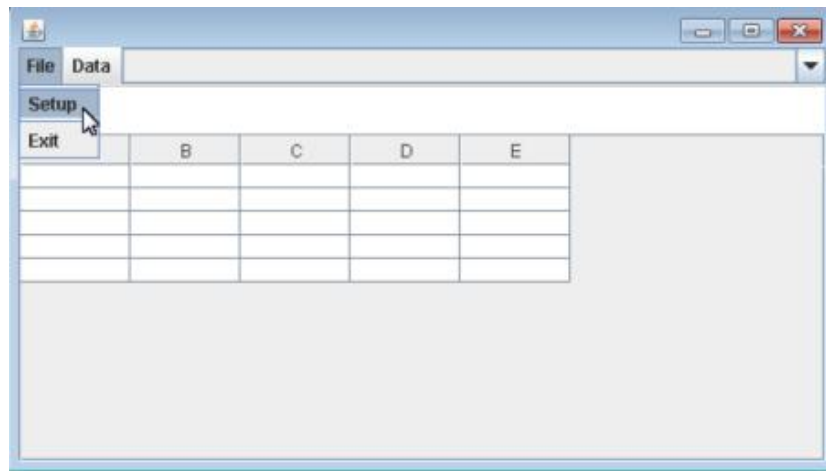


Figure 3.7.3. SVF Mapping Tool V1.1 software layout: Input directory table (Source: <http://urban-path.hu/>)

Building footprints with height in ESRI Shapefile format.

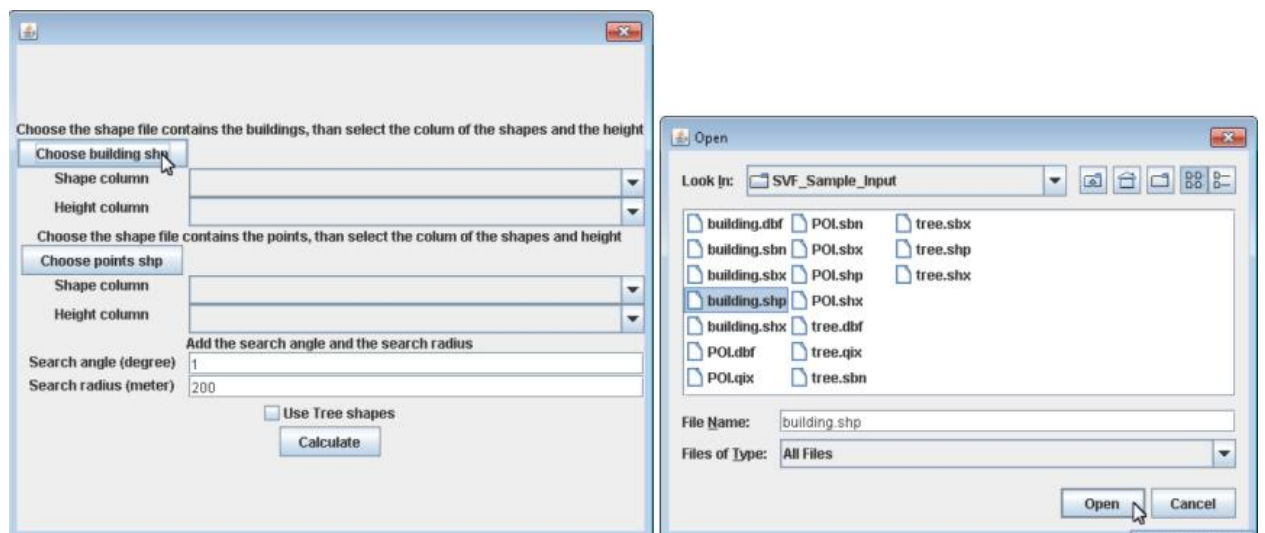


Figure 3.7.4. SVF Mapping Tool V1.1 software layout: Feature insert (Source: <http://urban-path.hu/>)

Shape column means the geometry. The name is always the_geom.

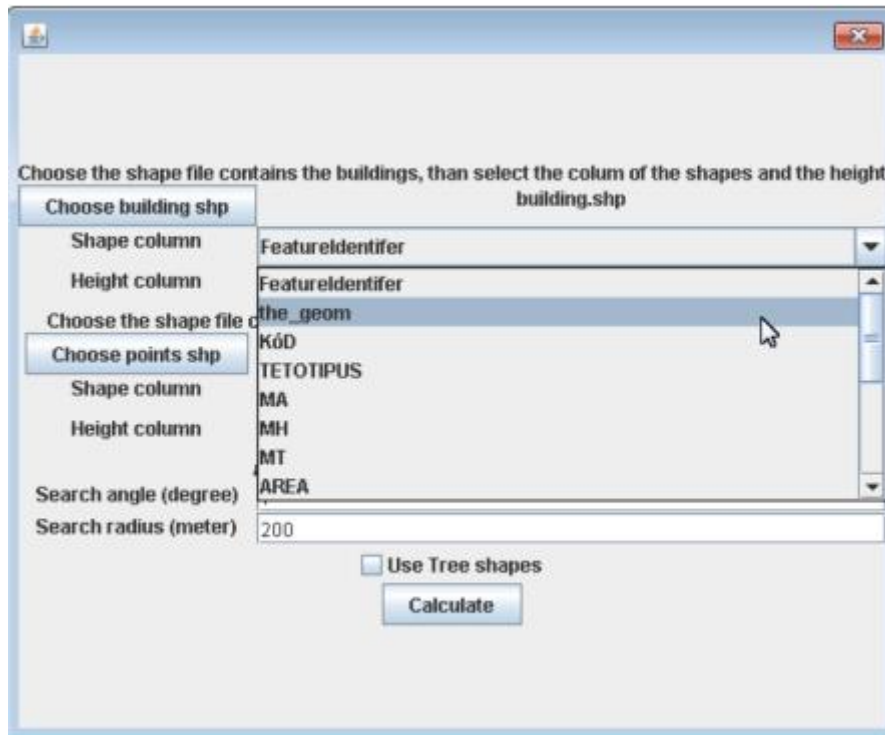


Figure 3.7.5. SVF Mapping Tool V1.1 software layout: Geometry selection (Source: <http://urban-path.hu/>)

Height column is the height or elevation of the buildings. meters above ground.

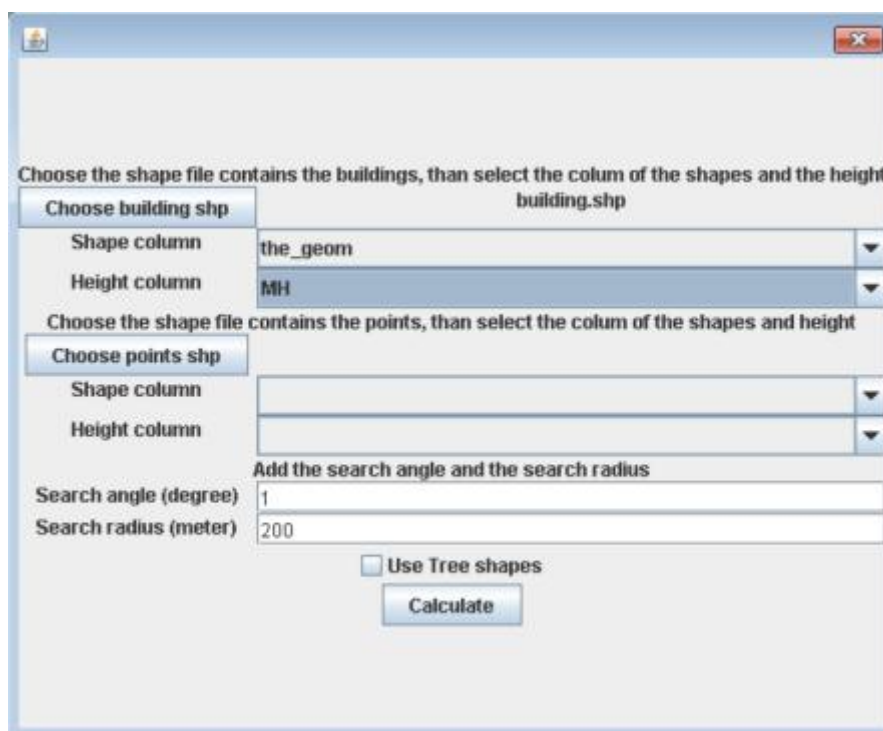


Figure 3.7.6. SVF Mapping Tool V1.1 software layout: Height selection (Source: <http://urban-path.hu/>)

Next, click Calculate. The software then reads the input files. Data -> Calculate is where the calculation begins.

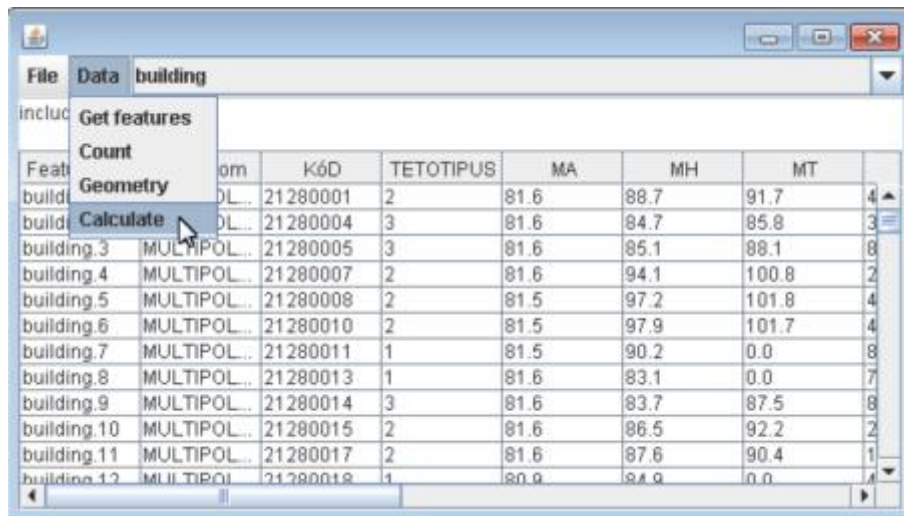


Figure 3.7.7. SVF Mapping Tool V1.1 software layout: Calculate step (Source: <http://urban-path.hu/>)

The software inquires about the output file's location when the computation is complete.

Additionally, SVF values can be computed using QGIS software using UMEP plug-in. using a computerized surface model of the ground and buildings, a pixel-by-pixel sky view factor map is produced.

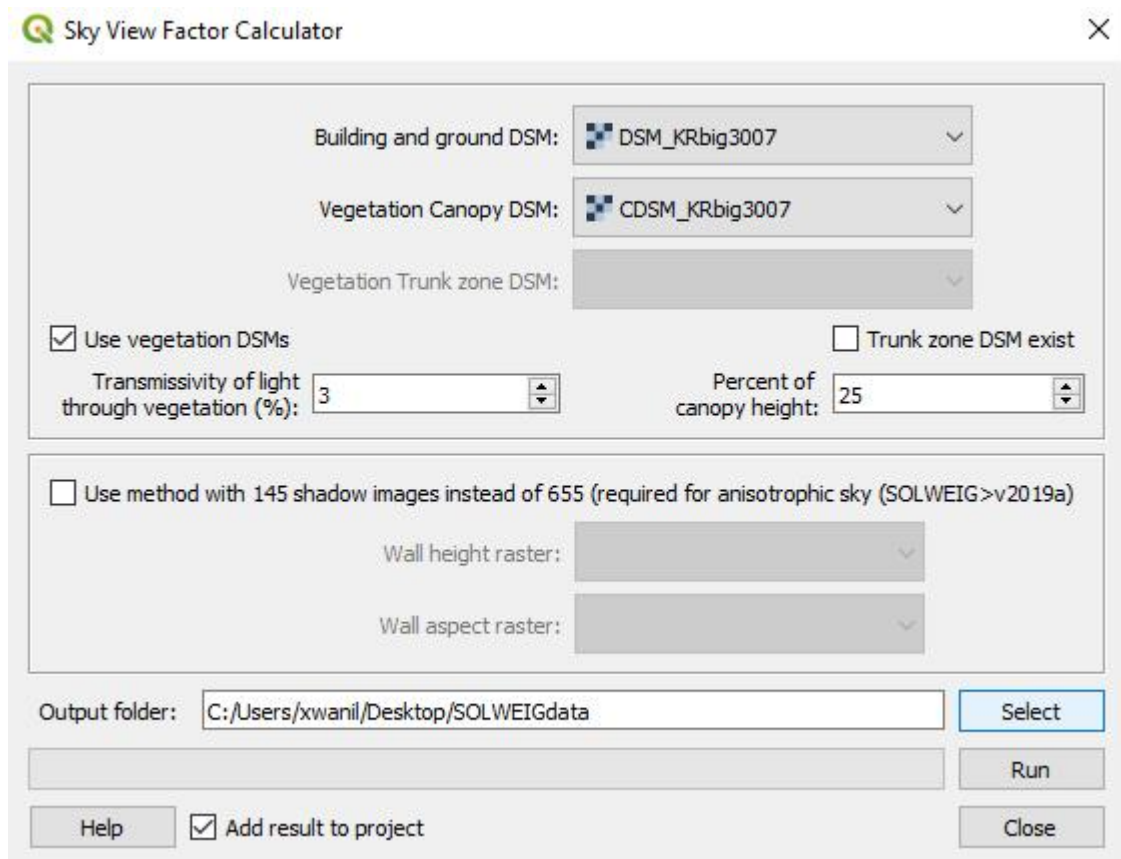


Figure 3.8. UMEP sky view factor calculator software layout (Source: <https://umep-docs.readthedocs.io/>)

C) SVF calculation using python script

The introduction of Python script aims to overcome the limitations of the existing SVF computing techniques. The program outputs a continuous sky view factor map in raster format and requires a DSM as input. In order to perform SVF from DSM data, a separate Python package (SVFpy) has been created. Rasterio to read DSM, Warp to keep projections, Scipy to maintain euclidean distance, Skimage to process images, Zarr to manage directions, and Numpy to perform numerical calculations are some of the modules used for this. Figure 5.4 displays the finished SVF map produced by the Python script. The following python script has been used to develop SVFpy.

```
import rasterio
from rasterio import warp
import math
from scipy.spatial.distance import euclidean
```

```

from skimage.draw import line
from skimage.util import view_as_windows
from scipy import ndimage, misc
import numpy as np
from rasterio.enums import Resampling
import zarr

class SVF:
    def __init__(self,
                  mds_path,
                  observer_height = 1.20,
                  kernel_size = 7,
                  max_radius = None):
        self.mds_src = rasterio.open(mds_path)
        self.observer_height = observer_height
        self.kernel_size = self._is_kernel_size_odd(kernel_size)
        if max_radius is None:
            self.max_radius = max(self.mds_src.shape)
        else:
            self.max_radius = max_radius
    def _is_kernel_size_odd(self, kernel_size):
        if int(kernel_size) % 2 == 0:
            raise ValueError("Kernel Size must be odd integer!")
        return int(kernel_size)
    def external_coordinates(self):
        kernel_size = self.kernel_size
        extremes = [[0,0], [kernel_size-1,0], [kernel_size-1, kernel_size-1], [0, kernel_size-1]]
        external_coords = []
        fuse_angles = []
        start_index = 1
        for i in range(4):
            l = line(*np.roll(extremes, -i, axis=0)[0:2].flatten())
            fuse_angles.append(np.arctan2(*(np.array(l) - kernel_size // 2)[:, start_index:]))
            external_coords.append(np.array(l, dtype='uint8').T[start_index:])

```



```

external_coords = np.concatenate(external_coords)
fuse_angles = np.concatenate(fuse_angles)
fuse_angles_range = np.diff(fuse_angles, append=fuse_angles[0])
fuse_angles_range[np.where(fuse_angles_range>np.pi)] =
fuse_angles_range[np.where(fuse_angles_range>np.pi)] - 2 * np.pi
return external_coords, fuse_angles, fuse_angles_range
def distance_matrix(size=11):
    kernel_simple = np.ones((size, size), dtype='float16')
    center_point = (int(kernel_simple.shape[0]//2), int(kernel_simple.shape[1]//2))
    distances = np.zeros((size, size), dtype='float16')

    for i in range(size):
        for j in range(size):
            distances[i][j] = euclidean([0., 0.], [i - center_point[0], j - center_point[1]])
    return distances
def zoom2d(matrix, times:int):
    shape = matrix.shape
    dims = len(shape)
    matrix_zomed = \
    np.tile(
        np.expand_dims(
            np.tile(
                np.expand_dims(matrix, axis=2),
                tuple(np.concatenate([np.array([1,1, times]), np.ones(dims-2, dtype='int')]))
            ).reshape(
                tuple(np.array(shape) * np.concatenate([np.array([1,times]), np.ones(dims-2,
dtype='int')]))
            ),
            axis=1
        ),
        tuple(np.concatenate([np.array([1,times]), np.ones(dims-1, dtype='int')]))
    ).reshape(
        tuple(np.array(shape) * np.concatenate([np.array([times,times]), np.ones(dims-2,
dtype='int')]))

```

```

)
return matrix_zomed

def lines_mask(svf:SVF):
    lines_mask = np.zeros((_fuse_lines(svf).shape[0], svf.kernel_size, svf.kernel_size),
dtype='bool')
    for k, fl in enumerate(_fuse_lines(svf)):
        lm = np.zeros((svf.kernel_size, svf.kernel_size), dtype='bool')
        lm[fl[:, 0], fl[:, 1]] = True
        lines_mask[k] = lm
    return lines_mask

def calculate(svf:SVF):
    pixel_max_size = math.ceil(svf.max_radius / math.floor(svf.kernel_size / 2) *
max(svf.mds_src.res))
    downscale_times = math.ceil(math.log2(pixel_max_size / max(svf.mds_src.res)) + 1)
    itens_quantity_by_scale = int(((svf.kernel_size//2) + 1) / 2)
    kernel_border_quantity = (svf.kernel_size * 4) - 4
    pixels_per_angle = downscale_times * itens_quantity_by_scale + itens_quantity_by_scale
    fuse_lines = _fuse_lines(svf)
    mds = svf.mds_src.read(1).astype('float16')
    mdss, transformations = [], []
    masks = lines_mask(svf)
    distance_rows = np.zeros((kernel_border_quantity, pixels_per_angle), dtype='float16')
    result_temp = np.zeros((svf.mds_src.width,
svf.mds_src.height, kernel_border_quantity, pixels_per_angle), dtype='float16')
    for i in np.arange(downscale_times):
        resolution = tuple([r * (2 ** i) for r in svf.mds_src.res])
        fuse_angle_range = svf.external_coordinates()[-1]
        mds, transform = warp.reproject(source=svf.mds_src.read(1),
src_transform=svf.mds_src.transform,
src_crs=svf.mds_src.crs,
dst_crs=svf.mds_src.crs,
dst_nodata=svf.mds_src.nodata,
dst_resolution=resolution,
resampling=Resampling.max)

```

```

mds = np.pad(np.squeeze(mds), svf.kernel_size // 2)
windows = view_as_windows(mds, (svf.kernel_size, svf.kernel_size))
if i == 0:
    index = (0, itens_quantity_by_scale * 2)
    print(index)
    distance_rows[:, index[0]:index[1]] = distance_matrix(size=svf.kernel_size)[fuse_lines[:, :,
0], fuse_lines[:, :, 1]][:, :] * resolution[0]
    distance_row = distance_matrix(size=svf.kernel_size)[fuse_lines[:, :, 0], fuse_lines[:, :,
1]][:, :] * resolution[0]
    rows = windows[:, :, fuse_lines[:, :, 0], fuse_lines[:, :, 1]]
    points = np.expand_dims(rows[:, :, :, 0], axis=3)
else:
    index = (int(i * itens_quantity_by_scale) + itens_quantity_by_scale, int(i *
itens_quantity_by_scale) + itens_quantity_by_scale * 2)
    print(index)
    distance_row = distance_matrix(size=svf.kernel_size)[fuse_lines[:, :, 0], fuse_lines[:, :,
1]][:, itens_quantity_by_scale:itens_quantity_by_scale*2] * resolution[0]
    rows = windows[:, :, fuse_lines[:, :, 0], fuse_lines[:, :, 1]]
    rows = zoom2d(rows, 2*i)[0:svf.mds_src.width, 0:svf.mds_src.width, :,
itens_quantity_by_scale:]
    result_max = np.max(np.arctan2(rows - points - svf.observer_height, distance_row), axis=3)
    print('calculating SVF ..')
    svf_result = np.sum(((fuse_angle_range/np.pi/-2) * (1 - np.sin(np.where(result_max >= 0.,
result_max, np.deg2rad(0)))/1), axis=2)
    return svf_result
def _fuse_lines(svf:SVF):
    external_coords = svf.external_coordinates()[0]
    lines = []
    center_point = (int(svf.kernel_size//2), int(svf.kernel_size//2))
    for c in external_coords:
        lines.append(line(*center_point, *c))
    fuse_lines = np.array([np.array(l).T for l in np.array(lines)])
    return fuse_lines

```

The final script for calculation SVF is

```

import svf
import rasterio
import numpy as np
import zarr

#loading tif file
path = input("Enter your DSM Path -")
path = r'{}'.format(path)
data = path
#loading tif file using base class
svf_data = svf.SVF(mds_path=data, kernel_size=15)
#checking the profile
profile1 = svf_data.mds_src.profile
#result checking
svf_result = svf.calculate(svf_data)
print(svf_result)

```

3.5 Local Climate Zones

Local Climate Zone is referred to as a localized collection of atmospheric conditions that can range in size from a few square meters to several square kilometers on a horizontal scale and are caused by the existence of uniform surface cover, structure, material, and human activity. For UHI experiments, Stewart & Oke (2012) developed a novel, rigorous strategy for defining land use. They found that each LCZ has a distinct temperature regime, which is most noticeable on dry surfaces on calm, clear nights. This regulation of temperature is related to homogeneous habitats or the urban ecosystem. The main way of offering the WUDAPT (World Urban Database and Access Portal Tools) project identifies the climate zones of Kolkata. Kolkata has a lot of low-rise structures, a bit of open space, and a lot of buildings. In comparison to the shadows cast by nearby structures and obstacles, the surfaces of the densest areas warm far more slowly.

The idea of local climate zone mapping was introduced by Bechtel & Daneke (2012). Due to the diversity among cities, a generic classification system for LCZs was formalized using a variety of techniques and strategies. The classification scheme was developed in accordance with Bechtel (2011), Conrad et al. (2015), Stewart & Oke (2012). The technique was then used by the community project known as World Urban Database and Access Portal Tools (WUDAPT) in order to create uniform LCZ maps of the world's cities (Ching et al., 2018). The scheme has 17 zones that are essentially determined by surface structure characteristics (such building and tree height and density) and surface cover (pervious vs. impervious). At the local scale, each zone spans horizontal distances of a few hundred meters to several kilometers (Stewart & Oke, 2012).

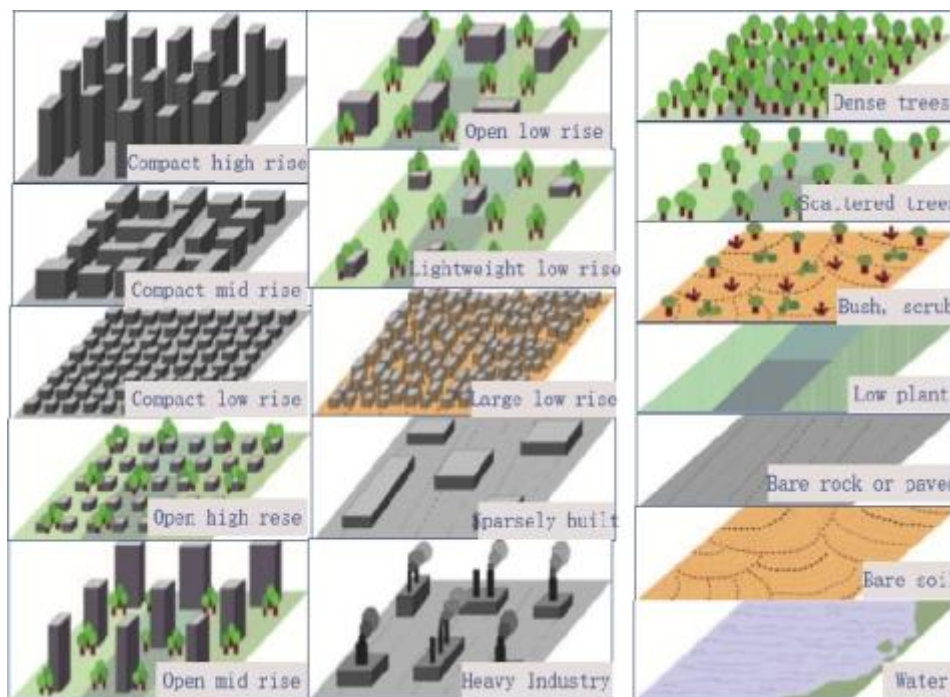


Figure 3.9. Local Climate Zone (Source: Stewart & Oke, 2012)

3.5.1 Types of Local Climate Zones

Stewart and Oke's local climate zone (LCZ) classification system is a widely used method for classifying urban areas based on their surface structure, cover, and human activity. The system consists of 17 zones, which can be grouped into two broad categories:

Built types (LCZ 1-10): These zones are characterized by high levels of impervious surface cover and building density. Examples include compact high-rise zones (LCZ 1), compact mid-rise zones (LCZ 2), and open high-rise zones (LCZ 3).

Land cover types (LCZ A-G): These zones are characterized by lower levels of impervious surface cover and building density. Examples include sparsely built areas (LCZ A), low plant cover (LCZ B), and tall plant cover (LCZ C).

Each LCZ has a unique set of physical characteristics that influence its local climate. For example, compact high-rise zones (LCZ 1) are typically warmer than sparse built areas (LCZ A) due to their high levels of impervious surface cover and shading.

The LCZ classification system has been used in a wide range of studies on urban climate and energy. It is a valuable tool for understanding the impacts of urbanization on local climate and for developing strategies to mitigate the negative effects of urban heat islands and other urban climate challenges.

Here is a brief overview of the 17 LCZs, as defined by Stewart and Oke:

Built types:

- LCZ 1: Compact high-rise
- LCZ 2: Compact mid-rise
- LCZ 3: Compact low-rise
- LCZ 4: Open high-rise
- LCZ 5: Open mid-rise
- LCZ 6: Open low-rise
- LCZ 7: Lightweight low-rise
- LCZ 8: Large low-rise
- LCZ 9: Sparsely built
- LCZ 10: Heavy industry

Land cover types:

LCZ A: Dense trees
LCZ B: Scattered trees
LCZ C: Tall plant cover
LCZ D: Bush, Scrub
LCZ E: Bare rock/paved
LCZ F: Bare soil
LCZ G: Water

It is important to note that the LCZ classification system is a simplification of the real world. In reality, urban areas are often a mix of different LCZs. However, the LCZ system provides a useful framework for understanding the impacts of urbanization on local climate and for developing strategies to mitigate the negative effects of urban heat islands and other urban climate challenges.

3.5.2 Application of World Urban Database and Access Portal Tools (WUDAPT) to the Workflow of Local Climate Zone Classification

The WUDAPT-based classification approach primarily uses supervised classification (Random Forest) on Landsat images with a 100m resolution in GIS and remote sensing-based mapping. WUDAPT's accuracy is frequently subpar because it focuses largely on an approach's universal applicability and excludes complex auxiliary classification procedures (Ma et al., 2021).



Figure 3.10. The workflow to classify LCZ as per the WUDAPT method

The WUDAPT classification method has recently taken over as the standard approach for LCZ classification. We more carefully selected the training samples to ensure optimum accuracy.

Based on climate-relevant surface characteristics, natural and urban landscapes are categorized using the local Climate Zone (LCZ) scheme by the WUDAPT approach (Bechtel & Daneke, 2012; Danylo et al., 2016). Collecting signatures from Google Earth pictures is the initial stage in creating LCZ, which is then followed by field verification of the acquired signatures. SAGA GIS software was used to complete the LCZ map using Landsat photos and signatures.

3.5.3 Dataset used to classify Local Climate Zone of Kolkata

WUDAPT-based classification approach follows to classify local climate zones of Kolkata. Historical building data set of Google Earth Pro is used to finalize signature file. The signature files were verified with KMC personnel and old maps before final process. The details of the used software to classify LCZ is as follows.

Table 3.3 Summary of software used to classify local climate zones of Kolkata

Software Name	Version
Google Earth Pro	7.8.1
Saga GIS	8.1.4

3.6 Chapter Summary

The research methodology chapter, which presents a thorough explanation of the tactics and practises used to address the research objectives and provide answers to the research questions, is an essential part of the study. It explores the methodical and structured strategy used to plan, carry out, and analyse the study, assuring the validity and dependability of the results. The methodology chapter establishes the reliability and strength of the study findings by explaining the research methodologies, data gathering approaches, and analytical tools, opening the door for significant contributions to the body of existing knowledge.

This study describes the urban built form typology in different micro climatic areas of Kolkata and how changes in urban heat island and sky view factor affect it. All open-source data set and software are used for this study. Only ArcGIS Pro is proprietary software and is used for this study. The methodology used in this study offers a different, simple, and most recent approach to the precise and accurate outcomes.

It serves as a road map for a clear and logical growth of the research process, making it possible to understand the justification for the decisions made. This chapter's organization is intended to provide a thorough and transparent account of the research design, covering the overall research approach, the justification for the methodology selected, data collection strategies, data analysis techniques, and any ethical issues raised during the research process. The methodology chapter strives to improve the study's repeatability and transparency by painstakingly documenting every step done, ultimately adding to the research's overall credibility and trustworthiness.

Chapter 4. COMPARATIVE ANALYSIS OF LAND-USE LAND- COVER WITH LOCAL CLIMATE ZONE APPROACH FOR URBAN HEAT ISLAND IN KOLKATA

4.1 Introduction

The impact of built form on the urban microclimate in Kolkata is a complex and multifaceted issue. While it is known that urban form directly influences urban microclimates, the complete demolition of entire blocks or heritage buildings in order to improve factors such as wind flow in outdoor spaces is unlikely (Tamminga et al., 2020). Instead, a more sustainable approach to improving the urban microclimate would involve taking action upon existing buildings and infrastructures. This strategy is consistent with Lenzholzer's notion of the climatope, an urban area or district with typical micro-climatic features due to the density of buildings and major land use. Studies have shown that the quality of the built environment in terms of urban form has a significant impact on various environmental outcomes in cities (Navickas et al., 2020). These outcomes include energy consumption, mobility patterns, and the provision of services. Urban design and landscape design also play a crucial role in shaping the microclimate of cities. Furthermore, it is important to acknowledge that the urban microclimate strongly influences building operation. The local atmospheric conditions, modified by energy exchanges with the surrounding built environment context, have a direct impact on the performance and operation of buildings. Moreover, the built environment is not solely comprised of buildings but also encompasses the physical manifestations of economic, social, and environmental processes.

The impact of built form on the urban microclimate in Kolkata is a subject that has received significant attention from urban planners and architects alike. Due to the city's densely built environment, it is susceptible to certain micro-climatic conditions such as heat island effects, air pollution, and poor ventilation.

The design of buildings can significantly affect these conditions; for example, taller buildings can create wind tunnels that exacerbate air pollution while selectively building green spaces can help mitigate heat island effects. Additionally, factors such as surface materials used in construction (e.g., concrete vs. vegetation) and methods of waste management (e.g., incineration vs. recycling) also play a role.

In short, thoughtful consideration of built form plays an essential role in shaping the urban microclimate in Kolkata – one that directly impacts both quality of life and public health outcomes for its residents.

4.2 Land use and land cover (LULC) scenario of Kolkata

Land Use and Land Cover (LULC) analysis is a critical component of urban planning and environmental management. Kolkata has witnessed substantial urbanization over the years, leading to the expansion of residential areas. Older neighborhoods have experienced densification, while newer satellite towns and housing developments have emerged on the peripheries. The change in land use is characterized by the conversion of agricultural land, wetlands, and green areas into residential zones.

The LULC information can be used to effectively describe the spatial-temporal pattern of LST in Kolkata. To extract the LULC map of Kolkata (Figure 4.1), supervised image classification methodology was utilized on Landsat 8 OLI images (November 2017). The outcome reveals that 69% of the land is built up. Whereas just 5% of the area is made up of water bodies, 7% is open space, and 19% is covered in vegetation. Another set of temporal images from 2003 and 2010 were taken into account to better comprehend the trend. It has been noted that there has been an overall 20.68% increase in built-up area, a 36.01% loss in vegetation, a 20.17% drop in water bodies, and a 2.29% decrease in open space

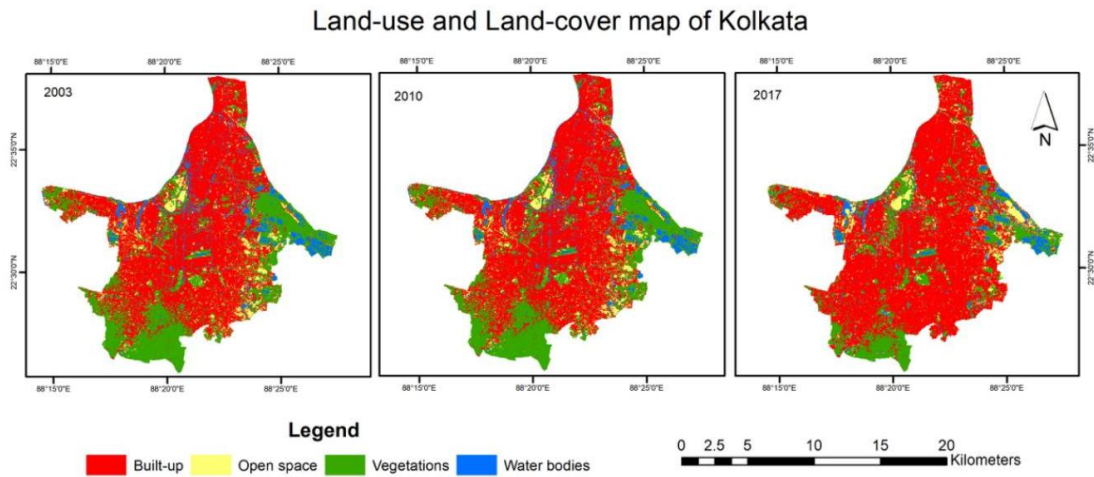


Figure 4.1. Land use and land cover map of Kolkata of 2003, 2010 and 2017 (Source: Author)

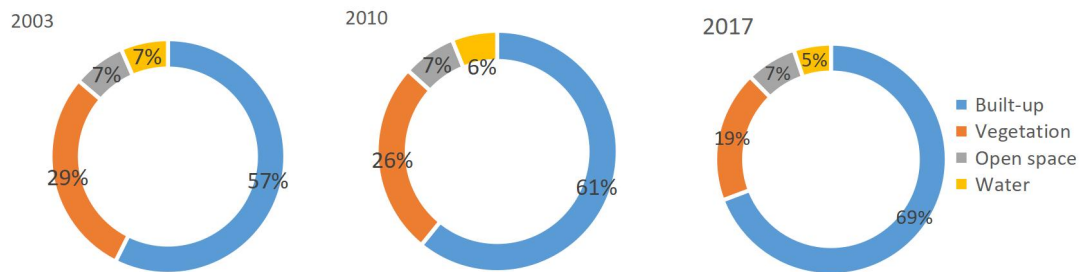


Figure 4.2. Proportion of LULC class in Kolkata of 2003, 2010 and 2017 (Source: Author)

Table 4.1. Temporal changes of LULC in Kolkata (Area in Sq. KM)

LULC Class	2017		2010		2003	
Built-up	140.22	69.24%	123.23	60.86%	116.19	57.38%
Vegetation	37.34	18.44%	52.38	25.87%	58.36	28.82%
Open space	14.39	7.11%	14.54	7.18%	14.73	7.28%
Water	10.55	5.21%	12.35	6.10%	13.21	6.52%

The analysis summarizes that increasing growth of urbanization promotes the surface level heat emission in the city. Very positive diurnal LST deviation has been found at Chitpur, Shyambazar, Cossipore, Bagbazar, Bara Bazar, Narkeldanga, Garden Reach, Rajabagan areas where the mean diurnal LST values range from 33°C to 35°C. At the south and south-eastern fringe areas of Kolkata is very active zone of urbanization. Built-up density is gradually increasing in Jadavpur, New Garia, Santoshpur and Baghajatin where the NDBI values have increased but NDVI values have decreased. These new urbanized zones of Kolkata are gradually decreasing the

fraction of vegetation surface and contribute to increase surface heat emission in this part of the Kolkata city.

4.3 Local Climate Zones in Kolkata

In the present study the local climate zones in the KMC area have been prepared at ward level after considering urban structure, diurnal and nocturnal LST, surface albedo, LULC, NDBI, NDVI information layer and ground truth verification (GTV). It is a GIS based technique where different raster and vector layers are stored, processed and analyzed with an overlay method. Finally, the LCZs are corrected with high spatial resolution Google Earth images. The extracted information has been presented in Table 4.2 and Figure 4.4 of this chapter as follows.

Table 4.2 LCZs in the Kolkata

Local climate zone	Ward No	Characteristics
LCZ2: Compact mid-rise LCZB: Scattered trees LCZG: Water	2, 3, 4, 14, 30, 33, 34, 66, 67, 69, 76, 91, 92, 95, 96, 98, 99, 100, 101, 102, 103, 104, 105, 117, 118, 19, 120, 121, 130, 131 & 132	1. High temperature variation. UHI present. 3. Narrow urban canyon. 4. 15 % to 18% surface albedo.
LCZ2: Compact mid-rise LCZB: Scattered trees	7, 8, 9, 10, 11, 12, 15, 16, 17, 18, 19, 20, 21, 22, 23, 24, 25, 26, 27, 28, 29, 37, 38, 39, 40, 41, 42, 43, 44, 47, 48, 49, 50, 51, 52, 53, 54, 55, 60, 61, 62, 68, 77, 83 & 84	1. High temperature variation. UHI present. 2. Presence of wide urban Canyon. (e.g. Central Avenue) 3 8 % to 12 % surface albedo.
LCZ8: Large low-rise LCZB: Scattered trees LCZG: Water	1, 6, 13, 79 & 80	1. Industrial and commercial buildings 2. High temperature variation. UHI present. 3. 10 % to 15 % surface albedo.
LCZ2: Compact mid-rise LCZ8: Large low-rise LCZB: Scattered trees	5 & 137	1. Commercial, industrial and residential buildings 2. Moderate temperature variation. 4. 15 to 16 % surface albedo
LCZ1: Open high-rise LCZ2: Compact mid-rise LCZ8: Large low-rise LCZB: Scattered trees	31, 32, 63, 64, 65, 70, 71, 72, 73, 75, 81, 82, 85, 86, 87, 88, 89, 93, 106, 107, 115 & 116	1. High temperature variation. UHI present. 2. Many deep and wide urban canyon 3. 13 % to 14 % surface albedo
LCZ2: Compact mid-rise LCZ3: Compact low-rise LCZB: Scattered trees	35 & 78	1. Moderate temperature variation.

LCZ3: Compact low-rise LCZ4: Open high-rise LCZB: Scattered trees	36 56	1. Moderate temperature variation.
LCZ1: Compact high-rise LCZB: Scattered trees	45, 46 & 74	1. Moderate temperature variation. 2. Prominent urban canyon
LCZ2: Compact mid-rise LCZB: Scattered trees LCZD: Low plants LCZG: Water	57, 58 & 90	1. Moderate temperature variation.
LCZ2: Compact mid-rise LCZB: Scattered trees LCZG: Water	59, 94, 97, 110, 111, 112, 113, 138, 139, 140, 141 & 144	1. Moderate temperature variation 2. 18 % to 20% surface albedo
LCZG: Water LCZ4: Open high-rise LCZ2: Compact mid-rise	108 & 109	1. Moderate temperature variation 2. More than 20% surface albedo
LCZ6: Open low-rise LCZ2: Compact mid-rise LCZB: Scattered trees LCZG: Water	114, 122, 123, 124, 125 & 126	1. Low temperature variation
LCZ3: Compact low-rise LCZ6: Open low-rise LCZ9: Sparsely built LCZG: Water	127, 128, 129, 142 & 143	1. Low temperature variation
LCZ3: Compact low-rise LCZ8: Large low rise LCZE: Bare rock or paved LCZG: Water	133, 134, 135 & 136	1. High temperature variation. UHI present.

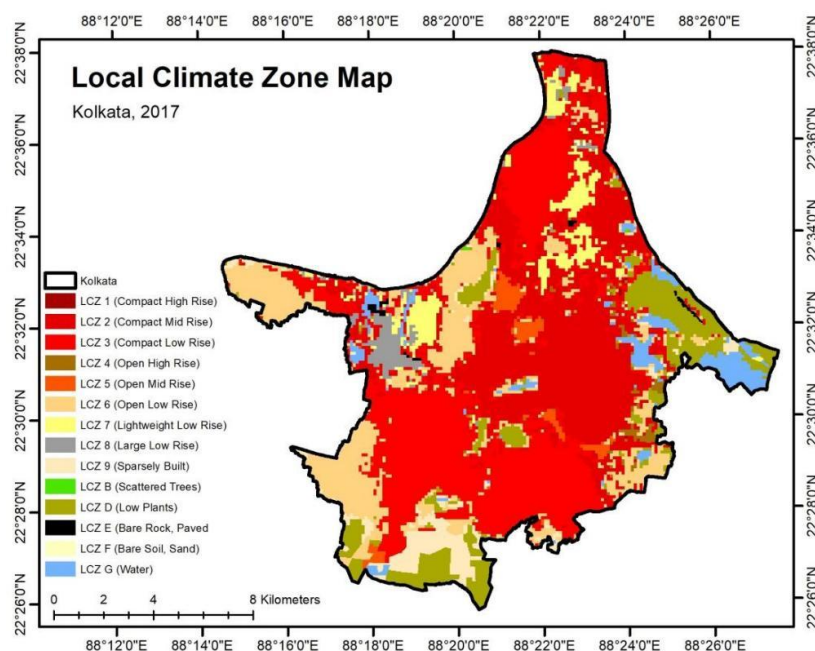


Figure 4.3. Local Climate Zone Map of Kolkata (Source: Author)

4.3.1 Accuracy assessment

The accuracy of Climate Zones is evaluated by supervised classification using images from Landsat 8. For classification, LCZ classes are produced by altering the training pixels. Google Earth was used to obtain the signature of LCZ, which was then confirmed by field survey.

With the aid of reference data that is readily available, climatic factors from each place are compared with the same variables in order to classify local climate. It was observed that the southern and eastern portions of the newly constructed areas had cooler temperatures than the central metropolis (center and north Kolkata).

To produce the final LCZ map, all input characteristics and training regions are integrated. The matching total accuracies are also calculated, as shown in Table 4.3.

Table 4.3. LCZ Classification Accuracy Assessment

Year	Overall Accuracy (OA)	Urban Class Accuracy (OAu)	Built versus natural class (OAbu)	Weighted Accuracy (OAw)
2017	0.59	0.62	0.90	0.88
2010	0.54	0.58	0.94	0.86
2003	0.58	0.61	0.88	0.81

4.3.2 Comparison between classified Local Climate Zone during the year 2003, 2010 and 2017 of Kolkata

The LCZ maps of Kolkata are shown in figure 4.3 and the descriptive statistics are summarized in table 4.3. From the analysis of time series maps, a significant increase in urbanized areas (LCZ 1 to LCZ 10 and LCZ E, LCZ F) is observed. In the year 2003, the urbanized area covers 74.32% whereas it is found that in 2010 the total area covers 76.59% and in 2017 the total area became 86.03%. In contrast to these, the vegetated area (LCZ B, LCZ C, LCZ D) and water bodies (LCZ G) were continuously decreasing. In the year 2003, the vegetated area covered almost 15.22%, but it covered only 14.61% in the year 2010 and 9.70% in the year 2017. Similarly, we found that the area covered by water bodies is 9.10%, 8.29%, and 3.87% for the years 2003, 2010, and 2017 respectively.

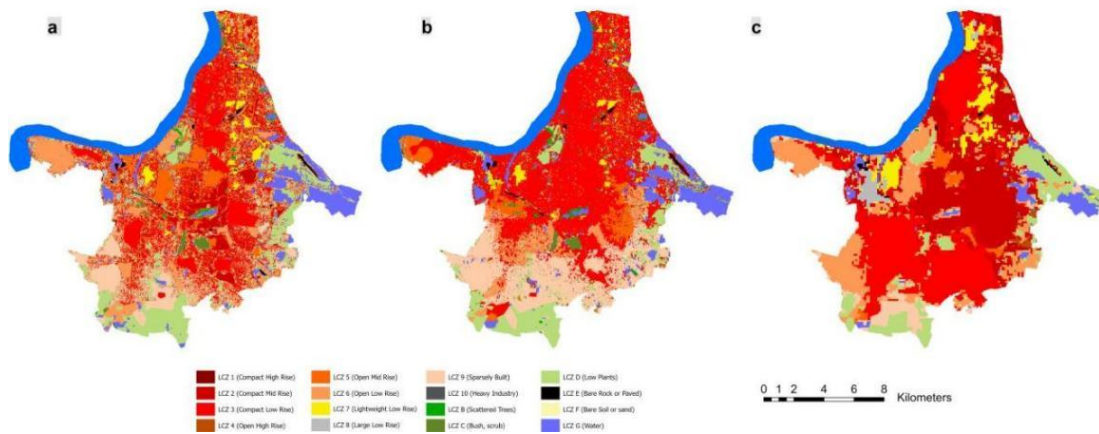


Figure 4.4. Local climate zone map for the year (a) 2003, (b) 2010, and (c) 2017
(Source: Author)

Table 4.4. Proportion of area of LCZs during the year 2003, 2010 and 2017

Sl No	LCZ Type	2003		2010		2017	
		Area (Sq Km)	%	Area (Sq Km)	%	Area (Sq Km)	%
1	Compact High Rise	0.20	0.10%	0.23	0.11%	0.72	0.36%
2	Compact Mid Rise	21.61	10.67%	29.00	14.32%	53.39	26.36%
3	Compact Low Rise	47.21	23.31%	61.49	30.36%	59.37	29.32%
4	Open High Rise	0.28	0.14%	0.53	0.26%	1.76	0.87%
5	Open Mid Rise	18.58	9.17%	8.61	4.25%	4.08	2.01%
6	Open Low Rise	28.42	14.03%	11.09	5.47%	32.38	15.99%
7	Lightweight Low Rise	9.64	4.76%	6.73	3.32%	9.44	4.66%
8	Large Low Rise	3.05	1.50%	2.28	1.13%	4.03	1.99%
9	Sparsely Built	21.09	10.41%	34.81	17.19%	8.26	4.08%
10	Heavy Industry	0.45	0.22%	0.40	0.20%	0.01	0.01%
11	Dense Trees	NA	NA	NA	NA	NA	NA
12	Scatter Trees	1.55	0.76%	3.06	1.51%	0.04	0.02%
13	Bush, Scrub	3.38	1.67%	2.84	1.40%	0.78	0.39%
14	Low Plant	25.90	12.79%	23.69	11.70%	19.53	9.65%
15	Bare Rock or Paved	2.53	1.25%	0.88	0.43%	0.62	0.31%
16	Bare Soil or Sand	0.23	0.12%	0.15	0.08%	0.20	0.10%
17	Water	18.43	9.10%	16.74	8.27%	7.89	3.90%

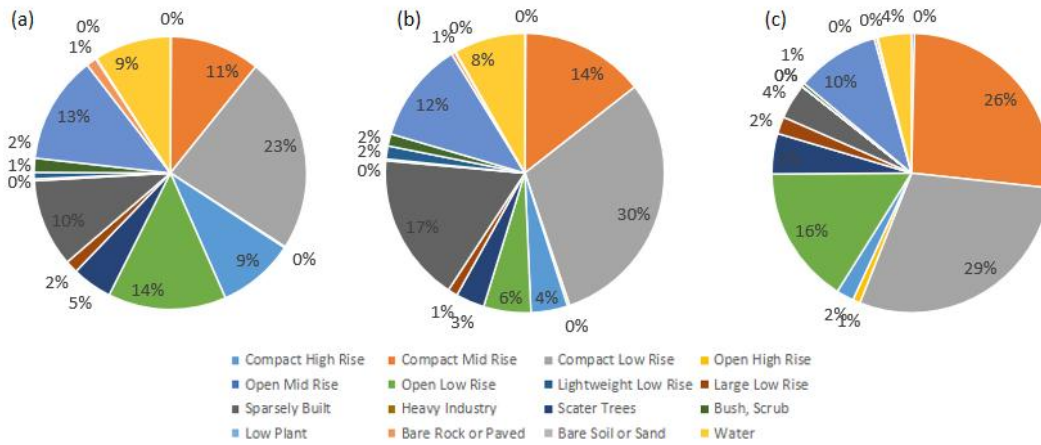


Figure 4.5. Proportion of area of LCZs during the year (a) 2003, (b) 2010 and (c) 2017 (Source: Author)

Transformation of LCZ occurred with the rapid change of urban morphology, which plays a major role in temperature variations. From the analysis, the mean LST variation within climate zones is observed as 2.48°C, 3.58°C, and 5.53°C respectively for the years 2003, 2010, and 2017. In 2017 the city is dominated by 'LCZ 2' and 'LCZ 3' almost 56% area, whereas in 2010 that category was only 46% and in 2003 was 34%. Continuously decreasing LCZ B, LCZ C, LCZ D, and LCZ G have a major impact on city weather change. The transformation mainly occurred from low rise (LCZ 3, LCZ 6, LCZ 7, LCZ 8, and LCZ 9) to mid-rise (LCZ 2 and LCZ 5) and high-rise (LCZ 1 and LCZ 4) urban morphology. There were 11% of vegetation land (LCZ B, LCZ C, and LCZ D) changed to built-up (LCZ 1 to LCZ 10) land. At the same time, there was a conversion of LCZ 3 to LCZ 2 (7%).

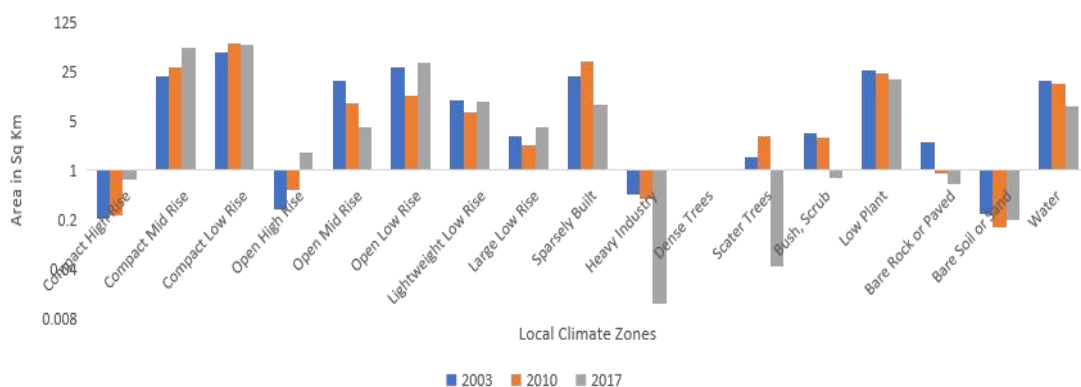


Figure 4.6. Transformation of LCZ in the year 2003, 2010 and 2017 (Source: Author)

Table 4.5. Transition matrix of Local Climate Zones, between 2003 to 2017

		Local Climate Zone 2017														Total
Local Climate Zone 2003		1	2	3	4	5	6	7	8	9	B	D	E	F	G	
	1	0.0003	0.0542	0.0404	0.0085	0.0111	0.0174	0.0016	0.0046	0.0054		0.0013		0.0003	0.0005	0.1456
	2	0.0026	8.4544	5.0672	0.0556	0.1721	0.4852	0.7096	0.2834	0.0337		0.0812	0.0168	0.0078	0.0223	15.3919
	3	0.0053	6.8738	7.238	0.0943	0.2325	12612	1.3279	0.5357	0.1019		0.2152	0.0409	0.0112	0.0732	18.0112
	4	0.0072	0.1046	0.0286	0.0104	0.0113	0.0162	0.0049	0.007	0.001		0.004	0.0003	0.0006	0.0015	0.1976
	5	0.004	4.0508	3.1726	0.0972	1.4109	3.0601	0.4883	0.3393	0.12	0.0002	0.3086	0.0306	0.0072	0.0734	13.1644
	6	0.0053	3.3223	5.2582	0.0391	0.1385	2.454	0.3237	0.2929	0.3811	0.0026	0.437	0.0544	0.0075	0.064	12.8293
	7	0.0017	2.1755	1.9712	0.0505	0.0264	0.186	2.0991	0.2767	0.021		0.0363	0.0062	0.0422	0.0082	6.9015
	8		0.6046	0.5084	0.0035	0.0136	0.1006	0.2482	0.6458	0.0075		0.0109	0.0016	0.0146	0.0073	2.1667
	9	0.0015	1.6927	4.361	0.1048	0.0459	5.3631	0.0829	0.0385	0.5455	0.0027	0.4073	0.0134	0.0015	0.04	12.7508
	10		0.1174	0.0712	0.0008	0.0081	0.0202	0.07	0.0181	0.0019		0.0026			0.0025	0.313
	B		0.106	0.1734	0.0022	0.0103	0.5317	0.005	0.0131	0.0651	0.0185	0.1002	0.0022		0.0303	1.0584
	C		0.3219	0.4402	0.0102	0.0121	0.5371	0.1239	0.062	0.0521		0.8153	0.0075	0.0003	0.0093	2.3925
	D	0.0185	2.0565	2.208	6.4553	0.0728	2.5954	0.0545	0.0328	0.6851		4.405	0.0171	0.0029	0.1458	12.7995
	E	0.0008	0.5419	0.3851	0.0153	0.0169	0.188	0.0917	0.0922	0.0212	0.0003	0.0436	0.0901	0.0062	0.0098	1.5033
	F	0.0014	0.0619	0.0381	0.0132	0.0131	0.0292	0.0012		0.0006		0.0019				0.1639
	G		0.0005	0.0559		0.0028	0.0857			0.0399		0.0155				0.2103
		0.0486	30.539	31.0117	1.0111	2.1986	16.9314	5.6325	2.7453	2.083	0.0242	6.886	0.2813	0.103	0.4982	100

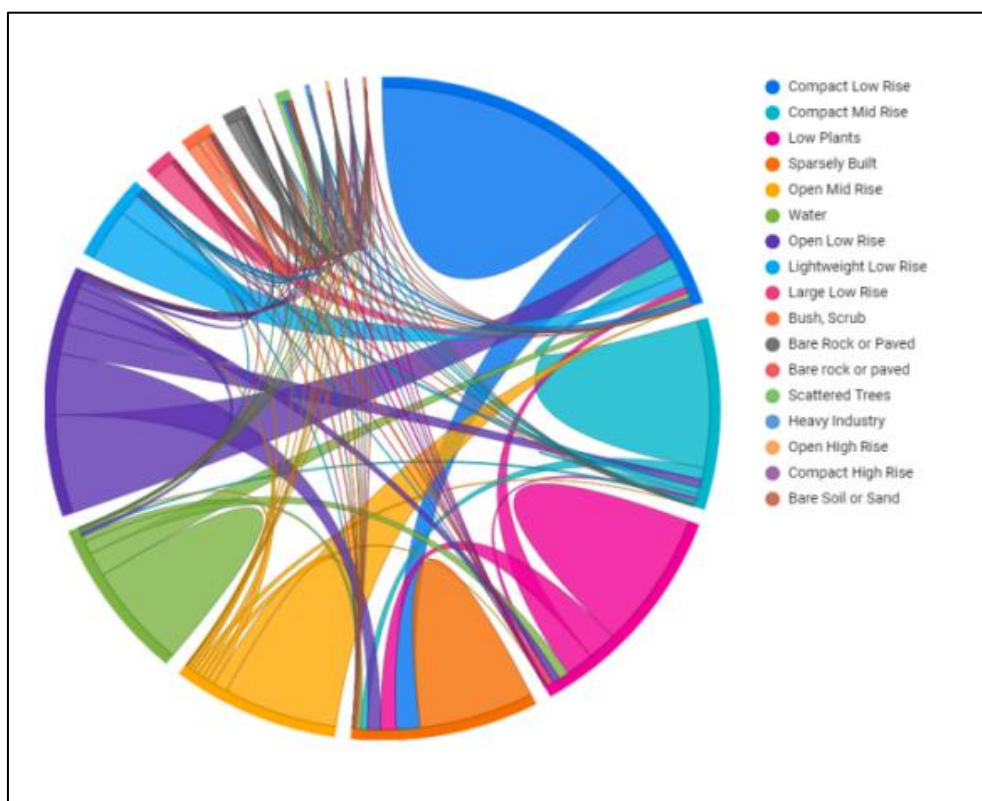


Figure 4.7. Shifting of Local Climate Zones 2003 to 2010 (Source: Author)

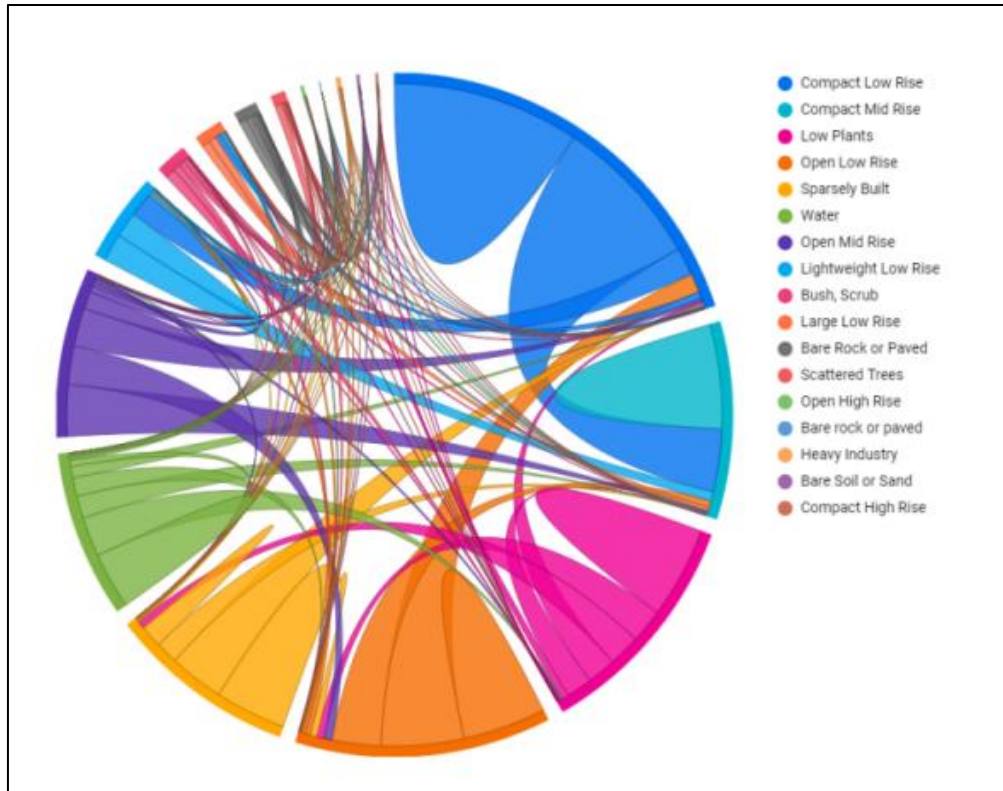


Figure 4.8. Shifting of Local Climate Zones 2010 to 2017 (Source: Author)

4.4 Comparative Analysis of Land-Use Land-Cover and Local Climate Zone Approach on Formation of Urban Heat Island

Local Climate Zone (LCZ) and Land Use/Land Cover (LULC) are two different concepts used in urban and environmental planning and analysis, each with its own focus and **purpose:**

Local Climate Zone (LCZ) is a classification system used to characterize different types of urban and suburban areas based on their surface cover characteristics, thermal properties, and influence on the local climate. LCZ classification helps in understanding how different urban areas impact the local microclimate, including temperature, wind patterns, and humidity. LCZ classification is more concerned with the micro scale climatic effects of various urban forms and materials.

Land Use/Land Cover (LULC) refers to the physical and functional features of the Earth's surface as categorized based on how the land is utilized and what types of coverage (natural or artificial) are present. It includes the categorization of areas into different types such as residential, commercial, industrial, agricultural, forested, water bodies, and more. LULC classification is important for various purposes like urban planning, environmental assessment, natural resource management, and land use planning.

LCZ **focuses** on the local climate and micro scale effects of urban features on temperature, wind patterns, and other climatic factors. Whereas LULC focuses on the characterization of the Earth's surface based on land usage and land cover types for purposes like land management, planning, and environmental analysis.

LCZ is concerned with a micro scale assessment of the local climate within urban areas and their immediate surroundings. LULC is more general and can encompass regional, citywide, or even larger **scale** analysis of land use and land cover patterns.

LCZ classification considers **factors** like surface cover, thermal properties, and their impact on microclimate. LULC classification considers factors like land use categories (e.g., residential, commercial, agricultural) and land cover types (e.g., forests, water bodies, barren land).

Table 4.6. Comparison between class of LULC and LCZ

LULC Class	LCZ Class
Built-up	LCZ 1: Compact high rise
	LCZ 2: Compact mid rise
	LCZ 3: Compact low rise
	LCZ 4: Open high rise
	LCZ 5: Open mid rise
	LCZ 6: Open low rise
	LCZ 7: Lightweight low rise
	LCZ 8: Large low rise
	LCZ 9: Sparsely built
	LCZ 10: Heavy Industry
Vegetation	LCZ A: Dense trees
	LCZ B: Scattered trees

Open space	LCZ C: Bush, scrub
	LCZ D: Low plants
	LCZ E: Bare rock or paved
	LCZ F: Bare soil or sand
Water	LCZ G: Water

In summary, LCZ is specific to analyzing the local climate effects of urban features, while LULC provides a broader understanding of how land is utilized and the types of coverage across a region. Both LCZ and LULC are essential for urban and environmental planning, allowing for better decision-making and sustainable development. Both LCZ and LULC are important and complementary in urban climate studies.

LCZ is more suitable for detailed analysis of the local climate within urban areas, providing insights into the microclimates and urban heat island effects. It is especially useful when focusing on understanding temperature variations and airflow patterns within a city.

LULC, on the other hand, provides a broader view of land use patterns and land cover characteristics across a larger region. It helps in understanding the overall urban structure, the distribution of different land use types, and how these patterns might affect the overall climate and environmental conditions.

Hence the purpose of this study is to ‘Investigating the Relationship between Urban Heat Island, Sky View Factor’, local climate zone is considered for detailed and precise understanding.

4.5 Chapter Summary

This chapter is an attempt to analyze the comparison between LULC and LCZ characteristics of urban structure and urban cover of the Kolkata city in order to understand the suitable approach for UHI studies as per set objectives of this research. Subsequently 4 types of LULC and 16 types of LCZs have been identified. The generic built forms were formed based on the building by laws of Kolkata

Municipal Corporation. For analysis, 12 survey locations were selected. The points at which the measurements were carried were selected on the basis of its orientation (in this case North-South and NESW), road width varying from 3m to 30m, built form types with horizontal and vertical uniformness and randomness. In north Kolkata the street canyon is mainly continuous type with no side setbacks, but in south Kolkata the side setbacks are present. Therefore, the optimal orientation for a continuous type of street canyon is NE-SW, uniformity in building geometry is preferred, and more variability in constructed form geometry should be avoided in order to achieve the desired thermal comfort level outside.

The size of the SUHI effect in Kolkata has been calculated, and the estimated SUHI is between 5 and 6 degrees Celsius. The KMC area's intra-urban gradient of LST suggests that Kolkata is experiencing a strong UHI effect. The strong positive association between LST and NDBI indicates that one of the main causes of this city's UHI effect is its built-up density. The amount of green space and water bodies in Kolkata has decreased during the previous 20 years, raising the mean LST in the city.

It can be said that the multifaceted built environment in Kolkata is formed by the multifunctional characteristics of the city and is characterized by diversity and bears witness to the city's rich history, blending colonial-era architecture with contemporary urban development. As one of India's oldest and most significant cities, Kolkata's built environment reflects the cultural, economic, and social transformations it has undergone over the centuries.

The emergence of urban heat islands in Kolkata is significantly influenced by the unique features and characteristics of the built environment. Kolkata's architecture is strongly influenced by its British colonial past. During the British Raj, the city served as the capital of British India, leading to the construction of numerous iconic buildings and landmarks. Structures like the Victoria Memorial, St. Paul's Cathedral, the General Post Office, and the Writer's Building showcase an eclectic blend of neo-Gothic, Indo-Saracenic, and Renaissance architectural styles. These buildings serve as enduring symbols of the city's colonial heritage and are significant tourist attractions.

Kolkata boasts an extensive collection of heritage buildings, many of which have been well-preserved over the years. The city's northern part, particularly areas like B.B.D. Bagh (formerly Dalhousie Square), College Street, and Esplanade, is home to a plethora of such structures. Many of these buildings house government offices, educational institutions, libraries, and cultural centers, contributing to the city's cultural and administrative identity. Kolkata's residential neighborhoods are characterized by rows of century-old houses and apartment buildings that showcase architectural styles prevalent during the British era. These buildings often feature ornate facades, intricate balconies, and spacious courtyards. While some have been carefully maintained, others have undergone modifications over the years, blending historical elements with modern amenities. As a rapidly growing metropolis, Kolkata has witnessed extensive urban development and the construction of high-rise buildings, particularly in newer areas and suburbs. These contemporary structures cater to the city's burgeoning population and house residential apartments, commercial spaces, and modern amenities. The skyline of Kolkata has evolved significantly in recent decades due to these developments. As Kolkata continues to grow, urban redevelopment and revitalization efforts have become crucial for preserving its heritage while adapting to modern demands. Striking a balance between conserving historical structures and accommodating contemporary development remains a significant challenge for city planners and policymakers.

The oldest portion of the city region is located in north, central, and south-west Kolkata and is made up of the primarily commercial and industrial land use, includes Chitpur, Cossipore, Bagbazar, Shyambazar, Barabazar, Esplanade, and Garden Reach sectors. The city expanded to the south and east when the country gained its independence, in places like Tollygunge, Alipore, Ballygunge, Garia, The Eastern Metropolitan Area, and Joka, new buildings and roadways are being built in a comparatively organized manner. The newest urbanized area of the city is the southern periphery. The rural portions of Joka I and Joka II were included in Kolkata's purview in 2015. The biophysical environment of Kolkata, which contrasts with the built-up area, is a key factor in determining microclimates.

Chapter 5. COMPARATIVE ANALYSIS OF EXISTING AND PROPOSED SKY VIEW FACTOR ANALYSIS IN KOLKATA

5.1 Introduction

The study and analysis of Sky View Factor in relation to the Urban Heat Island phenomenon in Kolkata is of great importance. Kolkata, like many other urban areas, is experiencing the effects of heat islands due to its dense urban development and high population density. According to Oke, one significant aspect causing urban heat island is the urban geometry and how much it protects the urban area from the chilly night sky. In assessing the degree to which an urban region is protected from the sky, Oke highlights the importance of the sky view factor. The ratio of the sky viewed from an urban area's buildings to an unobstructed, clear sky is known as the "sky view factor". The concept of sky view factor analysis involves quantifying the amount of sky visible from different areas within a city. This analysis provides valuable insights into the level of exposure to the sun and the potential for heat accumulation within urban areas. The impact of sky view factor on the urban heat island effect in Kolkata can be assessed by understanding how changes in building height, density, and arrangement affect the amount of sky view factor in different parts of the city (Ying et al., 2022).

Sky view factor analysis is a method that evaluates the degree to which the sky is visible from a certain point. It involves analyzing aerial images or digital elevation models to calculate the percentage of visible sky in different directions. This information can be used by urban planners and scientists to assess how much sunlight reaches specific areas, as well as how hot they are likely to become.

In terms of urban heat islands (UHIs), sky view factor analysis has been shown to have a significant impact on understanding their formation and effects. The areas with low sky view factors tend to trap more heat and experience higher temperatures than those with high sky view factors. By using this type of analysis, we can better understand how UHIs form and identify strategies for mitigating their

negative impacts on human health, ecological systems, and energy consumption in urban environments.

5.2 Sky View Factor Analysis of Kolkata

SVF has been calculated using Python script that takes advantage of Digital Elevation Model data. To verify the correctness of the Python-based SVF calculation strategy, two standard approaches are used to validate, the photographic method, which analyses fish-eye lens images; and the preferred way, which uses remote sensing and GIS.

5.2.1 Sky View Factor Analysis using Fish-eye lens

As previously mentioned, a fish-eye lens, GIS software, and a Python script are used to get the sky view factor for a particular area in Kolkata. To extract SVF values from fish-eye lens and point vector data, we chose 18 locations inside the study area. Continuous SVF data are extracted using both the raster approach and a Python script. Fish-eye images were captured using a Nikon 610D camera and a Nikon 16 mm f/2.8D lens (Figure 5.1). Sky View Factor Calculator software, developed by Johnson & Watson (1984) is used to process all images.



Figure 5.1. Fisheye lens photographs (Source: Author)

5.2.2 Sky View Factor Analysis using GIS Software

The University of Szeged's Urban Climate Research Group created the SVF mapping program V1.1, which is used to determine SVF values from a database of vector

buildings. We used a calibrated radius of 200 m and an angle of 180° for this analysis. The study requires building polygons in the shape (.shp) file format with a point layer for the area where the SVF value is determined and a height field. The results are displayed as points.

Additionally, SVF values can be computed using QGIS software using UMEP plug-in. using a computerized surface model of the ground and buildings, a pixel-by-pixel sky view factor map is produced. The range of SVF values is from 1 to 0.0245. SVF ratings for high-rise building roofs are 1 since there is no blockage. Within an obscured area encircled by the building, SVF 0.0245 is visible.



Figure 5.2. Sky View Factor Map was created in QGIS using UMEP plugins. Spatial resolution is 10 meters (Source: Author)

5.2.3. Suggested method for calculating the Sky View Factor using Python

A Python-based script was created to assess from a digital surface model (DSM) on any platform with an Integrated Development Environment in order to get beyond the shortcomings of the current SVF computation methodologies. In order to maintain the best image quality, the script outputs a continuous sky view factor map in raster format, ideally ".tiff." A DSM is required as input.

The SVF map is produced by adding the SVF values at the pixel level, which produces a continuous SVF map. The script works well and can generate SVF results for a bigger area. SVF values are generated using Python 3.0 and the rasterio, numpy, math, and scipy modules. SVF values are extracted using the SVFpy module, which developed by Fernando Gomes of the Centro de Estudos da Metrópole, Brazil. The original script was working with Lidar data. The script was modified and corrected to extract SVF values from DSM. DSM is a necessary component that can be obtained by processing vector 3D building data or by using a set of Lidar data. The scripts are processed using the provided Observer height, Kernel size, and Radius. Until the process is complete, DSM checks the values at the pixel level.

The DEM's SVF values are extracted using a Python script. The GIS processing uses the EPSG 32645 (UTM Zone 45N) projection system, while the Python processing uses the DEM. All structures are thought to have flat roofs, and each structure's walls are the same height. To create input for a Python script, SRTM DEM was downloaded and edited with a 3D building database.

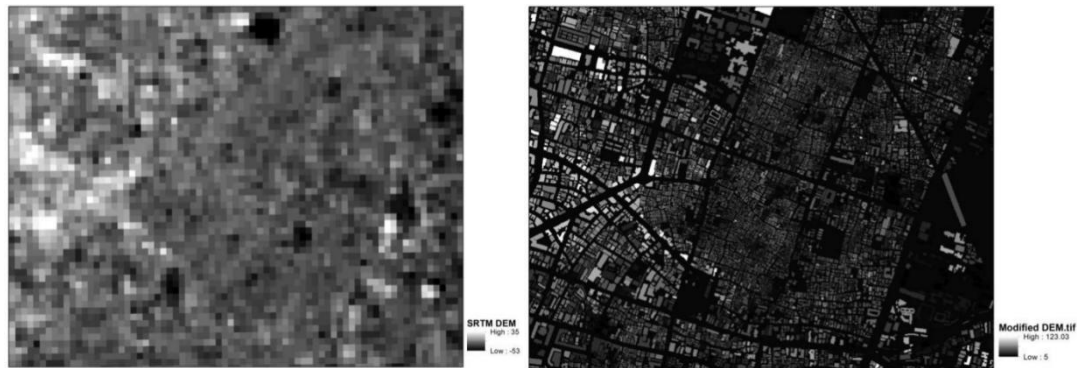


Figure 5.3. The spatial resolution of the SRTM DEM that hasn't been processed is 90 metres (first), whereas the processed DEM's spatial resolution is 10 metres (second) (Source: Author)



Figure 5.4. Python script was used to prepare the Sky View Factor map. 10 metre spatial resolution (Source: Author)

5.2.4 Comparative analysis of proposed method with existing method

SVF is calculated at 18 locations (Table 5.1) using various methods. These four approaches' SVF values are quite comparable to one another. The SVF steadily declines near buildings and narrow lanes, with low building density areas and building roofs displaying, correspondingly, higher values. With the exception of fish-eye lens techniques, vegetation and other obstructions are invalidated during SVF calculation. Because to vegetation and other obstructions (wires, poles, flex, banners, etc.), SVF values deviate from other methods by roughly 0.069. There is a significant correlation ($R^2 = 0.8734, 0.8677, \text{ and } 0.8490$) between the SVF Mapping tools V1.1, QGIS, Fish-eye lens, and Python Script approaches.

Table 5.1. Sky View Factor Analysis comparison

Point of Analysis	Python Script	SVF Mapping Tool V1.1 (radius 200m, direction 180°)	QGIS	Fish Eye Lens
1	0.812	0.903	0.892	0.821
2	0.621	0.581	0.570	0.501
3	0.721	0.703	0.714	0.583
4	0.786	0.843	0.795	0.651
5	0.923	0.882	0.853	0.855
6	0.972	0.932	0.927	0.869

7	0.824	0.878	0.731	0.697
8	0.623	0.625	0.598	0.61
9	0.618	0.561	0.546	0.527
10	0.746	0.765	0.704	0.683
11	0.834	0.815	0.798	0.787
12	0.678	0.692	0.665	0.631
13	0.432	0.534	0.486	0.401
14	0.591	0.599	0.545	0.565
15	0.310	0.317	0.301	0.270
16	0.841	0.845	0.840	0.839
17	0.398	0.438	0.422	0.390
18	0.512	0.518	0.503	0.478

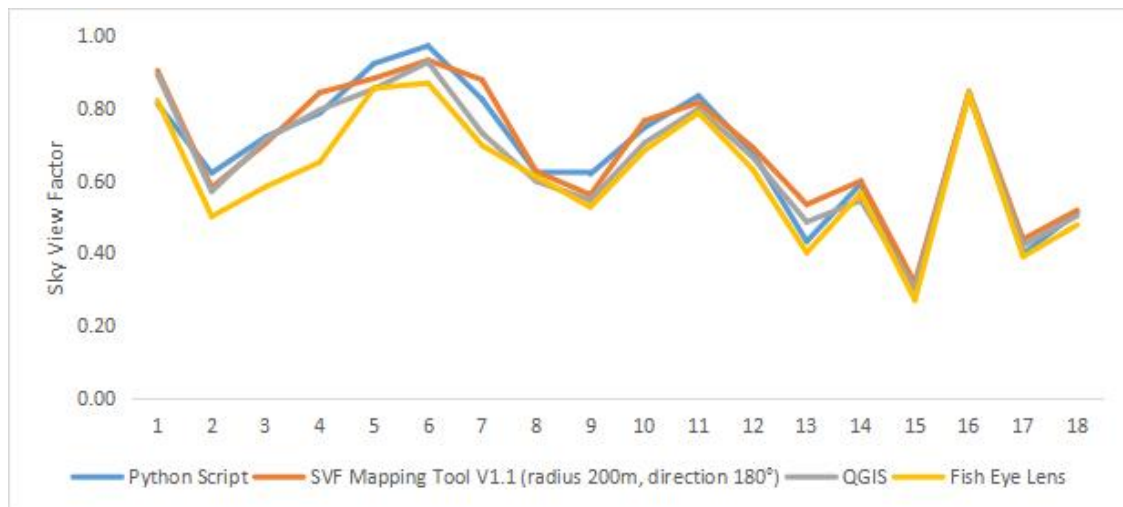


Figure 5.5. Comparison of SVF values between the SVF calculation methods at 18 locations (Source: Author)

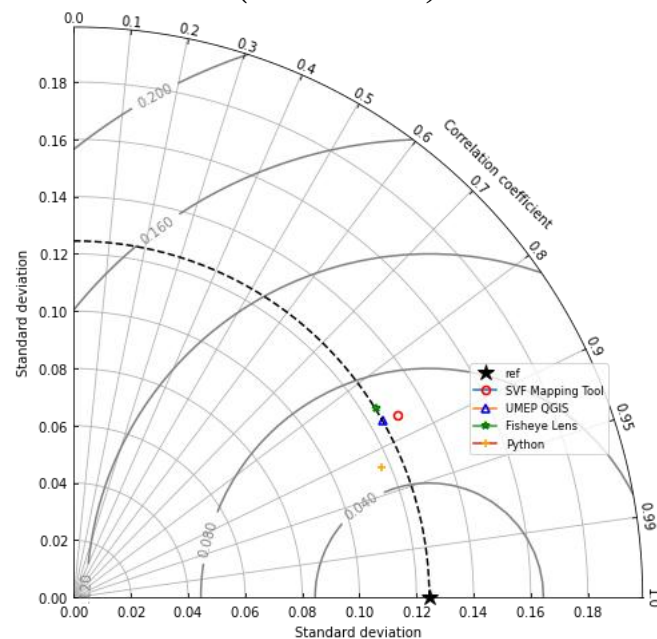


Figure 5.6. Validation results through Taylor Diagram between the SVFs calculated by the SVF mapping tool V1.1, QGIS, fish-eye images and Python script (Source: Author)

Fish-eye lens photographs, UMEP tool of QGIS, and Python script all indicated greater impediments; however, SVF Mapping Tool V1.1 regarded sky to be more visible. The data set should include all sky barriers, such as buildings, trees, and signboards, in a city like Kolkata in order to obtain findings with the highest degree of accuracy. As Kolkata is located in a tropical deciduous climate region, where trees lose their leaves in the winter, trees may instead have a significant impact on SVF, and that impact may change over time. The SVF value could therefore change between summer and winter. Only buildings were taken into account as sky obstructions in the GIS and Python script approaches, even if we are analyzing computing performance on certain SVF calculation methods.

To compare the results, the SVF values for the UMEP approach and the Python method were calculated 1 m above ground level, and SVF mapping tool V1.1 and fish-eye lens at pedestrian level photography were also carried out from 1 m ground. As a restriction, trees and other pieces of street furniture that are necessary to accurately portray the area could not be replicated using the remote sensing and GIS methods. It was anticipated that the SVF would be larger than those from the fish-eye lens photos due to the limitation of the Remote Sensing and GIS model, which did not take into account the obstruction produced by trees and other characteristics .

GIS and remote sensing techniques processed data more quickly than photography did. Python script employs free open-source frameworks, making it the most efficient and economical method for calculating SVF. Figure 5.6 demonstrates the connection between the Python script (Orange plus), the SVF Mapping Tool (Red circle), UMEP QGIS (Blue triangle), and the Fish-eye lens (Green star). A black dotted line representing the reference SVF is displayed, with the SD value normalized to 0.1245. Python's model works better with observations, as can be seen. SVF Mapping Tool model is larger than seen whereas fish-eye lens and UMEP QGIS are on par with observed standards.

5.3 Chapter Summary

This chapter delves into the various methods currently utilized to calculate sky view factors while highlighting their respective advantages and drawbacks. The photographic method, despite being meticulous and time-consuming, is recognized for its enhanced accuracy in determining sky view factors. On the other hand, techniques such as GIS and RS methods are preferred for their efficiency in conducting analysis; however, concerns arise regarding the data accuracy they provide. In light of these considerations, it is proposed to introduce a novel approach based on Python programming that promises to deliver precise results in a significantly reduced time frame, thus offering a balanced combination of accuracy and efficiency in sky view factor calculations. By incorporating this innovative Python-based methodology, noteworthy improvements can be achieved in streamlining the analysis process while maintaining high levels of precision, proving to be advantageous for researchers and practitioners in the field of sky view factor assessment.

The entire procedure has been carried out to determine the sky view factor in Kolkata, India, a city with a flat topography. The analysis of the existing morphological in the chosen area as a consequence of this research yielded an average sky view factor of 0.7364. When using a fish-eye lens to take pictures of glass buildings, which reflect solar radiation, there have been various problems that have led to variations in SVF readings. The approach outlined can be applied to studies and projects dealing with urban climate modeling and climate planning.

Chapter 6. ANALYSIS OF THE RELATIONSHIP BETWEEN THE URBAN HEAT ISLAND AND THE SKY VIEW FACTOR FOR VARIOUS CLIMATE ZONES IN KOLKATA

6.1 Introduction

Following a review of relevant literature and data analysis, the assessment procedures for the relationship between the screen levels (air) temperature or SUHI intensity (ΔT), SVF, and LCZ were developed. Concrete road pavements, compact urban-built form, and a sizable percentage of compact mid-rise and compact low-rise buildings are the main features that set the Kolkata region apart. Several meteorological parameters and WUDAPT techniques were used to investigate the local climate zone. Numerous sampling locations are compared with the appropriate spot-on Google Earth photos from the same time period in order to validate LCZ. Additionally, the SVF derived using the four techniques and the local meteorological data from the same time period were used to validate the LST. The findings of a few significant studies are compiled in the paragraphs that follow. It is not a simple task to estimate the SVF for an entire urban environment in reality; for this reason, a sample region of sixteen sites was chosen. UHI intensity was estimated from these sites and LCZs were found. SVF values were calculated using both approaches, yielding all SVF values for each point. The analytical process (Figure 6.1) used by SVF, UHI, and LCZ.

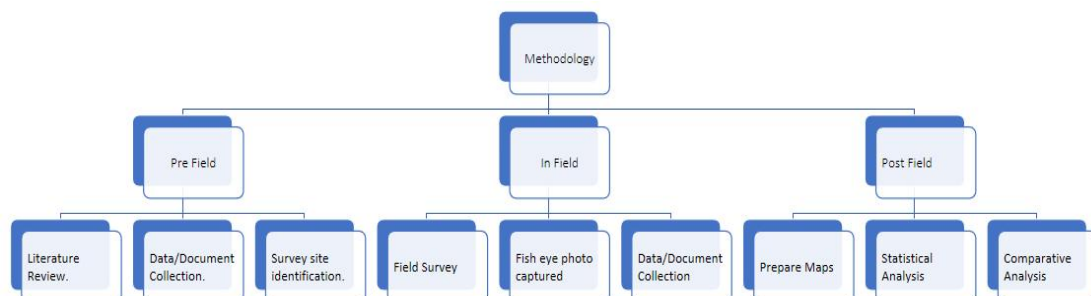


Figure 6.1. Flow diagram of comparative analysis study (Source: Author)

6.2 The Relationship between UHI and LCZ

Kolkata is highly urbanized with large areas classified as built-up LCZs. Kolkata's downtown, particularly in the north and center, is incredibly congested and packed and is primarily divided into LCZs 2, 3, 5, 6, and 7, which demonstrate the potential for significant UHI intensity. The increasing surface roughness over the cities due to higher building heights increases the frictional drag against the wind and has an impact on UHI. There is little visible separation between the city center and the suburbs, indicating high levels of urbanization and a big potential UHI distribution region. Some classes, including LCZs 1, 4, 5, and 6, as well as B and E, only include a few pixels in their samples. The UHI map shows hot spots in Kolkata's downtown areas to the north and southwest. It should be mentioned that over Dhapa in east Kolkata, there were significant hotspots. The temperature varies significantly between LCZ classes. The highest UHI among built-up LCZs is found in LCZ 8 (large low rise), whereas the highest LST among land covering LCZs is found in LCZ E (rock or paved cover). The complex and varied urban morphology of Kolkata's many LCZs may be the reason for the temperature drop from LCZ 3 to LCZ 6, which results in notable temperature variations between the LCZ classes. They might share similar thermal properties with the built-up LCZs because LCZ E in Kolkata represents the port and areas that have been reinforced with concrete and steel. Of all the LCZs, LCZ G (Water) has the lowest LST.

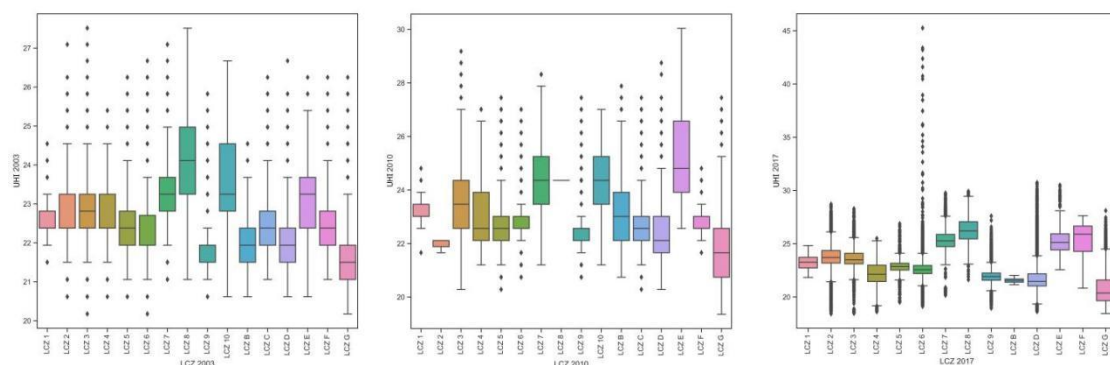


Figure 6.2. Boxplot showing the relationship between UHI and LCZ for the year 2003, 2010 and 2017 (Source: Author)

6.3 Urban heat Island extraction of Kolkata

Kolkata, India, is a prime example of a city with a severe UHI problem. The city's population has been growing rapidly in recent years, and this has led to an increase in the amount of impervious surfaces in the city. As a result, Kolkata experiences some of the highest UHI temperatures in the world. The land surface temperature pattern shows the concentration of UHI above or below mean LST based on the diurnal LST distribution maps. Standard score or Z-score had been calculated and mapped to determine the anomaly in UHI distribution. The peak thermal zone or urban heat islands were calculated from the Z-score map where the value of Z-score was equal to or greater than 1.5°C.

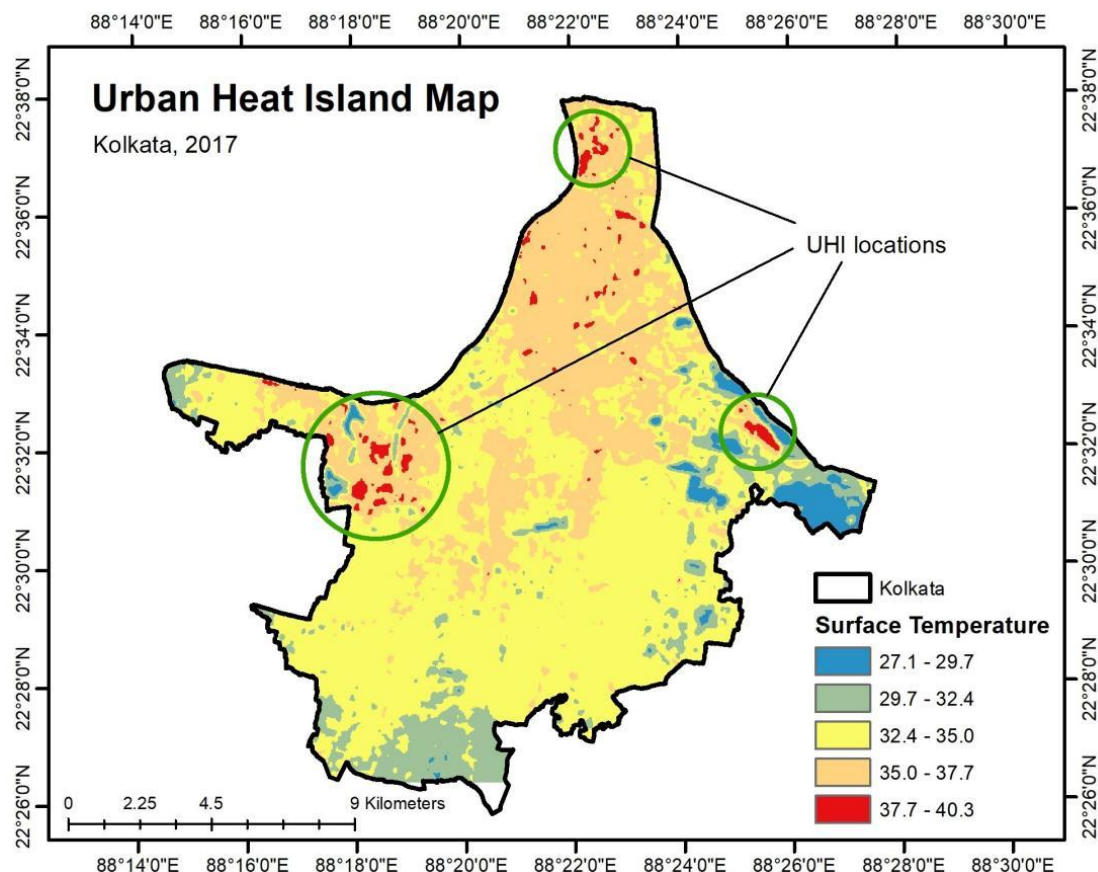


Figure 6.3. Urban Heat Island maps of Kolkata (Source: Author)

6.3.1 Comparison between classified Urban Heat Island during the year 2003, 2010 and 2017 of Kolkata

There are many urban hotspots found in KMC area where the Land Surface Temperature (LST) is almost 5 to 6°C higher than the surrounding urban areas. Hot spots are larger in size at South-West Kolkata but larger in number at North Kolkata. Old, flat roofed, metal roofed commercial buildings and mud tiles roofed slums are generating major urban hotspots. High-rise buildings are frequently found at Southern and South-Eastern Kolkata but interestingly this area is devoid of such hotspots due to dissected urban landscape and presence of vegetation than the rest part of KMC area. The LST map shows hot spots in Kolkata's downtown regions to the north and west. It is also reported that there were extended periods of high temperatures above Dhapa in east Kolkata.

Table 6.1. Minimum, Maximum and Mean temperature of Kolkata for the year 2003, 2010, and 2017

Year	UHI Minimum	UHI Maximum	UHI Mean	Standard Deviation
2003	20.17	27.52	22.39	0.87
2010	19.36	30.04	22.99	1.21
2017	18.42	45.26	23.26	1.43

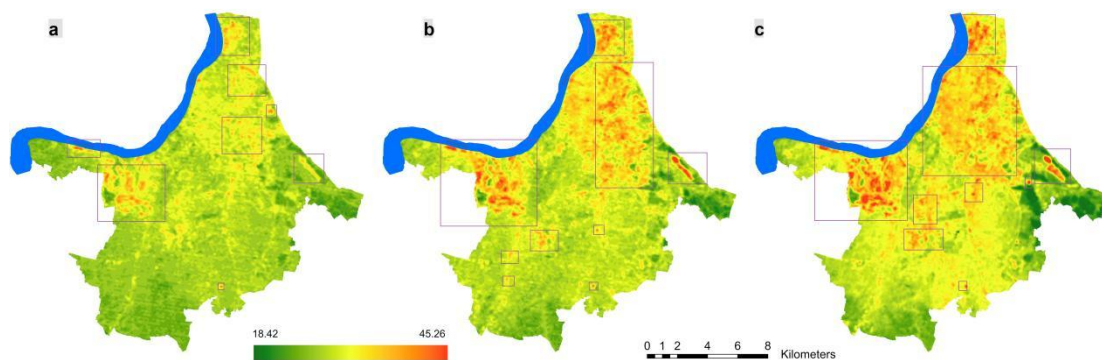
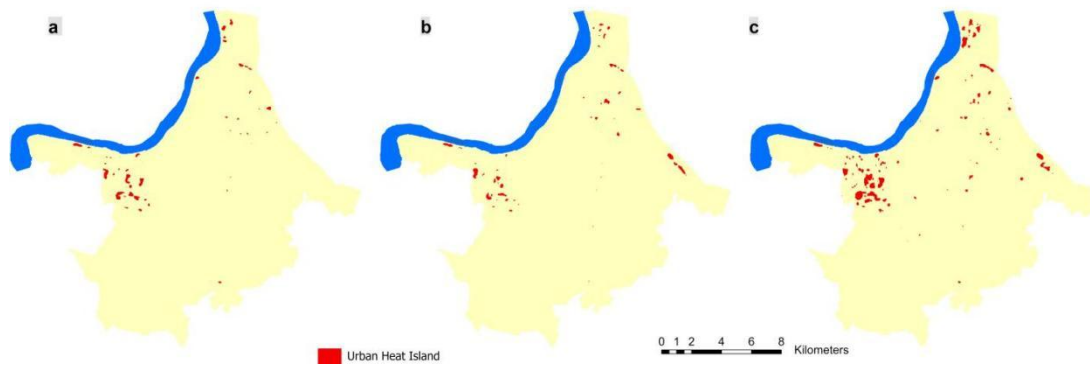


Figure 6.4. Land Surface Temperature Map of the year (a) 2003, (b) 2010 and (c)2017 showing the locations of Urban Heat Islands(Source: Author)



*Figure 6.5. Locations of Urban Heat Island of the year (a) 2003, (b) 2010 and (c) 2017
(Source: Author)*

UHI estimates are difficult since the planet's surface is formed of a variety of materials. (Qin & Karnieli, 1999). UHI is a critical governing factor in the physical processes of water balance and surface energy (Brunsell & Gillies, 2003; Kustas & Anderson, 2009; Qin & Karnieli, 1999). The characteristics of the urban heat island (UHI) influence have been explained using LST and surface imperviousness (Vlassova et al., 2009).

6.4. The impact of sky view factor on thermal environments in Kolkata

The results of the qualitative analysis show a negative correlation between UHI and SVF ($R^2 = -0.22$). Building height and degree of compactness also affect SVF values. Compact mid-rise building regions had the lowest SVF because of their less dense base and thin urban canopy layer. The old, dense urban core has fewer values and a much lower function trend. The presence of vegetation cover and overhead urban amenities causes some changes in SVF values in the photographic and GIS computation methods (i.e., electric posts, cables, hoardings, etc.). These facilities are not taken into account in GIS calculating methods. The unusually low mean SVF value is most likely a result of the deciduous leaf cover. This correlation shows that open urban building environments absorbed more solar radiation, while shading effects from trees might minimize sun exposure, which would eventually lead to a cooler climate on a diurnal scale. The huge low-rise urban environment's urban thermal heterogeneity has a lower SVF (0.598) score but absorbs more heat (31.34°C) mostly

because of its reduced green cover and metal roof. According to study, the climate in open building areas was therefore cooler than in compact building areas. UHI and a surface's ability to receive sunlight are closely connected. Given the existence of buildings and obstacle shadows, the surfaces of the densest sections warm more slowly.

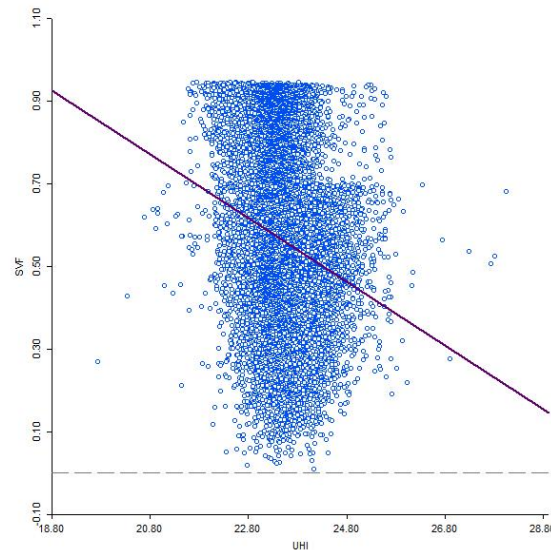


Figure 6.6. Correlation between SVF and UHI (Source: Author)

The result summarizes that increasing growth of urbanization reduces sky visibility and promotes the surface level heat emission in the city. Very positive land surface temperature deviation has been found at Chitpur, Shyambazar, Cossipore, Bagbazar, Bara Bazar, Narkeldanga, Garden Reach, Rajabagan areas where the mean diurnal LST values range from 33°C to 35°C. At the south and south-eastern fringe areas of Kolkata is very active zone of urbanization. Built-up density is gradually increasing in Jadavpur, New Garia, Santoshpur and Baghajatin. These new urbanized zones of Kolkata are gradually decreasing the SVF and contribute to increase surface heat emission in this part of the KMC area. Magnitude of UHI effect in the KMC area has been calculated in this study where the estimated UHI is 5°C to 6°C. This intra-urban gradient of LST in the KMC area indicates a strong UHI effect over Kolkata during the month of November.

Very Positive Correlation between LST and NDBI proves the built-up density is the one of the main causes of UHI effect of this metro city. Decreasing proportion of

green surfaces and water bodies also been observed during past two decades in the KMC area leads to increase of mean LST of Kolkata.

6.5 The Relationship between SVF and LCZ

Kolkata has a lot of low-rise structures, a lot of open space, and a lot of buildings. Compact mid-rise (LCZ 2) and compact low-rise (LCZ 3) make up about 60% of the area. Compact low rise and compact mid-rise have the lowest SVF values when it comes to open low rise and open mid-rise, which suggests a dense urban morphology and a smaller height-width ratio. Compact high rise (LCZ 1) can be seen on the eastern side of the city, scattered with a few patches.

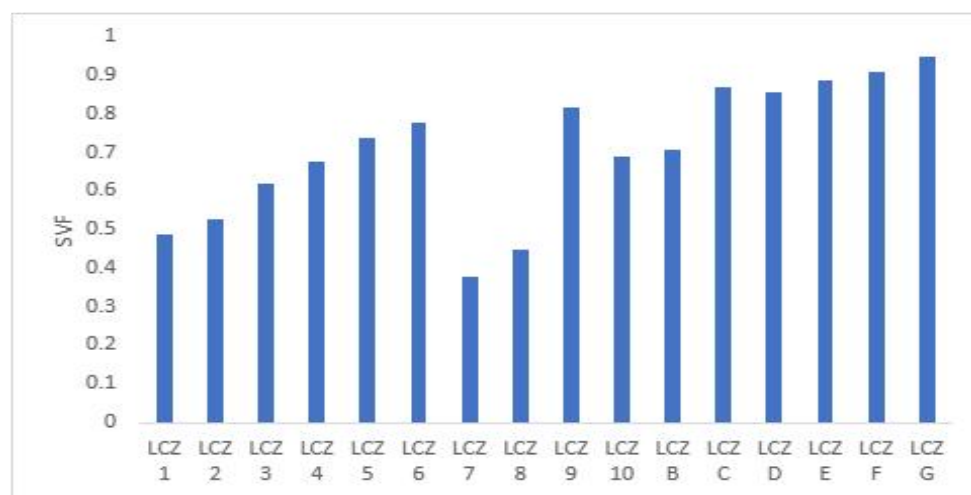


Figure 6.7. Mean SVF value on each LCZs (Source: Author)

6.6 Comparative Analysis between SVF, UHI and LCZ

A comparative study and analysis are conducted to identify the relationship of the UHI and SVF to each local climate zone. Urban development triggered a rapid change to the cities' landforms and as an impact land surface temperature varies within a short distance. The result of this analysis gives valuable information on urban climate study.

We found 16 local climate zones in Kolkata in 2017. 2 sq km area from each climate zone is selected for analysis. LCZ 7 and LCZ 8 are warmer within built-up classes and LCZ E and LCZ F are warmer within natural classes. This may be due to the surface

reflectance from old mud, asbestos, or flat roofs and congested built-up with narrow lanes. High rise areas (LCZ 1 and LCZ 4) are comparatively less warm than mid rise (LCZ 2 and LCZ 5) and low rise (LCZ 3, LCZ 6, and LCZ 9) areas. This may be due to the presence of rooftop vegetation and respectively wider roads that help to blow wind. LCZ 10 (Heavy Industry) is less warm than LCZ 7 and LCZ 8 but warmer than other built-up classes. Open or bare land (LCZ E and LCZ F) are warmer than vegetated land (LCZ B, LCZ C, and LCZ D). Water bodies (LCZ G) are relatively cooler within all LCZs.

Compact mid rise (LCZ 2) and low-rise regions (LCZ 3, LCZ 7, and LCZ 8) exhibit smaller NDVI, while open built-up classes (LCZ 4, LCZ 5, LCZ 6, and LCZ 9) and compact high rise (LCZ 1) have larger NDVI. The industrial area (LCZ 10) contains more NDVI indicating the presence of vegetation. As with the NDVI trend, a reverse trend is observed on NDBI. Lower NDVI and NDBI are observed on the bodies of water (LCZ G) due to the presence of algae and pollutants. It also observed that higher SVF are concentrated within the high rise and mid rise built-up areas. We extract SVF values by using the shadow casting method, so the maximum SVF is 1 as the building roofs have minimal or no shadows.

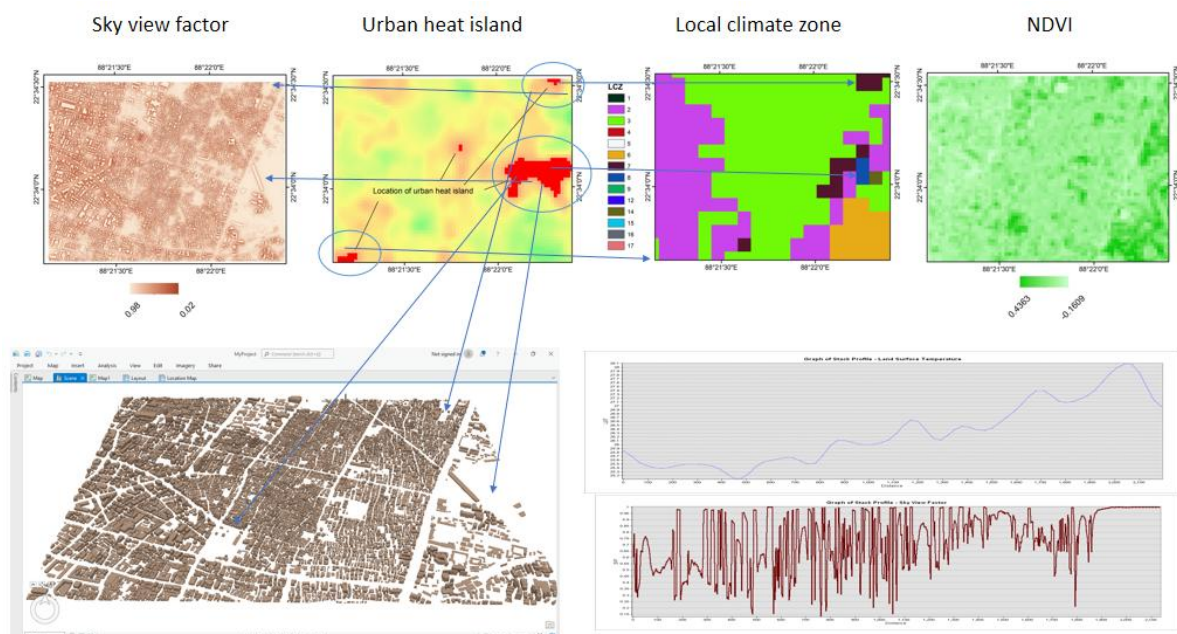


Figure 6.8. SVF, UHI, and LCZ comparison on a chosen (2 x 2 Sq Km) area in Kolkata. Building height is confirmed by a 3D map to affect sky visibility, temperature, and local climate zones. On the NDVI map, there is less vegetation and greater heat. Lower sky view factor in relation to increased temperature is seen by the stack profile.(Source: Author)

The following figures compare UHI and SVF for each local climate zone.

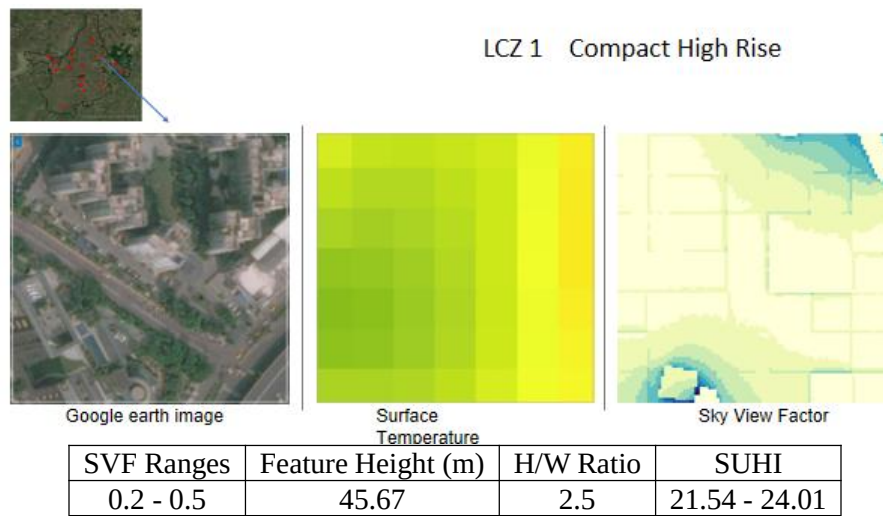


Figure 6.9. UHI and SVF comparison at local climate zone 1 (Source: Author)

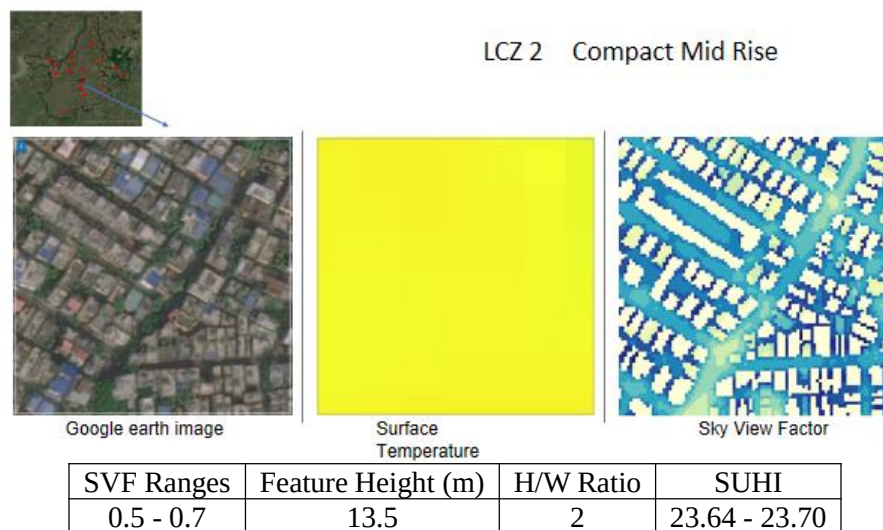


Figure 6.10. UHI and SVF comparison at local climate zone 2 (Source: Author)

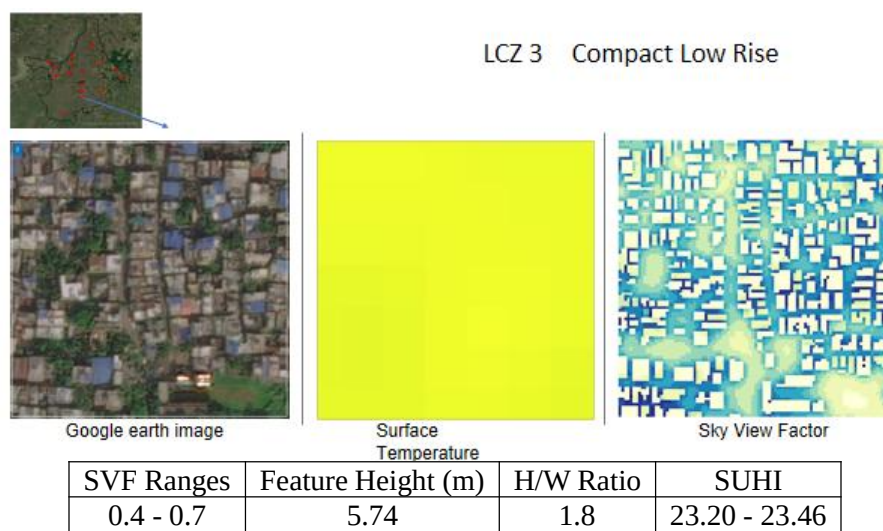


Figure 6.11. UHI and SVF comparison at local climate zone 3 (Source: Author)

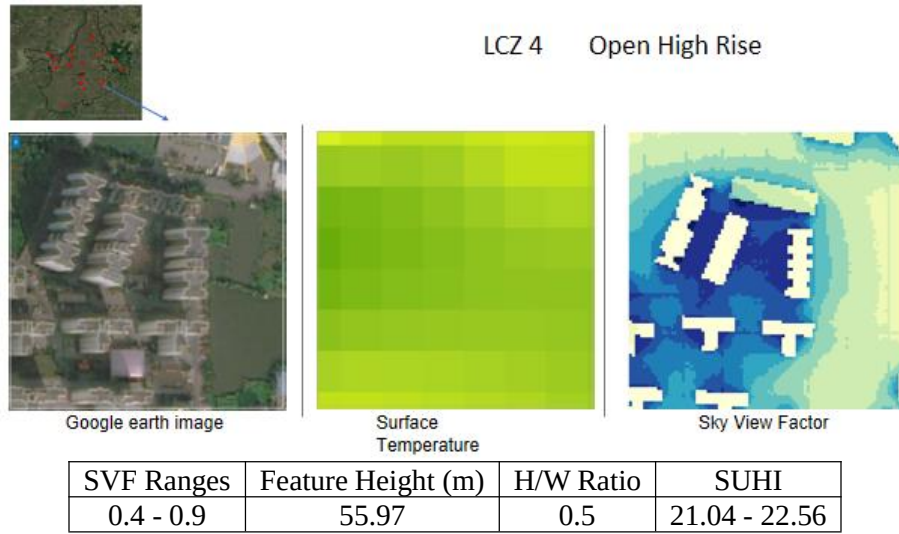


Figure 6.12. UHI and SVF comparison at local climate zone 4(Source: Author)

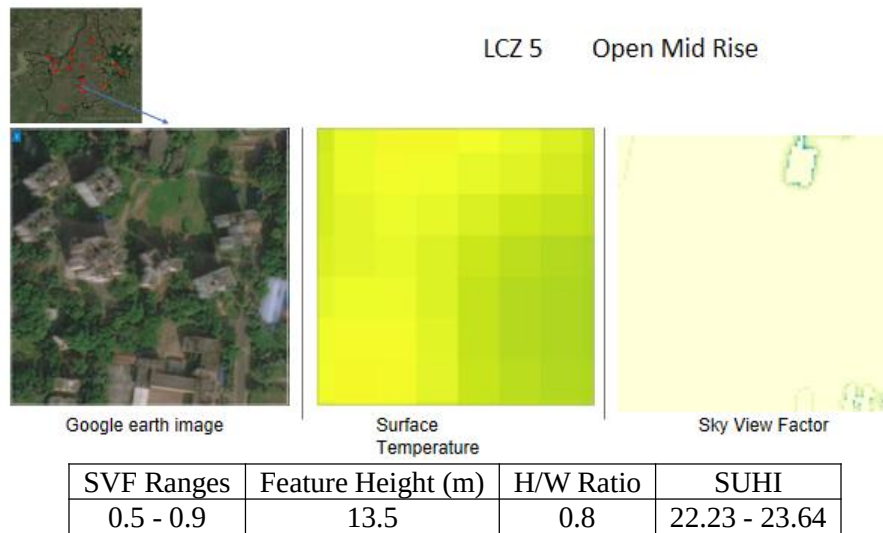


Figure 6.13. UHI and SVF comparison at local climate zone 5(Source: Author)

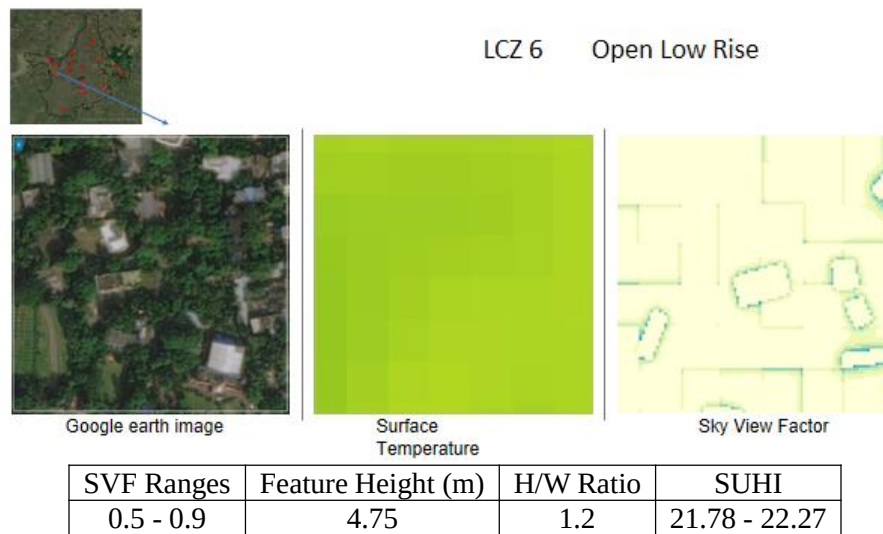


Figure 6.14. UHI and SVF comparison at local climate zone 6(Source: Author)

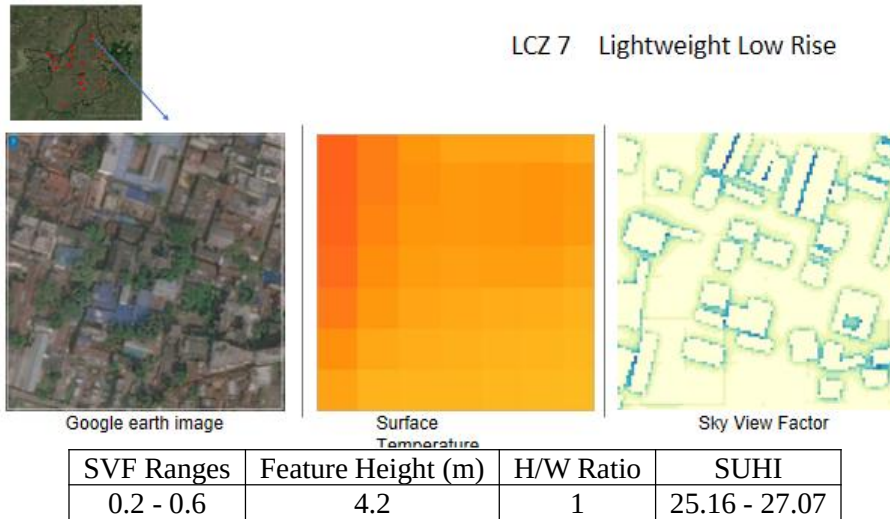


Figure 6.15. UHI and SVF comparison at local climate zone 7(Source: Author)

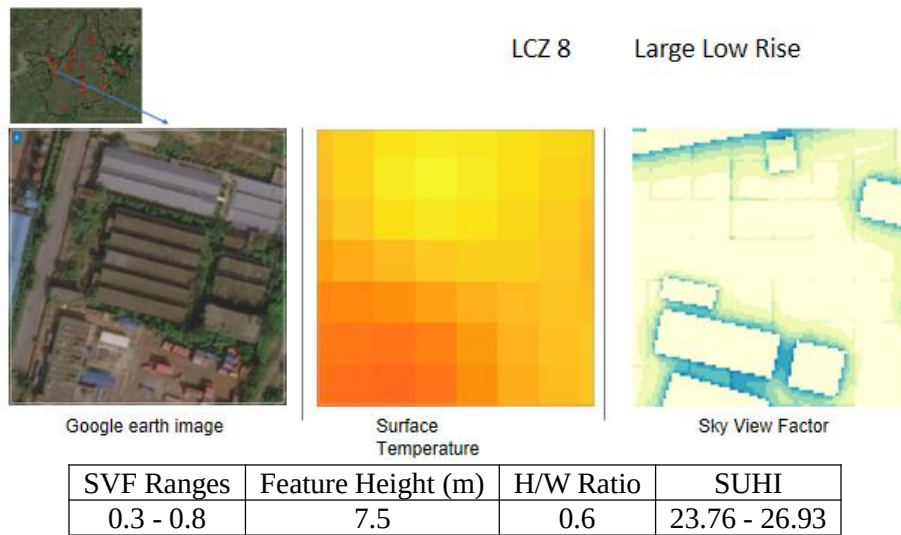


Figure 6.16. UHI and SVF comparison at local climate zone 8(Source: Author)

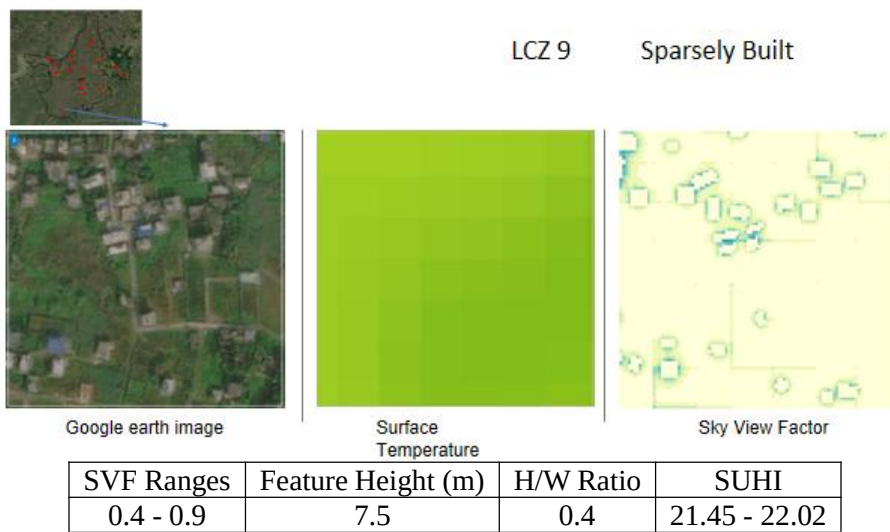


Figure 6.17. UHI and SVF comparison at local climate zone 9(Source: Author)

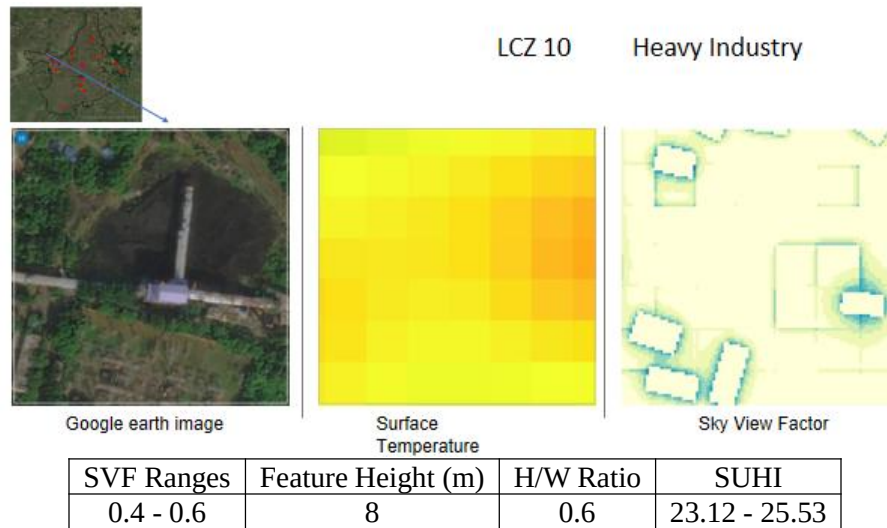


Figure 6.18. UHI and SVF comparison at local climate zone 10(Source: Author)

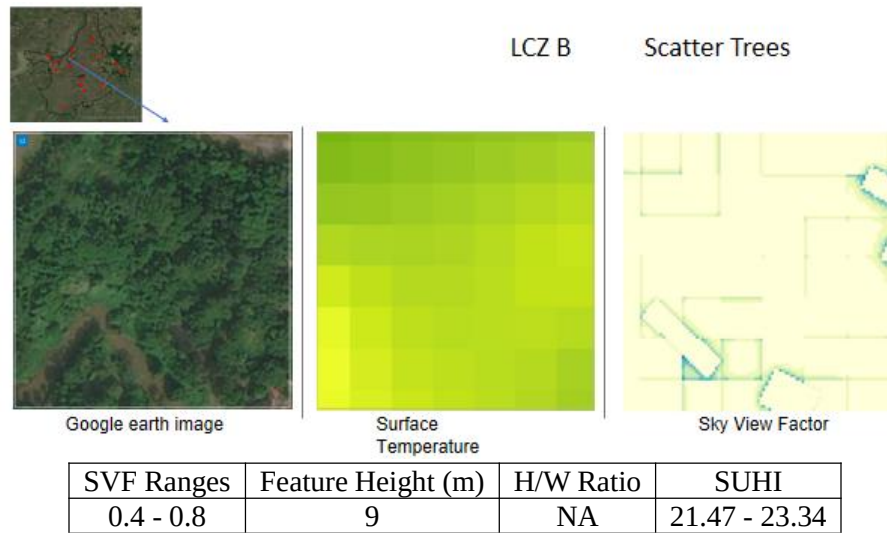


Figure 6.19. UHI and SVF comparison at local climate zone B(Source: Author)

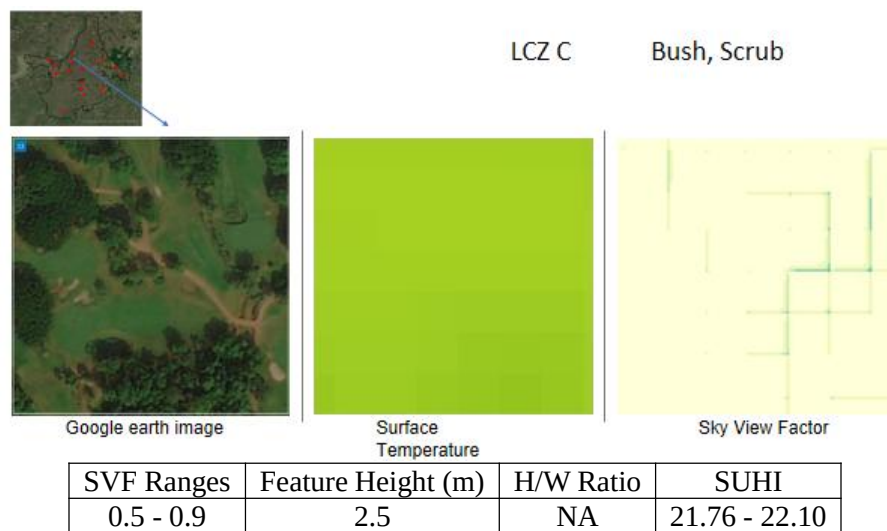


Figure 6.20. UHI and SVF comparison at local climate zone C(Source: Author)

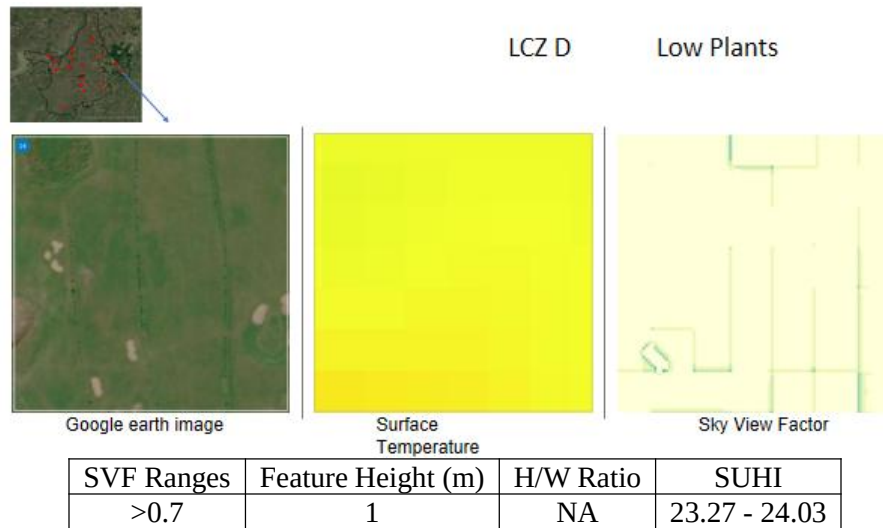


Figure 6.21. UHI and SVF comparison at local climate zone D(Source: Author)

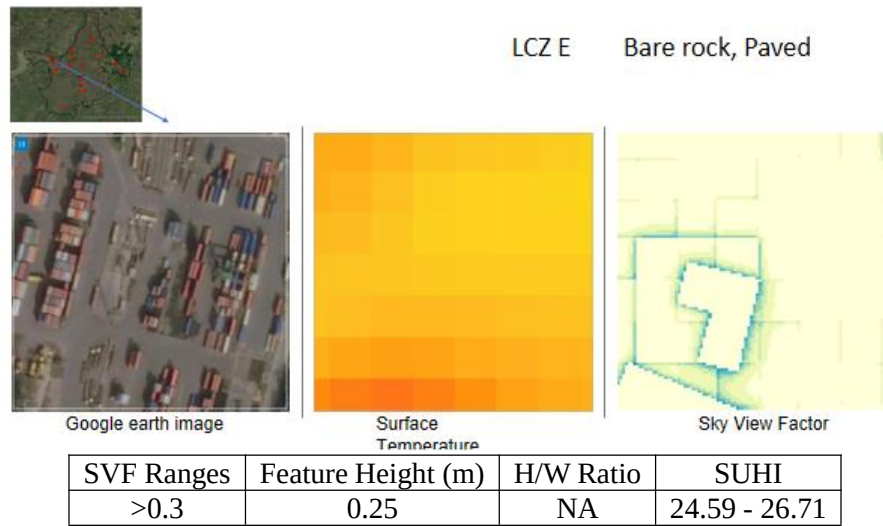


Figure 6.22. UHI and SVF comparison at local climate zone E(Source: Author)

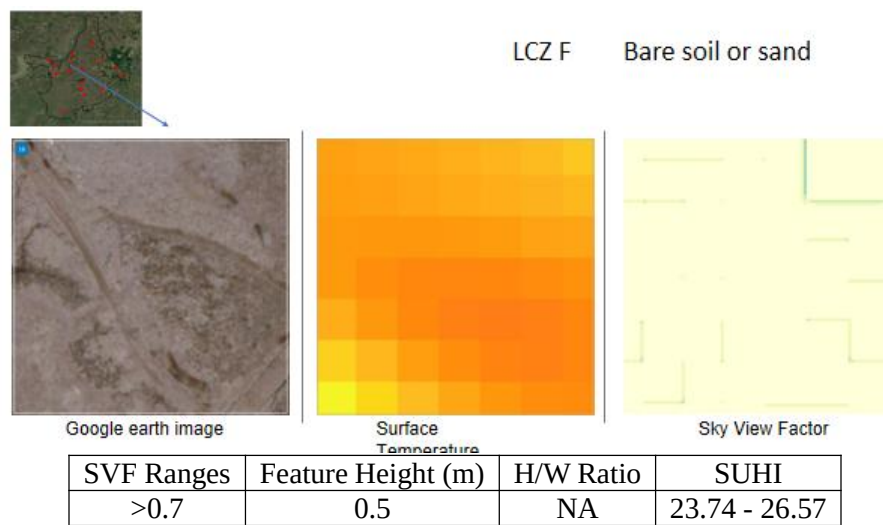


Figure 6.23. UHI and SVF comparison at local climate zone F (Source: Author)

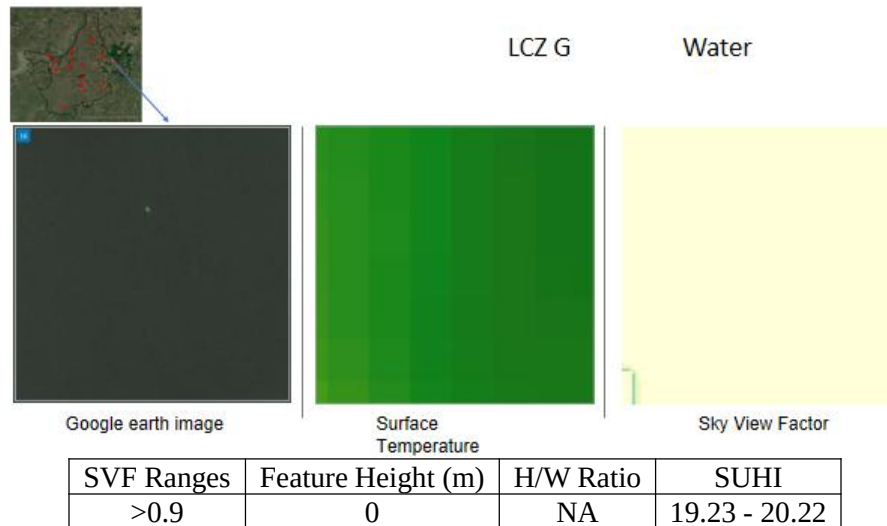


Figure 6.24. UHI and SVF comparison at local climate zone G (Source: Author)

6.7 Findings from analysis

The analysis's findings highlight the significance of urban design elements in SVF and SUHI at the local level. Because of this, the SUHI intensities rise as building density or the percentage of impermeable surfaces increases. This outcome is in strong agreement with the increase of vegetation the SUHI intensities decrease as the vegetation cover ratio raises latent heat fluxes in the air through evaporation and transpiration. Surface area ratio has a negative impact on SUHI, showing that areas with greater building shadowing and higher building heights have lower SUHI. Building height increases have a detrimental effect on SHUI as SVF lowers and congested or densely populated areas reveal. The SUHI intensity for Kolkata is $\Delta\text{TLCZ } 1-10 - \text{LCZ B-G} = 0.73^{\circ}\text{C}$. The SUHI intensity was calculated by "Average LST value of all available built up LCZs - Average LST value of all available natural LCZs". The positive values indicate the presence of SUHI at Kolkata (Shi et al., 2019). Built up LCZs are categorized as per various urban design factor into two groups, one group is with LCZ 2, 3, 4, 7, 8, and 10 and another group is with LCZ 1, 5, 6, and 9. Polling LCZs of a similar type into a data group for analysis could yield significant information for the construction of urban built-up regions. It is important to note that LCZ E, which forms SUHI, LCZ 9 and other naturally occurring LCZs (LCZ B, C, D, F, and G) are generating surface urban cool islands. SUHI intensity on LCZ 2, 3, 4, 7, 8, and 10 is $\Delta\text{TLCZ } 2, 3, 4, 7, 8, 10 - \text{LCZ B-G} = 1.17^{\circ}\text{C}$ and LCZ 1, 5, 6, and 9 is $\Delta\text{TLCZ } 1, 5, 6, 9 - \text{LCZ}$

B-G = 0.29°C. The factors of sky view factor and building density revealed significant correlations in LCZs 2, 3, 4, 7, 8, and 10. There are a low positive correlation is observed with LCZ 1, 5, 6, and 9.

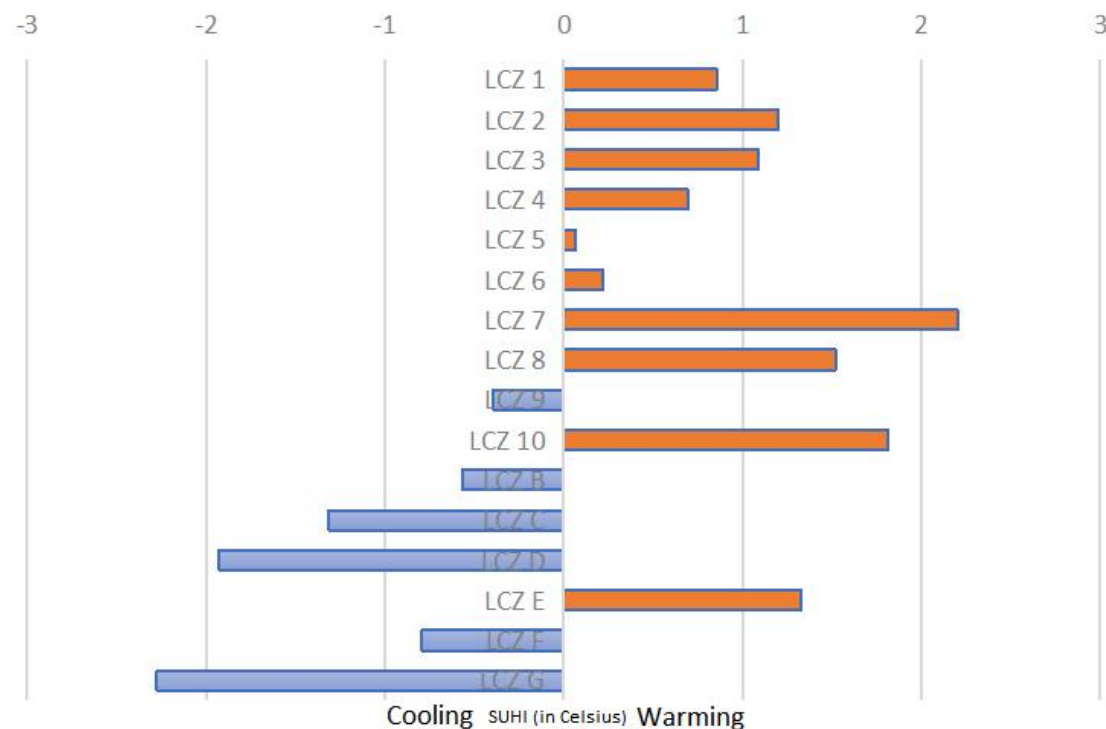


Figure 6.25. Intensity of heat islands and cool islands on LCZs (Source: Author)

The main findings from the analysis are as follows.

- ✓ Local climate zone 7 (lightweight low rise) and local climate zone 8 (large low rise) has maximum impact of SVF over UHI.
- ✓ UHI of Local climate zone 2 (Compact mid rise), 3 (Compact low rise), and 10 (heavy industry) is moderately impacted by SVF.
- ✓ In the local climate zones of 1 (compact high rise), 4 (open high rise), 5 (open mid rise), 6 (open low rise), and 9 (sparsely built), there is a low impact of SVF on UHI.
- ✓ Almost negligible impact of SVF on UHI is noticed on all natural local climate zones.
- ✓ The heat islands in an urban context can be formed by specific land uses and properties, including densely populated areas close to ports.
- ✓ A new approach is proposed to calculate sky view factor by using python script to overcome the difficulty of available SVF calculation methods.

6.8 Chapter Summary

An understanding of Kolkata's surface urban heat island generation in relation to the sky view factor may be gained from this study's distribution of land surface temperature and its variability. Furthermore, Kolkata's hot spot locations allow for up-close inspection of structures with large thermal capacities.

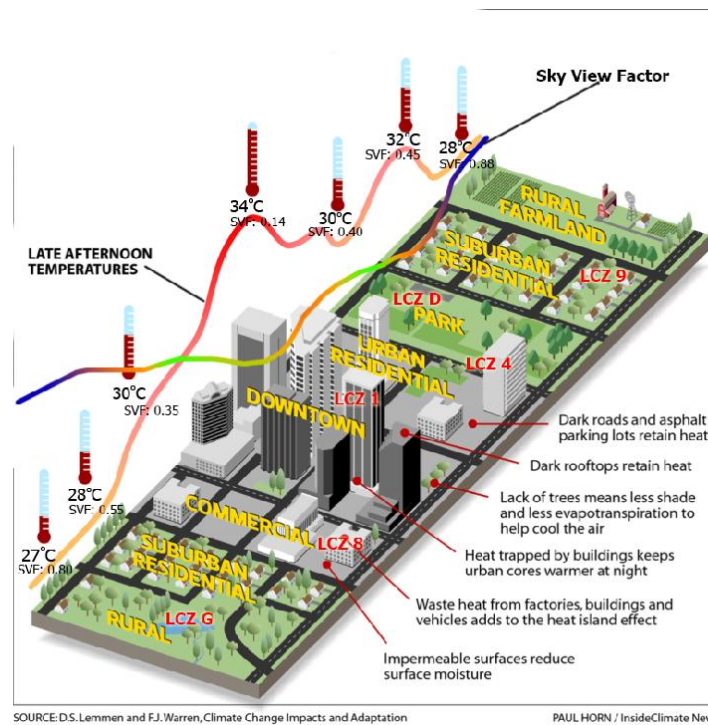


Figure 6.26. Schematic diagram of city, showing the variation of UHI and SVF over different local climate zones

The primary hotspots in Kolkata are evidently the enlarged flat-roofed buildings and the old residences with metal roofs, as confirmed by the ground verification and analysis of the Google Earth images.

Urban Heat Island and Climate zone study was conducted on entire Kolkata region, but Sky View is calculated only from sample site. Further need more details and elaborate sample to conclude and prospects.

This research was seen as a stepping stone in the research process since the findings will be used to provide the complete picture of the urban surface features in the study location. Around identifying the locations that were found to be hot spots or cold spots of the surface temperature along the study region, the data were also

used as a basic map to identify the various types of existing urban structure. The urban spaces are actually divided into various zones by the variability of the intra-urban spatial distribution of land surface temperature. Urban climate is an open system with energy continuously coming from space as solar radiation, with some of this solar energy converting to heat or terrestrial thermal radiation that warms the city air through convection, conduction, and advection processes. An important factor in creating climate-sensitive cities, particularly in tropical nations, is the regulation of urban surface heat. Urban planning currently gives great importance to sustainable urban growth and ecological balance. Urban climatic study has taken into consideration the identification of urban thermal zones in the city area and the spatial identity of Kolkata in terms of the urban thermal behaviour of various built-up areas.

The mean minimum atmospheric temperature over Kolkata is 2°C to 3°C higher than the rural surroundings. Urban heat islands and the sky view factor superimposed on local climate zones provide a clear indicator of which local climate zones are susceptible to urban heating.

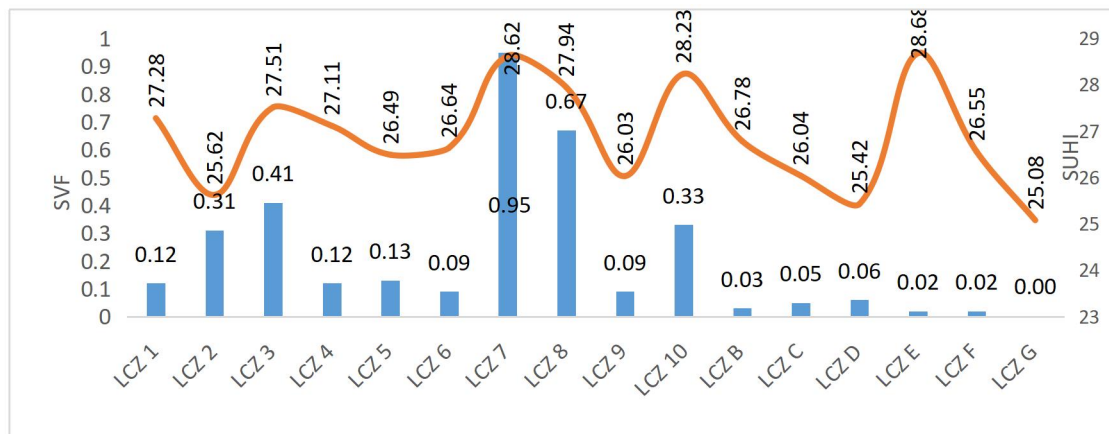


Figure 6.27. Correlation bar between UHI and SVF on different LCZs at Kolkata
(Source: Author)

Table 6.2. Demonstrates the SVF of Kolkata deviates slightly from Stewart and Oke's suggested range in various LCZ classes. Temperatures are higher for LCZ 1, LCZ 2, LCZ 3, LCZ 7, LCZ 8 and LCZ 10 compared to other LCZs.

Local Climate Zones		Properties of Other Cities as per Iain D. Stewart, Stewart & Oke (2012)			Properties of Kolkata			
		SVF Ranges	Feature Height (m)	H/W Ratio	SVF Ranges	Feature Height (m)	H/W Ratio	SUHI (Celsius)
LCZ 1	Compact High Rise	0.2 - 0.4	>25	>2	0.2 - 0.5	45.67	2.5	21.54 - 24.01
LCZ 2	Compact Mid Rise	0.3 - 0.6	10 - 25	0.75 - 2	0.5 - 0.7	13.5	2	23.64 - 23.70
LCZ 3	Compact Low Rise	0.2 - 0.6	3 - 10	0.75 - 1.5	0.4 - 0.7	5.74	1.8	23.20 - 23.46
LCZ 4	Open High Rise	0.5 - 0.7	>25	0.75 - 1.25	0.4 - 0.9	55.97	0.5	21.04 - 22.56
LCZ 5	Open Mid Rise	0.5 - 0.8	10 - 25	0.3 - 0.75	0.5 - 0.9	13.5	0.8	22.23 - 23.64
LCZ 6	Open Low Rise	0.6 - 0.9	3 - 10	0.3 - 0.75	0.5 - 0.9	4.75	1.2	21.78 - 22.27
LCZ 7	Lightweight Low Rise	0.2 - 0.5	2 - 4	1 - 2	0.2 - 0.6	4.2	1	25.16 - 27.07
LCZ 8	Large Low Rise	>0.7	3 - 10	0.1 - 0.3	0.3 - 0.8	7.5	0.6	23.76 - 26.93
LCZ 9	Sparsely Built	>0.8	3 - 10	0.1 - 0.25	0.4 - 0.9	7.5	0.4	21.45 - 22.02
LCZ 10	Heavy Industry	0.6 - 0.9	5 - 15	0.2 - 0.5	0.4 - 0.6	8	0.6	23.12 - 25.53
LCZ A	Dense Trees	<0.4	3 - 30	>1	NA	NA	NA	NA
LCZ B	Scatter Trees	0.5 - 0.8	3 - 15	0.25 - 0.75	0.4 - 0.8	9	NA	21.47 - 23.34
LCZ C	Bush, Scrub	0.7 - 0.9	<2	0.25 - 1	0.5 - 0.9	2.5	NA	21.76 - 22.1
LCZ D	Low Plant	>0.9	<1	<0.1	>0.7	1	NA	23.27 - 24.03
LCZ E	Bare rock, paved	>0.9	<0.25	<0.1	>0.3	0.25	NA	24.59 - 26.71
LCZ F	Bare Soil or sand	>0.9	<0.25	<0.1	>0.7	0.5	NA	23.74 - 26.57
LCZ G	Water	>0.9	0	<0.1	>0.9	0	NA	19.23 - 20.22

Positive correlation exists between the sky view factor and urban heat island. The fact that there is a modest association suggests that other factors, such as street orientation, wind flow, building and roof materials, appliance use, vehicle emissions, the presence of flora and water-bodies, etc., may also be at play. The correlation bars between SVF and UHI on each LCZ in Figure 6.27 reveal that LCZ 7 has the most influence from SVF, whereas LCZ 2, LCZ 3, LCZ 8, and LCZ 10 have a moderate impact. The impact of SVF on heat generation is minimal in LCZ 1, LCZ 4, LCZ 5, LCZ 6, and LCZ 9. Natural LCZs LCZ B, LCZ C, and LCZ D have minimal effects on SVF, but LCZ E, LCZ F, and LCZ G have insignificant effects.

Chapter 7 CONCLUSION AND RECOMMENDATION

7.1 Conclusion

The urban morphology, built up structures, roof materials and landscape play major role to increase relatively higher temperature. Over time, the overall urban heat islands rises for all local climate zones. Sky View Factor can be identified as an important indicator to analyze urban heat island effects, also providing a reliable basis for urban construction and planning.

The overall idea of the study is to investigate the relationship between UHI and SVF for different LCZs in Kolkata city is not prevalent as per global warming effects are concerned. As seen from the research, the thermal level varies considerably within the city with a direct relationship to land use and vegetation. High temperatures that have been reported in the city's environs can have an effect on the local community by raising peak energy use, air conditioning expenses, air pollution, and the risk of heat-related disease and death. If ignored, hot air over cities can potentially affect regional wind and precipitation patterns.

Kolkata is surrounded by the river Ganges in the west, East Kolkata wetland in the east and other municipalities in the north and south. As city expansion is limited, with the increase of population and various economic activities the city face land shortage, which force towards vertical expansion and environmental challenges like increase of temperature, decrease of natural vegetation and water bodies. These activities accelerate the transformation mainly from low rise (LCZ 3, LCZ 6, LCZ 7, LCZ 8 and LCZ 9) to mid-rise (LCZ 2 and LCZ 5) and high-rise (LCZ 1 and LCZ 4) urban morphology. From the study it been identified that 11% of vegetation land (LCZ B, LCZ C and LCZ D) changed to built-up (LCZ 1 to LCZ 10) land within 2003 to 2017. At the same time, there was conversion (7%) of compact low rise (LCZ 3) to compact mid rise(LCZ 2). Regular changes of local climate zones have major environmental impact, may generate various health problems and change the level of urban comfort.

Appropriate land use planning, climate responsive building guidelines, planning for green areas, open space and water bodies should be taken into account by the urban planners and civic body. It can be summarized that Local climate zone is an important parameter for framing any regulatory guidelines and development control tools for sustainable urban planning.

It has been found that the high thermal zone throughout the day and night is a compact mid-rise with a few dispersed trees. As most diurnal and nocturnal heat islands are connected to this micro-climate zone, it contributes to the rise in surface temperature in north and central Kolkata. Most upscale areas of east, central, and south Kolkata are open high-rise and compact mid-rise with sporadic trees and water. The major characteristic of this LCZ is the presence of deep urban canyons, which trap heat during the day and increase nocturnal thermal radiation in this urban climatic zone of Kolkata. In the KMC region, LCZ 2 and LCZ G were cool local climate zones with compact mid-rise buildings covered in dense trees and bodies of water. Due to the high surface albedo (18% to 20%), it was the coolest LCZ in Kolkata, and multiple urban cold spots were discovered here. Due to the existence of the East Kolkata Wetland and numerous other large bodies of water, the LCZ G, LCZB, LCZ 4, and LCZC microclimate zones in the eastern half of the KMC area constitute a diurnal cold area and a night-time potential thermal region.

The study will implement diverse possibilities and will be useful for future urban studies. The morphological factors, which are important for influencing urban climate in order to know and understand the process.

The study also built the possibility for the estimation of relevant meteorological information in complex structures and environments.

Urban centres have low solar radiance factors (SVFs), which can create a shadow effect that cools the city, particularly in the early morning during low sun angle periods. While some studies have identified a correlation between SVF and urban air

temperatures, there are significant differences between the two, and caution must be exercised when equating low SVF values with high amounts of urban heating.

To effectively assess the extent of the UHI effect, a thorough method that examines a variety of extra variables in addition to SVF values, such as albedo, heat capacity, surface emissivity, and surface roughness, would be more appropriate.

The study takes into account how building geometry affects the microclimate in cities. Future research is anticipated to provide additional light on other variables, including vegetation, geography, human heat output, and heat fluxes associated to urban planning. By examining the local climate zone map, it has been determined which form of development has the most impact on urban heat islands. It is obvious that LCZs 1, 2, 3, 7, 8, and E have the greatest potential to produce heat islands. While LULC-based approaches can only identify where there are more built-up regions that produce heat. In connection with this, it may be claimed that there is a greater possibility for heat generation when the sky view factor is less than 0.5.

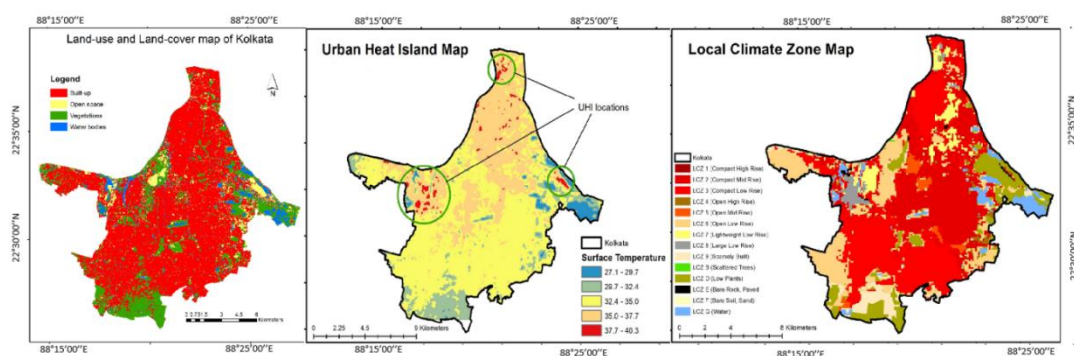


Figure 7.1. LULC, UHI, and LCZ in Kolkata (Source: Author)

The microclimate analysis of the urban built form, together with experimenting with mitigation techniques, is one of the most crucial approaches toward planning for climate-resilient cities, according to a comparison of building and urban environments between 2003 and 2017. It is crucial to note that the results are only applicable to a small number of sample study areas and certain hours of the day. Therefore, it may be inferred that more research is necessary to incorporate these factors in a more comprehensive perspective. This suggested study should be broadened by utilizing other satellite sensors, taking into account various times of the day, and repeating the analysis.

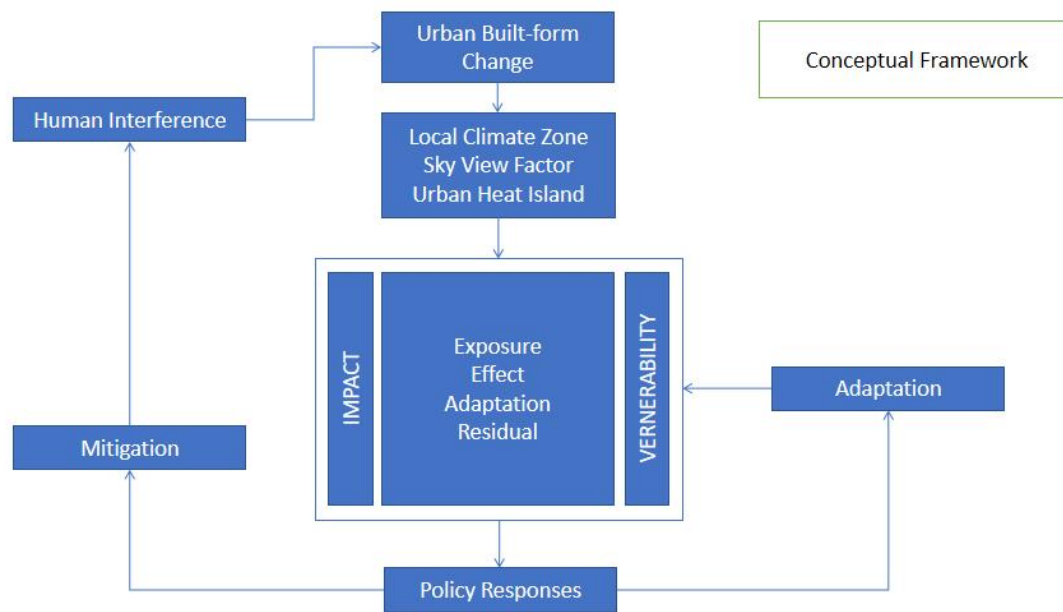


Figure 7.2. Conceptual framework of the study (Source: Author)

Urban designing and spatial planning in Kolkata should pay particular attention to these urban local-climate zones to reduce UHI and increase surface albedo in high thermal micro-climate zones, restore greenery, and conserve urban water bodies. This will make the city more comfortable and environmentally friendly. The study's results are discussed below.

7.1.1 Comprehend the facets of urban heat island in cities alongside how it affects the local climate zone.

The Kolkata city is primarily distinguished by compact urban-built form, concrete road pavements, and a significant portion of compact mid-rise and compact low-rise structures. Kolkata's downtown districts, particularly those in the north and center, are incredibly packed and compact and are mostly categorized into LCZs 2, 3, 5, 6, and 7, which exhibit the potential for significant UHI intensity. There is little visible separation between the city center and the suburbs, indicating high levels of urbanization and a big potential UHI distribution region. In the northern part of the city the street canyon is mainly continuous type with no side setbacks. The H/W ratio is >2 . In the southern part wider in respect to northern part with newly developed high rises.



Figure 7.3. Height-width ratio of Kolkata streets (Source: Author)

The study has shown a rapid landscape transformation occurred in the last 15 years. In 2003, the vegetated area and water body contain more land use type, but it continuously decreased until 2017. There had been a certain increase in the urbanized sector (76.12% to 83.72%) and it is observed that the maximum city transformation occurred in 2010 – 2017 in respect to 2003 – 2010.

A comparative study and analysis are conducted to identify the relationship of the urban aspects on each local climate zone. Urban development triggered a rapid change to the city's landforms and as an impact land surface temperature varies within short distance. The result of this analysis gives valuable information on urban climate study.

We found 16 local climate zones at Kolkata in the year 2017. 2 sq km area from each climate zone is selected to analysis.

From the analysis, it has been observed that LCZ 7 and LCZ 8 are warmer within built-up classes and LCZ E and LCZ F are warmer within natural classes. This may be due to the surface reflectance from old mud, asbestos or flat roofs and congested built-up with narrow lanes. High rise areas (LCZ 1 and LCZ 4) are comparatively less warm than mid-rise (LCZ 2 and LCZ 5) and low rise (LCZ 3, LCZ 6 and LCZ 9) areas. This may be due to the presence of roof top vegetation and respectively wider road that help to blow wind. LCZ 10 (Heavy Industry) is less warm from LCZ 7 and LCZ 8 but warmer than other built-up classes. Open or bare land (LCZ E and LCZ F) are warmer than vegetated land (LCZ B, LCZ C and LCZ D). Water bodies (LCZ G) are relatively cooler within all LCZs.

Smaller NDVI is observed on compact midrise (LCZ 2) and low-rise areas (LCZ 3, LCZ 7 and LCZ 8) whereas higher NDVI is observed on compact high rise (LCZ 1) and open built-up classes (LCZ 4, LCZ 5, LCZ 6 and LCZ 9). Industrial area (LCZ 10) contains more NDVI indicate presence of vegetation. Like NDVI trend, a reverse trend is observed on NDBI. Lower NDVI and NDBI are observed on the bodies of water (LCZ G) due to presence of algae and pollutant. It also observed that higher SVF are concentrated within high rise and midrise built-up areas. We extract SVF values by using shadow casting method, so the maximum SVF is 1 as the building roofs have minimal or no shadows.

7.1.2 Analyze the relationship between the urban heat island and the sky view factor

In Kolkata, there is an inverse link between the sky view factor (SVF) and the urban heat island (UHI). This implies that regions with a lower sky view factor typically have hotter temperatures, which exacerbates the UHI effect. The highest SVF recorded 0.93 (in LCZ 9), indicate sky is almost open and the lowest SVF is recorded 0.14 (in LCZ 3), indicate that the sky is almost obstructed by any standing object. The difference between highest and lowest SVF is 0.86 showing the huge variation of sky view factor within the study area. The mean SVF is 0.71 signifies that about 71% sky is visible in Kolkata's and the temperature distribution shares a low positive relationship in Kolkata. The minimum and maximum SVF values are similar for compact built-up areas (LCZ 1, LCZ 2, LCZ 3) and it can be summarized that only around ~10% sky is visible from these climatic zones. Whereas around ~50% of the sky is visible from open built-up areas (LCZ 5, LCZ 6). It also be observed that only around 7% of the sky is visible from open high built-up (LCZ 4), this may be due to building height and presence of vegetation within this climate zone. 8. Interestingly from lightweight low-rise areas (LCZ 7), the sky visibility is around 25%. Congested built-up creates narrow lanes cause high height-width ratio. Large Low Rise and Heavy Industry (LCZ 8 and LCZ 10) characterized with large low built-up with narrow lane whereas sparsely built-up (LCZ 9) area also show lower sky visibility, the reason can be presence of vegetation on this climate zone.

In addition to the previously stated component, surface material and roof material are important UHI control factors in Kolkata. It has been noted that certain places with wide skies and low-rise buildings also produce UHI. A thorough analysis reveals that built-up LCZs predominate there and that natural LCZs are barely noticeable. Additionally, areas with low SVF and high rise are comparatively less temperate. One of the main influences in those places is most likely the duration of the sun, wind and the pollution.

7.1.3 Urban built form characteristics and how they relate to SVF and UHI in respect to various LCZs.

Urban built form is the study of the three-dimensional shape of urban areas, with a focus on the relationship between buildings and streets. It is an important area of study for urban planning and design, as it can have a significant impact on the microclimate, air quality, and pedestrian comfort of urban spaces.

Kolkata is a dense and rapidly growing city with a diverse range of urban built forms. The city's historic core is characterized by narrow streets and tall buildings, while its newer suburbs are characterized by wider streets and lower buildings. Aspects of urban built form canyon geometry that are relevant to Kolkata include:

Aspect ratio (H/W Ratio): The aspect ratio of a street canyon is the ratio of its height to its width. A high aspect ratio indicates that the buildings are tall, and the street is narrow, while a low aspect ratio indicates that the buildings are shorter, and the street is wider. Kolkata has a mix of street canyons with both high and low aspect ratios. Chatterjee and Goswami (2015) found that street canyons with high aspect ratios had higher temperatures and lower wind speeds than street canyons with low aspect ratios.

Street orientation: The orientation of a street canyon can affect the amount of sunlight it receives and the prevailing wind patterns. Streets that are oriented north-south typically receive more sunlight than streets that are oriented east-west. Kolkata has a mix of street canyons with different orientations. Banerjee and

Chakraborty (2016) found that north-south oriented street canyons had higher temperatures and lower wind speeds than east-west oriented street canyons.

Building setbacks: Building setbacks are the distances between the edges of buildings and the property lines. Large building setbacks can help to create more open and airy street canyons. Kolkata has a mix of buildings with both large and small building setbacks. Mondal et al. (2017) found that buildings with large building setbacks had lower temperatures and higher wind speeds than buildings with small building setbacks.

Vegetation: Vegetation can help to shade and cool street canyons and improve air quality. Kolkata has a relatively low level of vegetation in its street canyons. Sen and Ray (2018) found that street canyons with more vegetation had lower temperatures and higher wind speeds than street canyons with less vegetation.

Table 7.1. Street width (m), aspect ratio, built form, and street orientation measured at the survey points.

Point	Street Width (m)	Aspect Ratio	Built form	Street orientation
1	3.8	1.2	Compact mid rise Compact low rise Low plant Water	N-S
2	20	1	Compact mid rise Scattered plant	E-W
3	18	2.4	Compact high rise Compact mid rise Scattered plant Water	E-W
4	3	3.1	Compact mid rise	NW-SE
5	6	2.5	Open mid rise Open low rise Scattered trees Low plants	NE-SW
6	8	1.8	Compact mid rise Scattered trees	E-W
7	6	4.2	Compact mid rise Compact low rise Scattered plant	N-S
8	6	3.8	Compact mid rise Scattered trees	N-S
9	6	5.4	Compact mid rise	NW-SE
10	30	0.4	Compact high rise Compact mid rise	N-S
11	18	0.8	Compact mid rise Scattered plant Water	NW-SE
12	6	1.7	Compact mid rise Scattered plant	N-S



1 (H/W 1.2)



2 (H/W 1)



3 (H/W 2.4)



4 (H/W 3.1)



5 (H/W 2.5)



6 (H/W 1.8)



7 (H/W 4.2)



8 (H/W 3.8)



9 (H/W 5.4)



10 (H/W 0.4)



11 (H/W 0.8)



12 (H/W 1.7)

Figure 7.4 Urban Built Form Canyon Geometry aspects on selected survey points in Kolkata
(Source: Author)

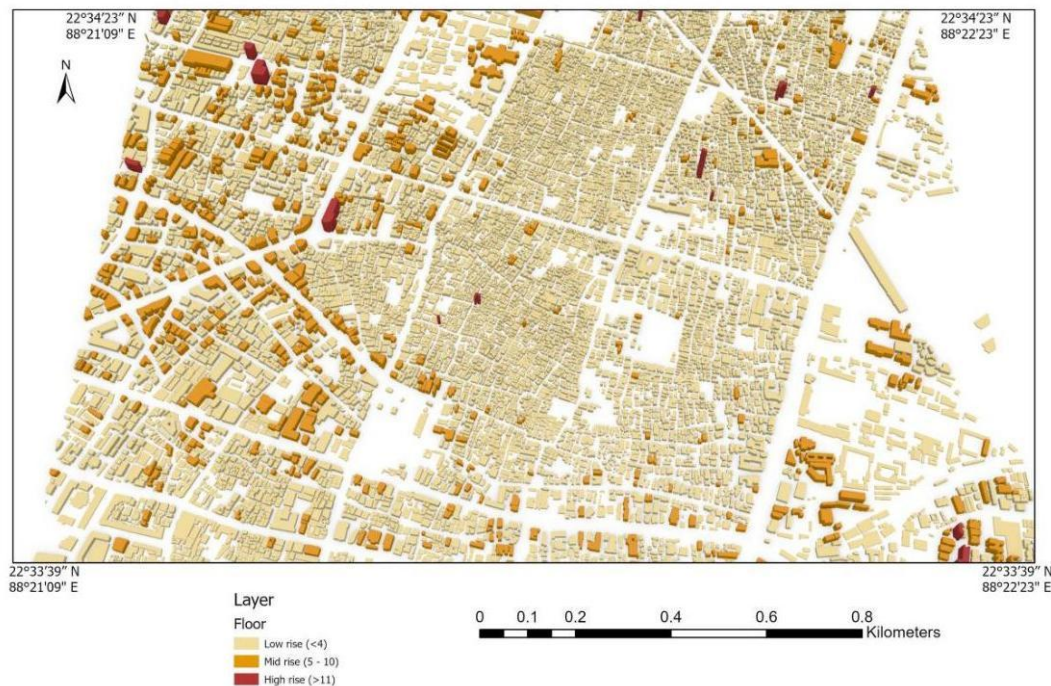


Figure 7.5 3D view of portion of Kolkata (Source: Author)

The UHI effect isn't uniform across a city. LCZs with more vegetation ("Parks") will experience lower temperatures compared to densely built zones ("Compact Mid-Rise"). Higher temperatures due to UHIs can trap pollutants closer to the ground, impacting air quality more in specific LCZs like "Large Low-Rise" zones with limited ventilation. Activities like running vehicles and buildings generate waste heat trapped in the urban environment, further elevating temperatures in all LCZs, but especially densely built zones.

By mapping LCZs, we can identify areas most susceptible to the UHI effect. Here's how:

Targeted strategies: Focus on planting trees in "Large Low-Rise" zones for shade and cooling.

Material choices: Promote lighter-colored pavements in "Compact High-Rise" zones to reflect sunlight and reduce heat absorption.

Green infrastructure: Encourage green roofs and walls in all LCZs for insulation and cooling benefits.

7.1.4 Suggest and put forth various SVF ratios of the urban environment for reducing the effects of UHI.

It is crucial for the biophysical thermal comfort of city residents to identify the best method and technology for reducing the effects of surface urban heat islands in tropical urban areas.

Urban vegetation, fountains, cool pavements, and cool roofs have all been shown to be practical and cost-effective solutions for reducing local air pollutant concentrations in tropical cities like Kolkata and managing the effects of UHI. The shade provided by the urban tree canopy is a type of green infrastructure that lowers ambient temperatures and mitigates the Heat Island Effect. The efficiency of advantageous land use, land cover, and urban planning is recommended. Future research should focus on conducting model-based experiments on UHI mitigation technologies and strategies. Local climate zone 1, 2, 3, 7, 8, and 10 absorbed more heat and one of the reasons behind the formation of Urban Heat Island. It is recommended not to expand such types of LCZs.

The structure and design of metropolitan areas can have an impact on SVF ratios. These are a recommendation along with the corresponding SVF ratio:

Dense Urban Setting are characterized by high-rise buildings closely packed, narrow streets, limited green spaces (LCZ 1, LCZ 2, LCZ 3, LCZ 7, LCZ 8):

Suggested SVF Ratio: 0.1 - 0.3

Moderate Urban Setting are characterized by mix of medium-rise buildings, moderate street width, some green areas/parks (LCZ 4, LCZ 5, LCZ 6):

Suggested SVF Ratio: 0.3 - 0.5

Open Urban Setting are characterized by low-rise buildings, wider streets, ample green spaces, and parks (LCZ 9, LCZ A - G):

Suggested SVF Ratio: 0.5 - 0.7

In accordance to studies, an **SVF of 0.4 to 0.8 is thought to be ideal for reducing the effects of UHI**. This range facilitates natural ventilation and lowers heat retention by allowing enough solar radiation to reach the ground. Higher SVF values—which are getting close to 1—indicate an enclosed urban area with less sky visibility, which raises the temperature.

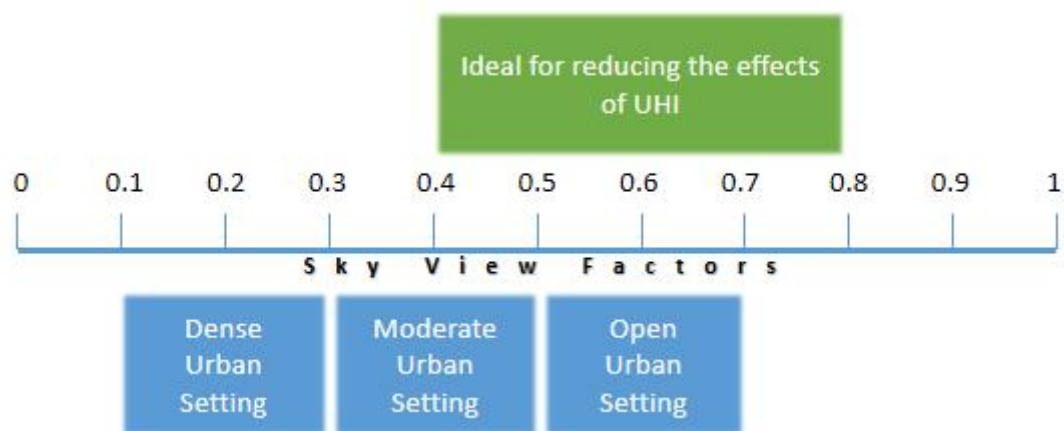


Figure 7.6 Corresponding SVF ratios of different urban settings and ideal for reducing the effects of UHI (Source: Author)

There are a few crowded climate zones (LCZ 1, LCZ 7, etc.) where heat concentrates and sky view factor is lower. It is recommended to use a sky view factor of 0.6 for the LCZ 1, LCZ 2, LCZ 3, LCZ 7, and LCZ 8.

The sky view factor influences many analyses, such as acoustics, thermic, ventilation, and solar radiation. In order to analyse SVF more precisely, it is important to comprehend the theoretical ideas and interactions among the variables involved. This can be done by integrating current areas that offer numerous types of blockage with hypothetical models. The sky view factor parameter is advised to be included as required by law in city planning.

7.2 Recommendation

Exploring the environmental impacts of reducing heat gain and mitigating the urban heat island effect is essential in our changing climate. It involves investigating various strategies like green roofs, reflective surfaces, and vegetation cover to understand their efficacy in cooling urban areas. This exploration could also extend to examining the effects on air quality, biodiversity, and overall urban ecology, paving the way for more sustainable and resilient cities.

Delving into urban biodiversity management is crucial. Preserving and enhancing green spaces within cities not only supports diverse flora and fauna but also positively impacts mental health, community well-being, and ecosystem services. Research in this domain could involve understanding the interplay between different species, their habitats, and human interaction, thereby guiding urban planning for biodiversity conservation.

The management of the built environment plays a pivotal role in shaping sustainable cities. Investigating building designs, materials, and construction techniques for energy efficiency and environmental sustainability is a vast yet vital area. It involves examining the life cycle of buildings, their energy consumption, and exploring innovative approaches to reduce the ecological footprint of urban infrastructure.

City planning is a multifaceted field encompassing various aspects like zoning, transportation, and public spaces. Future studies could focus on optimizing urban layouts for efficiency, accessibility, and inclusivity. Additionally, integrating green spaces, promoting walkability, and considering social dynamics in city planning can foster vibrant, equitable communities.

Qualitative research on the socioeconomic effects of urbanization is equally intriguing. Understanding how migration to urban areas influences livelihoods, social structures, and cultural dynamics is essential for informed policy-making. Additionally, exploring outdoor thermal comfort from a qualitative perspective involves

understanding people's perceptions, behaviors, and adaptations to weather conditions, thereby influencing urban design and public policy.

Each of these research areas presents a rich tapestry of opportunities to better understand, design, and manage cities of the future. What's most exciting is the potential for interdisciplinary collaboration and the practical implications these studies can have on creating more sustainable, livable, and inclusive urban environments. How do you envision these findings being applied in real-world scenarios?

Since the current study's constrained parameters, some indicators could not be measured. Every indicator that could not be measured represents a data and opportunity gap. Future studies could focus on issues like.

Investigation of the environmental effects of reduced heat gain, mitigation of the urban heat island, management of the urban biodiversity, management of the built environment, city planning, etc.

Qualitative research on the socioeconomic effects of urbanization and outdoor thermal comfort.

References

- Akbari, H., Pomerantz, M., & Taha, H. (2001). Cool surfaces and shade trees to reduce energy use and improve air quality in urban areas. *Solar Energy*, 70(3), 295–310. [https://doi.org/10.1016/S0038-092X\(00\)00089-X](https://doi.org/10.1016/S0038-092X(00)00089-X)
- Anas, A., Arnott, R., & Small, K. (1998). Urban Spatial Structure. *Journal of Economic Literature*, 36(3), 1426–1464.
- Anderson, M. C. (1964). Studies of the Woodland Light Climate: I. The Photographic Computation of Light Conditions. *The Journal of Ecology*, 52(1), 27. <https://doi.org/10.2307/2257780>
- Antonanzas-Torres, F., Martínez-de-Pisón, F. J., Antonanzas, J., & Perpignan, O. (2014). Downscaling of global solar irradiation in complex areas in R. *Journal of Renewable and Sustainable Energy*, 6(6), 063105. <https://doi.org/10.1063/1.4901539>
- Arnold, C. L., & Gibbons, C. J. (1996). Impervious Surface Coverage: The Emergence of a Key Environmental Indicator. *Journal of the American Planning Association*, 62(2), 243–258. <https://doi.org/10.1080/01944369608975688>
- Bajani, S., & Das, D. (2020). Sustainable Planning Interventions in Tropical Climate for Urban Heat Island Mitigation – Case Study of Kolkata. In M. Ghosh (Ed.), *Perception, Design and Ecology of the Built Environment* (pp. 167–182). Springer International Publishing. https://doi.org/10.1007/978-3-030-25879-5_10
- Bärring, L., Mattsson, J. O., & Lindqvist, S. (1985). Canyon geometry, street temperatures and urban heat island in malmö, sweden. *Journal of Climatology*, 5(4), 433–444. <https://doi.org/10.1002/joc.3370050410>
- Bechtel, B. (2011). Multitemporal Landsat data for urban heat island assessment and classification of local climate zones. *2011 Joint Urban Remote Sensing Event*, 129–132. <https://doi.org/10.1109/JURSE.2011.5764736>
- Bechtel, B., Alexander, P. J., Böhner, J., Ching, J., Conrad, O., Feddema, J., Mills, G., See, L., & Stewart, I. (2015). Mapping local climate zones for a worldwide database of the form and function of cities. *ISPRS International Journal of Geo-Information*, 4(1), 199–219. <https://doi.org/10.3390/ijgi4010199>
- Bechtel, B., & Daneke, C. (2012). Classification of Local Climate Zones Based on Multiple Earth Observation Data. *IEEE Journal of Selected Topics in Applied Earth Observations and Remote Sensing*, 5(4), 1191–1202. <https://doi.org/10.1109/JSTARS.2012.2189873>
- Bell, S. (2015). *Quantifying uncertainty in citizen weather data*. Aston University.
- Bhatta, B. (2011). *Remote Sensing and GIS* (3rd Edn.). Oxford University Press.

- Blennow, K. (1995). Sky View Factors from High-Resolution Scanned Fish-eye Lens Photographic Negatives. *Journal of Atmospheric and Oceanic Technology*, 12(6), 1357–1362. [https://doi.org/10.1175/1520-0426\(1995\)012<1357:SVFFHR>2.0.CO;2](https://doi.org/10.1175/1520-0426(1995)012<1357:SVFFHR>2.0.CO;2)
- Boschmann, E. E., & Kwan, M.-P. (2008). Toward Socially Sustainable Urban Transportation: Progress and Potentials. *International Journal of Sustainable Transportation*, 2(3), 138–157. <https://doi.org/10.1080/15568310701517265>
- Bourne, L. S. (1996). REURBANIZATION, UNEVEN URBAN DEVELOPMENT, AND THE DEBATE ON NEW URBAN FORMS. *Urban Geography*, 17(8), 690–713. <https://doi.org/10.2747/0272-3638.17.8.690>
- Bouyer, J., Musy, M., Huang, Y., & Athamena, K. (2011). Mitigating Urban Heat Island Effect by Urban Design: Forms and Materials. In *Cities and Climate Change: Responding to an Urgent Agenda* (pp. 164–181). The Worldbank.
- Brown, M. J., Grimmond, S., & Ratti, C. (2001). Comparison of Methodologies for Computing Sky View Factor in Urban Environments. *Proceedings of the 2001 International Symposium on Environmental Hydraulics, November 2016*, 6.
- Brunsell, N. A., & Gillies, R. R. (2003). Length Scale Analysis of Surface Energy Fluxes Derived from Remote Sensing. *Journal of Hydrometeorology*, 4(6), 1212–1219. [https://doi.org/10.1175/1525-7541\(2003\)004<1212:LSAOSE>2.0.CO;2](https://doi.org/10.1175/1525-7541(2003)004<1212:LSAOSE>2.0.CO;2)
- Bruse, M., & Fleer, H. (1998). Simulating surface-plant-air interactions inside urban environments with a three dimensional numerical model. *Environmental Modelling and Software*, 13(3–4), 373–384. [https://doi.org/10.1016/S1364-8152\(98\)00042-5](https://doi.org/10.1016/S1364-8152(98)00042-5)
- Cardoso, R. dos S., & Amorim, M. C. de C. T. (2018). Urban heat island analysis using the ‘local climate zone’ scheme in Presidente Prudente, Brazil. *Investigaciones Geográficas*, 69, 107. <https://doi.org/10.14198/INGEO2018.69.07>
- CHAPMAN, L., & THORNES, J. E. (2003). Real-Time Sky-View Factor Calculation and Approximation. *JOURNAL OF ATMOSPHERIC AND OCEANIC TECHNOLOGY*, 21, 730–741.
- Chapman, L., & Thornes, J. E. (2004). Real-Time Sky-View Factor Calculation and Approximation. *Journal of Atmospheric and Oceanic Technology*, 21(5), 730–741. [https://doi.org/10.1175/1520-0426\(2004\)021<0730:RSFCAA>2.0.CO;2](https://doi.org/10.1175/1520-0426(2004)021<0730:RSFCAA>2.0.CO;2)
- Chapman, L., Thornes, J. E., & Bradley, A. v. (2001). Rapid determination of canyon geometry parameters for use in surface radiation budgets. *Theoretical and Applied Climatology*, 69(1–2), 81–89. <https://doi.org/10.1007/s007040170036>
- Chen, L., Ng, E., An, X., Ren, C., Lee, M., Wang, U., & He, Z. (2012). Sky view factor analysis of street canyons and its implications for daytime intra-urban air temperature differentials in high-rise, high-density urban areas of Hong Kong: a GIS-based simulation approach. *International Journal of Climatology*, 32(1), 121–136. <https://doi.org/10.1002/joc.2243>
- Chen, M., Guo, S., Hu, M., & Zhang, X. (2020). The spatiotemporal evolution of population exposure to PM_{2.5} within the Beijing-Tianjin-Hebei urban agglomeration, China.

- Journal of Cleaner Production*, 265, 121708.
<https://doi.org/10.1016/j.jclepro.2020.121708>
- Chen, Y., Shan, B., Yu, X., Zhang, Q., & Ren, Q. (2022). Comprehensive effect of the three-dimensional spatial distribution pattern of buildings on the urban thermal environment. *Urban Climate*, 46, 101324. <https://doi.org/10.1016/j.uclim.2022.101324>
- Ching, J., Mills, G., Bechtel, B., See, L., Feddema, J., Wang, X., Ren, C., Brousse, O., Martilli, A., Neophytou, M., Mouzourides, P., Stewart, I., Hanna, A., Ng, E., Foley, M., Alexander, P., Aliaga, D., Niyogi, D., Shreevastava, A., ... Theeuwes, N. (2018). WUDAPT: An Urban Weather, Climate, and Environmental Modeling Infrastructure for the Anthropocene. *Bulletin of the American Meteorological Society*, 99(9), 1907–1924.
<https://doi.org/10.1175/BAMS-D-16-0236.1>
- Conrad, O., Bechtel, B., Bock, M., Dietrich, H., Fischer, E., Gerlitz, L., Wehberg, J., Wichmann, V., & Böhner, J. (2015). System for Automated Geoscientific Analyses (SAGA) v. 2.1.4. *Geoscientific Model Development*, 8(7), 1991–2007. <https://doi.org/10.5194/gmd-8-1991-2015>
- Danylo, O., See, L., Schepaschenko, D., Fritz, S., & Bechtel, B. (2016). Contributing to WUDAPT: A Local Climate Zone Classification of Two Cities in Ukraine. *IEEE Journal of Selected Topics in Applied Earth Observations and Remote Sensing*, 9(5).
<https://doi.org/10.1109/JSTARS.2016.2539977>
- de Morais, M., de Freitas, E., Marciotto, E., Guerrero, V., Martins, L., & Martins, J. (2018). Implementation of Observed Sky-View Factor in a Mesoscale Model for Sensitivity Studies of the Urban Meteorology. *Sustainability*, 10(7), 2183.
<https://doi.org/10.3390/su10072183>
- Denzin, N. K., & Lincoln, Y. S. (2005). *The Sage handbook of qualitative research* (3rd Ed). Sage Publications Ltd.
- Dirksen, M., Pagani, G., Ronda, R., & Theeuwes, N. (2019). Sky view factor calculations and its application in urban heat island studies. *Urban Climate*, 30.
<https://doi.org/10.1016/j.uclim.2019.100498>
- Donnay, J.-P., J.Barnsley, M., & A.Longley, P. (2001). *Remote Sensing and Urban Analysis* (1st ed.). Taylor & Francis.
- Dousset, B., & Gourmelon, F. (2003). Satellite multi-sensor data analysis of urban surface temperatures and landcover. *ISPRS Journal of Photogrammetry and Remote Sensing*, 58(1–2), 43–54. [https://doi.org/10.1016/S0924-2716\(03\)00016-9](https://doi.org/10.1016/S0924-2716(03)00016-9)
- Elsayed, I. S. M. (2012). Mitigation of the Urban Heat Island of the City of Kuala Lumpur, Malaysia. *Middle-East Journal of Scientific Research*, 11, 1602–1613.
- Emmanuel, M. R. (2005). *An urban approach to climate-sensitive design: strategies for the tropics*. Spon Press.
- Falcidieno, B. (1994). Modelling and visualization of spatial data in GIS: Guest editor's introduction. *Computers & Graphics*, 18(6), 759–761.

- Gál, T., Lindberg, F., & Unger, J. (2009). Computing continuous sky view factors using 3D urban raster and vector databases: Comparison and application to urban climate. *Theoretical and Applied Climatology*, 95(1–2), 111–123. <https://doi.org/10.1007/s00704-007-0362-9>
- Gál, T., & Unger, J. (2014). A new software tool for SVF calculations using building and tree-crown databases and its possible applications in urban climate studies. *Urban Climate*, 10(P3), 594–606. <https://doi.org/10.1016/j.uclim.2014.05.004>
- Geletiĉ, J., & Lehnert, M. (2016). GIS-based delineation of local climate zones: The case of medium-sized Central European cities. *Moravian Geographical Reports*, 24(3), 2–12. <https://doi.org/10.1515/mgr-2016-0012>
- Giuliano, G., Kang, S., & Yuan, Q. (2019). Agglomeration economies and evolving urban form. *The Annals of Regional Science*, 63(3), 377–398. <https://doi.org/10.1007/s00168-019-00957-4>
- Gillies, R. R., & Carlson, T. N. (1995). Thermal Remote Sensing of Surface Soil Water Content with Partial Vegetation Cover for Incorporation into Climate Models. *Journal of Applied Meteorology and Climatology*, 34(4), 745–756.
- Grimmond, C. S. B., Ward, H. C., & Kotthaus, S. (2015). How is urbanization altering local and regional climate? In K. C. Seto, W. D. Solecki, & C. A. Griffith (Eds.), *The Routledge Handbook of Urbanization and Global Environmental Change*. University of Reading.
- Hafner, J., & Kidder, S. Q. (1999). Urban Heat Island Modeling in Conjunction with Satellite-Derived Surface/Soil Parameters. *Journal of Applied Meteorology and Climatology*, 38(4), 448–465. [https://doi.org/10.1175/1520-0450\(1999\)038](https://doi.org/10.1175/1520-0450(1999)038)
- Hämmerle, M., Gál, T., Unger, J., & Matzarakis, A. (2011a). Comparison of models calculating the sky view factor used for urban climate investigations. *Theoretical and Applied Climatology*, 105(3), 521–527. <https://doi.org/10.1007/s00704-011-0402-3>
- Hämmerle, M., Gál, T., Unger, J., & Matzarakis, A. (2011b). Introducing a script for calculating the sky view factor used for urban climate investigations. In *ACTA CLIMATOLOGICA ET CHOROLOGICA* (Vols. 44–45, pp. 83–92).
- He, B.-J., Wang, J., Liu, H., & Ulpiani, G. (2021). Localized synergies between heat waves and urban heat islands: Implications on human thermal comfort and urban heat management. *Environmental Research*, 193, 110584. <https://doi.org/10.1016/j.envres.2020.110584>
- Herold, M., Hemphill, J., Dietzel, C., & Clarke, K. C. (2005). Remote Sensing Derived Mapping To Support Urban Growth Theory. *Joint Symposia URBAN - URS 2005*, 7. http://www.isprs.org/proceedings/xxxvi/8-w27/herold_hemphill_etal.pdf
- Ho, H. C., Knudby, A., Sirovyak, P., Xu, Y., Hodul, M., & Henderson, S. B. (2014). Mapping maximum urban air temperature on hot summer days. *Remote Sensing of Environment*, 154, 38–45. <https://doi.org/10.1016/j.rse.2014.08.012>

- Holmer, B., Postgård, U., & Eriksson, M. (2000). Sky view factors in forest canopies calculated with IDRISI. *Theoretical and Applied Climatology*, 68, 33–40.
- Hoornweg, D., & Pope, K. (2014). *Socioeconomic Pathways and Regional Distribution of the World's 101 Largest Cities*.
- Howard, L. (1833). *THE CLIMATE OF LONDON* (2nd ed.). Harvey and Darton, J. and A. Arch, Longman, Hatchard, S. Highley [and] R. Hunter.
- Hox, J. J., & Boeijs, H. R. (2005). Data Collection, Primary vs. Secondary. In *Encyclopedia of Social Measurement* (pp. 593–599). Elsevier. <https://doi.org/10.1016/B0-12-369398-5/00041-4>
- Hunt, J. C. R., Aktas, Y. D., Mahalov, A., Moustauoui, M., Salamanca, F., & Georgescu, M. (2018). Climate change and growing megacities: hazards and vulnerability. *Proceedings of the Institution of Civil Engineers - Engineering Sustainability*, 171(6), 314–326. <https://doi.org/10.1680/jensu.16.00068>
- Jamei, Y., Rajagopalan, P., & Sun, Q. (Chayn). (2019). Spatial structure of surface urban heat island and its relationship with vegetation and built-up areas in Melbourne, Australia. *Science of The Total Environment*, 659, 1335–1351. <https://doi.org/10.1016/j.scitotenv.2018.12.308>
- Jensen, J. R., & Cowen, D. C. (1999). Remote Sensing of Urban/Suburban Infrastructure and Socio-Economic Attributes. *Photogrammetric Engineering and Remote Sensing*, 65(5), 611–622.
- Johnson, G. T., & Watson, I. D. (1984). The Determination of View-Factors in Urban Canyons. *Journal of Climate and Applied Meteorology*, 23, 329–335.
- Kastendeuch, P. P. (2013). A method to estimate sky view factors from digital elevation models. *International Journal of Climatology*, 33(6), 1574–1578. <https://doi.org/10.1002/joc.3523>
- Kim, J.-P., Guldmann, J.-M., Merry, C. J., & Viton, P. A. (2009). *LAND-USE PLANNING AND THE URBAN HEAT ISLAND EFFECT*.
- Kłysiak, K., & Fortuniak, K. (1999). Temporal and spatial characteristics of the urban heat island of Łódź, Poland. *Atmospheric Environment*, 33(24–25), 3885–3895. [https://doi.org/10.1016/S1352-2310\(99\)00131-4](https://doi.org/10.1016/S1352-2310(99)00131-4)
- Kotharkar, R., & Bagade, A. (2018). Evaluating urban heat island in the critical local climate zones of an Indian city. *Landscape and Urban Planning*, 169, 92–104. <https://doi.org/10.1016/j.landurbplan.2017.08.009>
- Kustas, W., & Anderson, M. (2009). Advances in thermal infrared remote sensing for land surface modeling. *Agricultural and Forest Meteorology*, 149(12), 2071–2081. <https://doi.org/10.1016/j.agrformet.2009.05.016>
- Lee, K., & Levermore, G. J. (2019). Sky view factor and sunshine factor of urban geometry for urban heat island and renewable energy. *Architectural Science Review*, 62(1), 26–34. <https://doi.org/10.1080/00038628.2018.1536601>

- Lillesand, T., Kiefer, R. W., & Chipman, J. (2015). *Remote Sensing and Image Interpretation* (7th Edition). Wiley.
- Lin, Z., & Oguchi, T. (2006). DEM analysis on longitudinal and transverse profiles of steep mountainous watersheds. *Geomorphology*, 78(1–2), 77–89.
<https://doi.org/10.1016/j.geomorph.2006.01.017>
- Lindberg, F. (2007). Modelling the urban climate using a local governmental geo-database. *Meteorological Applications*, 14(3), 263–273. <https://doi.org/10.1002/met.29>
- Lindberg, F., & Grimmond, C. S. B. (2010). Continuous sky view factor maps from high resolution urban digital elevation models. *Climate Research*, 42(3), 177–183.
<https://doi.org/10.3354/cr00882>
- Lindberg, F., Grimmond, C. S. B., Gabey, A., Huang, B., Kent, C. W., Sun, T., Theeuwes, N. E., Järvi, L., Ward, H. C., Capel-Timms, I., Chang, Y., Jonsson, P., Krave, N., Liu, D., Meyer, D., Olofson, K. F. G., Tan, J., Wästberg, D., Xue, L., & Zhang, Z. (2018). Urban Multi-scale Environmental Predictor (UMEP): An integrated tool for city-based climate services. *Environmental Modelling & Software*, 99, 70–87.
<https://doi.org/10.1016/J.ENVSOFT.2017.09.020>
- Lindberg, F., & Holmer, B. (2012). *Sky View Factor Calculator*.
- Lindberg, F., Sun, T., Grimmond, S., & Tang, Y. (2022). *UMEP Manual Documentation*.
- Ma, L., Zhu, X., Qiu, C., Blaschke, T., & Li, M. (2021). Advances of Local Climate Zone Mapping and Its Practice Using Object-Based Image Analysis. *Atmosphere*, 12(9), 1146.
<https://doi.org/10.3390/atmos12091146>
- Masson-Delmotte, V., Zhai, P., Pörtner, H. O., Roberts, D., Skea, J., Shukla, P. R., Pirani, A., Moufouma-Okia, W., Péan, C., Pidcock, R., Connors, S., Matthews, J. B. R., Chen, Y., Zhou, X., Gomis, M. I., Lonnoy, E., Maycock, T., Tignor, M., & Waterfield, T. (2018). *Global Warming of 1.5 °C: An IPCC Special Report on the Impacts of Global Warming of 1.5 °C above Pre-Industrial Levels and Related Global Greenhouse Gas Emission Pathways, in the Context of Strengthening the Global Response to the Threat of Climate Change*.
- Matuschek, O., & Matzarakis, A. (2010). Estimation of sky view factor in complex environment as a tool for applied climatological studies. *Berichte Des Meteorologischen Instituts Der Albert-Ludwigs-Universität Freiburg*, 20, 534–539.
- McCloy, K. R. (1995). *Resource Management Information Systems Remote Sensing, GIS and Modelling* (2nd ed.). Taylor & Francis.
- McCoy, R. M. (2005). *Field methods in remote sensing*. Guilford Press.
- Memon, R. A., Leung, D. Y. C., & Liu, C.-H. (2009). An investigation of urban heat island intensity (UHI) as an indicator of urban heating. *Atmospheric Research*, 94(3), 491–500.
<https://doi.org/10.1016/j.atmosres.2009.07.006>

- Miao, C., Yu, S., Hu, Y., Zhang, H., He, X., & Chen, W. (2020). Review of methods used to estimate the sky view factor in urban street canyons. *Building and Environment*, 168, 106497. <https://doi.org/10.1016/j.buildenv.2019.106497>
- Middel, A., Lukasczyk, J., & Maciejewski, R. (2017). Sky view factors from synthetic fisheye photos for thermal comfort routing—A case study in Phoenix, Arizona. *Urban Planning*, 2(1), 19–30. <https://doi.org/10.17645/up.v2i1.855>
- Mirzaei, P. A., & Haghighat, F. (2010). Approaches to study Urban Heat Island – Abilities and limitations. *Building and Environment*, 45(10), 2192–2201. <https://doi.org/10.1016/j.buildenv.2010.04.001>
- Mohajerani, A., Bakaric, J., & Jeffrey-Bailey, T. (2017). The urban heat island effect, its causes, and mitigation, with reference to the thermal properties of asphalt concrete. *Journal of Environmental Management*, 197, 522–538. <https://doi.org/10.1016/j.jenvman.2017.03.095>
- Morgan, D. L. (1998). Practical Strategies for Combining Qualitative and Quantitative Methods: Applications to Health Research. *Qualitative Health Research*, 8(3), 362–376. <https://doi.org/10.1177/104973239800800307>
- Morris, K. I., Chan, A., Morris, K. J. K., Ooi, M. C. G., Oozeer, M. Y., Abakr, Y. A., Nadzir, M. S. M., & Mohammed, I. Y. (2017). Urbanisation and urban climate of a tropical conurbation, Klang Valley, Malaysia. *Urban Climate*, 19, 54–71. <https://doi.org/10.1016/j.uclim.2016.12.002>
- Nassar, A. K., Blackburn, G. A., & Whyatt, J. D. (2016). Dynamics and controls of urban heat sink and island phenomena in a desert city: Development of a local climate zone scheme using remotely-sensed inputs. *International Journal of Applied Earth Observation and Geoinformation*, 51, 76–90. <https://doi.org/10.1016/j.jag.2016.05.004>
- Nichol, J. (2013). Remote Sensing of Urban Heat Islands by Day and Night. *Photogrammetric Engineering & Remote Sensing*, 71(5), 613–621. <https://doi.org/10.14358/pers.71.5.613>
- Oke, T., Christen, A., Mills, G., & Voogt, J. (2017). *Urban climates*. <https://doi.org/10.1017/9781139016476>
- Oke, T. R. (1973). City size and the urban heat island. *Atmospheric Environment* (1967), 7(8), 769–779. [https://doi.org/10.1016/0004-6981\(73\)90140-6](https://doi.org/10.1016/0004-6981(73)90140-6)
- Oke, T. R. (1982). The energetic basis of the urban heat island. *Quarterly Journal of the Royal Meteorological Society*, 108(455), 1–24. <https://doi.org/10.1002/qj.49710845502>
- Oke, T. R. (1987). *Boundary Layer Climates*.
- Oke, T. R. (1988). Street design and urban canopy layer climate. *Energy and Buildings*, 11(1–3), 103–113. [https://doi.org/10.1016/0378-7788\(88\)90026-6](https://doi.org/10.1016/0378-7788(88)90026-6)

- Oke, T. R. (2006). *Initial guidance to obtain representative meteorological observations at urban sites Vancouver-Sunset Urban Flux Tower View project BUBBLE-Basel Urban Boundary Layer Experiment View project*.
<https://www.researchgate.net/publication/265347633>
- O'Neill, M. S., & Kristie L. Ebi. (2009). Temperature Extremes and Health: Impacts of Climate Variability and Change in the United States. *Journal of Occupational and Environmental Medicine*, 51(1), 13–25.
- Pandey, P., Kumar, D., Prakash, A., Masih, J., Singh, M., Kumar, S., Jain, V. K., & Kumar, K. (2012). A study of urban heat island and its association with particulate matter during winter months over Delhi. *Science of The Total Environment*, 414, 494–507.
<https://doi.org/10.1016/j.scitotenv.2011.10.043>
- Peiser, R. B. (1989). Density and Urban Sprawl. *Land Economics*, 65, 204.
<https://doi.org/10.2307/3146665>
- Qin, Z., & Karnieli, A. (1999). Progress in the remote sensing of land surface temperature and ground emissivity using NOAA-AVHRR data. *International Journal of Remote Sensing*, 20(12), 2367–2393. <https://doi.org/10.1080/014311699212074>
- Ramírez-Aguilar, E. A., & Lucas Souza, L. C. (2019). Urban form and population density: Influences on Urban Heat Island intensities in Bogotá, Colombia. *Urban Climate*, 29, 100497. <https://doi.org/10.1016/j.uclim.2019.100497>
- Ratti, C., & Richens, P. (1999). *Urban texture analysis with image processing techniques*.
- Ratti, C., & Richens, P. (2004). Raster Analysis of Urban Form. *Environment and Planning B: Planning and Design*, 31(2), 297–309. <https://doi.org/10.1068/b2665>
- Reis, S., Uzun, B., & Yalcin, A. (2003). *Monitoring Land Use Changes by GIS and Remote Sensing Techniques: Case Study of Trabzon*.
<https://www.researchgate.net/publication/237536692>
- Riebeek, H., & Simmon, R. (2010, June 3). *Global Warming*.
<https://Earthobservatory.nasa.gov/Features/GlobalWarming/Page1.Php>
- Ruiz-Arias, J. A., Tovar-Pescador, J., Pozo-Vázquez, D., & Alsamamra, H. (2009). A comparative analysis of DEM-based models to estimate the solar radiation in mountainous terrain. *International Journal of Geographical Information Science*, 23(8), 1049–1076.
<https://doi.org/10.1080/13658810802022806>
- Santamouris, M. (Ed.). (2013). *Energy and Climate in the Urban Built Environment*. Routledge.
<https://doi.org/10.4324/9781315073774>
- Santamouris, M., Paraponiaris, K., & Mihalakakou, G. (2007). Estimating the ecological footprint of the heat island effect over Athens, Greece. *Climatic Change*, 80(3–4), 265–276. <https://doi.org/10.1007/s10584-006-9128-0>

- Shi, Z., Jia, G., Hu, Y., & Zhou, Y. (2019). The contribution of intensified urbanization effects on surface warming trends in China. *Theoretical and Applied Climatology*, 138(1–2), 1125–1137. <https://doi.org/10.1007/s00704-019-02892-y>
- Shi, Y., Xiang, Y., & Zhang, Y. (2019). Urban Design Factors Influencing Surface Urban Heat Island in the High-Density City of Guangzhou Based on the Local Climate Zone. *Sensors*, 19(16), 3459. <https://doi.org/10.3390/s19163459>
- Souza, L. C. L., Rodrigues, D. S., & Mendes, J. F. G. (2003). Sky view factors estimation using a 3D-GIS extension. *8th International IBPSA Conference, 2001*, 1227–1234. <http://repositorium.sdum.uminho.pt/handle/1822/2206>
- Stewart, I. D. (2011). *Redefining the Urban Heat Island* (Issue October).
- Stewart, I. D., & Oke, T. R. (2012). Local climate zones for urban temperature studies. *Bulletin of the American Meteorological Society*, 93(12), 1879–1900. <https://doi.org/10.1175/BAMS-D-11-00019.1>
- Stewart, I., & Oke, T. R. (2009). Newly developed “thermal climate zones” for defining and measuring urban heat island “magnitude” in the canopy layer. *AMS Eighth Symposium on the Urban Environment, December*, J8.2A. <http://ams.confex.com/ams/pdfpapers/150476.pdf>
- Steyn, D. G. (1980). The calculation of view factors from fisheye-lens photographs: Research note. *Atmosphere-Ocean*, 18(3), 254–258. <https://doi.org/10.1080/07055900.1980.9649091>
- Steyn, D. G., Hay, J. E., Watson, I. D., & Johnson, G. T. (1986). The Determination of Sky View-Factors in Urban Environments Using Video Imagery. *Journal of Atmospheric and Oceanic Technology*, 3(4), 759–764. [https://doi.org/10.1175/1520-0426\(1986\)003<0759:TDOSVF>2.0.CO;2](https://doi.org/10.1175/1520-0426(1986)003<0759:TDOSVF>2.0.CO;2)
- Streutker, D. (2003). Satellite-measured growth of the urban heat island of Houston, Texas. *Remote Sensing of Environment*, 85(3), 282–289. [https://doi.org/10.1016/S0034-4257\(03\)00007-5](https://doi.org/10.1016/S0034-4257(03)00007-5)
- T. GÁL, M. RZEPA, B. G. and J. U. (2007). COMPARISON BETWEEN SKY VIEW FACTOR VALUES COMPUTED BY TWO DIFFERENT METHODS IN AN URBAN ENVIRONMENT. *ACTA CLIMATOLOGICA ET CHOROLOGICA*, 17–26.
- U.
- Tarekegn, T. H., Haile, A. T., Rientjes, T., Reggiani, P., & Alkema, D. (2010). Assessment of an ASTER-generated DEM for 2D hydrodynamic flood modeling. *International Journal of Applied Earth Observation and Geoinformation*, 12(6), 457–465. <https://doi.org/10.1016/j.jag.2010.05.007>
- Teller, J., & Azar, S. (2001). Townscope II - A computer systems to support solar access decision-making. *Solar Energy*, 70(3), 187–200. [https://doi.org/10.1016/S0038-092X\(00\)00097-9](https://doi.org/10.1016/S0038-092X(00)00097-9)
- Theeuwes, N. E., Steeneveld, G.-J., Ronda, R. J., & Holtslag, A. A. M. (2017). A diagnostic equation for the daily maximum urban heat island effect for cities in northwestern

- Europe. *International Journal of Climatology*, 37(1), 443–454.
<https://doi.org/10.1002/joc.4717>
- Tso, C. P. (1996). A survey of urban heat island studies in two tropical cities. *Atmospheric Environment*, 30(3), 507–519. [https://doi.org/10.1016/1352-2310\(95\)00083-6](https://doi.org/10.1016/1352-2310(95)00083-6)
- Tso, C. P., Chan, B. K., & Hashim, M. A. (1990). An improvement to the basic energy balance model for urban thermal environment analysis. *Energy and Buildings*, 14(2), 143–152.
[https://doi.org/10.1016/0378-7788\(90\)90033-F](https://doi.org/10.1016/0378-7788(90)90033-F)
- TV, R., Aithal, B. H., & Sanna, D. D. (2012). Insights to urban dynamics through landscape spatial pattern analysis. *International Journal of Applied Earth Observation and Geoinformation*, 18, 329–343. <https://doi.org/10.1016/j.jag.2012.03.005>
- Unger, J. (2004). Intra-urban relationship between surface geometry and urban heat island: review and new approach. *Climate Research*, 27, 253–264.
<https://doi.org/10.3354/cr027253>
- van der Hoeven, F., & Wandl, A. (2015). Amsterwarm: Mapping the landuse, health and energy-efficiency implications of the Amsterdam urban heat island. *Building Services Engineering Research and Technology*, 36(1), 67–88.
<https://doi.org/10.1177/0143624414541451>
- Verdonck, M.-L., Okujeni, A., van der Linden, S., Demuzere, M., de Wulf, R., & van Coillie, F. (2017). Influence of neighbourhood information on ‘Local Climate Zone’ mapping in heterogeneous cities. *International Journal of Applied Earth Observation and Geoinformation*, 62, 102–113. <https://doi.org/10.1016/j.jag.2017.05.017>
- Voogt, J. A. (2020). Urban Heat Islands. In *Atmosphere and Climate* (2nd Ed). CRC Press.
- Voogt, J. A., & Oke, T. R. (2003). Thermal remote sensing of urban climates. *Remote Sensing of Environment*, 86(3), 370–384. [https://doi.org/10.1016/S0034-4257\(03\)00079-8](https://doi.org/10.1016/S0034-4257(03)00079-8)
- Watson, I. D., & Johnson, G. T. (1987). Graphical estimation of sky view-factors in urban environments. *International Journal of Climatology*, 7(2), 193–197.
- Weng, Q. (2001). A remote sensing?GIS evaluation of urban expansion and its impact on surface temperature in the Zhujiang Delta, China. *International Journal of Remote Sensing*, 22(10), 1999–2014. <https://doi.org/10.1080/713860788>
- Weng, Q. (2009). Thermal infrared remote sensing for urban climate and environmental studies: Methods, applications, and trends. *ISPRS Journal of Photogrammetry and Remote Sensing*, 64(4), 335–344. <https://doi.org/10.1016/j.isprsjprs.2009.03.007>
- Wu, C., & Murray, A. T. (2003). Estimating impervious surface distribution by spectral mixture analysis. *Remote Sensing of Environment*, 84(4), 493–505.
[https://doi.org/10.1016/S0034-4257\(02\)00136-0](https://doi.org/10.1016/S0034-4257(02)00136-0)
- Xie, X., Huang, Z., & Wang, J. (2005). Impact of building configuration on air quality in street canyon. *Atmospheric Environment*, 39(25), 4519–4530.
<https://doi.org/10.1016/j.atmosenv.2005.03.043>

- Yang, L., Qian, F., Song, D.-X., & Zheng, K.-J. (2016). Research on Urban Heat-Island Effect. *Procedia Engineering*, 169, 11–18. <https://doi.org/10.1016/j.proeng.2016.10.002>
- Yang, X., Yao, L., Jin, T., Peng, L. L. H., Jiang, Z., Hu, Z., & Ye, Y. (2018). Assessing the thermal behavior of different local climate zones in the Nanjing metropolis, China. *Building and Environment*, 137, 171–184. <https://doi.org/10.1016/j.buildenv.2018.04.009>
- Yin, R. K. (2003). *Case Study Research : Design and Methods* (3rd ed.). SAGE Publications.
- Yin, S., Liu, J., & Han, Z. (2022). Relationship between urban morphology and land surface temperature—A case study of Nanjing City. *PLOS ONE*, 17(2), e0260205. <https://doi.org/10.1371/journal.pone.0260205>
- Yuan, F., & Bauer, M. E. (2007). Comparison of impervious surface area and normalized difference vegetation index as indicators of surface urban heat island effects in Landsat imagery. *Remote Sensing of Environment*, 106(3), 375–386. <https://doi.org/10.1016/j.rse.2006.09.003>
- Zeng, L., Lu, J., Li, W., & Li, Y. (2018). A fast approach for large-scale Sky View Factor estimation using street view images. *Building and Environment*, 135, 74–84. <https://doi.org/10.1016/j.buildenv.2018.03.009>
- Zeng, Y., Huang, W., Zhan, F., Zhang, H., & Liu, H. (2010). Study on the urban heat island effects and its relationship with surface biophysical characteristics using MODIS imageries. *Geo-Spatial Information Science*, 13(1), 1–7. <https://doi.org/10.1007/s11806-010-0204-2>
- Zheng, Y., Ren, C., Xu, Y., Wang, R., Ho, J., Lau, K., & Ng, E. (2018). GIS-based mapping of Local Climate Zone in the high-density city of Hong Kong. *Urban Climate*, 24, 419–448. <https://doi.org/10.1016/j.uclim.2017.05.008>
- Zhang, C. L., Chen, F., Miao, S. G., Li, Q. C., Xia, X. A., & Xuan, C. Y. (2009). Impacts of urban expansion and future green planting on summer precipitation in the Beijing metropolitan area. *Journal of Geophysical Research*, 114(D2), D02116. <https://doi.org/10.1029/2008JD010328>
- Zhou, B., Rybski, D., & Kropp, J. P. (2017). The role of city size and urban form in the surface urban heat island. *Scientific Reports*, 7(1). <https://doi.org/10.1038/s41598-017-04242-2>
- Zhou, L., Dickinson, R. E., Tian, Y., Fang, J., Li, Q., Kaufmann, R. K., Tucker, C. J., & Myneni, R. B. (2004). Evidence for a significant urbanization effect on climate in China. *Proceedings of the National Academy of Sciences*, 101(26), 9540–9544. <https://doi.org/10.1073/pnas.0400357101>

List of Publication and Conferences

Publications

1. Bajani, Santanu; Das, Debashish; Sustainable Planning Interventions in Tropical Climate for Urban Heat Island Mitigation – Case Study of Kolkata. DOI 10.1007/978-3-030-25879-5_10. “Perception, Design and Ecology of the Built Environment: A Focus on the Global South, Springer, Switzerland, 2020-01-01 | Book chapter
2. Santanu Bajani, Dr. Debashish Das, Analyzing Sky View Factor Calculation Methods for Urban Climate Studies: Case Study Kolkata, International Journal of Science and Research (IJSR), Volume 11 Issue 11, November 2022, pp. 129- 137, https://www.ijsr.net/get_abstract.php?paper_id=SR221030224259
3. Bajani, Santanu; Das, Debashish and Bhadra, Debasree (2022). On the Quantification of Local Climate Zone Change and its Impact on the Thermal and Urban Landscape Metrics in Kolkata. Available at SSRN: <https://ssrn.com/abstract=4305993> or <http://dx.doi.org/10.2139/ssrn.4305993>, Elsevier

Conference Attended

1. National Seminar On “Environmental Management with The Application of GIS and Geoinformatics”, dated 9th September 2017
2. International Conference On Mother Earth. Dated 11th to 13th January 2018. Relationship Between LST and NDVI with Their Impact to LCZ: A Case Study of Kolkata, India.

Plagiarism Report

**Investigating the Relationship between
Urban Heat Island (UHI), Sky View Factor
(SVF) and different Local Climatic
Zones (LCZs): Case study of Kolkata**

By Santanu Bajani

Investigating the Relationship between Urban Heat Island (UHI), Sky View Factor (SVF) and different Local Climatic Zones (LCZs): Case study of Kolkata

By Santanu Bajani

Investigating the Relationship between Urban Heat Island (UHI), Sky View Factor (SVF) and different Local Climatic Zones (LCZs): Case study of Kolkata

Santiraj
14/6/24

ORIGINALITY REPORT

8%
SIMILARITY INDEX

Debabrata Das..

PRIMARY SOURCES

Professor
Department of Architecture
Jadavpur University
Kolkata-700032

1	www.ijsr.net Internet	366 words — 1%
2	Emmanuel Matsaba Ochola, Elham Fakharizadehshirazi, Aggrey Ochieng Adimo, John Bosco Mukundi et al. "Inter-local climate zone differentiation of land surface temperatures for Management of Urban Heat in Nairobi City, Kenya", Urban Climate, 2020 Crossref	194 words — 1%
3	rmets.onlinelibrary.wiley.com Internet	126 words — < 1%
4	www.researchgate.net Internet	123 words — < 1%
5	www.jaduniv.edu.in Internet	103 words — < 1%
6	www.mdpi.com Internet	94 words — < 1%
7	pr.hec.gov.pk Internet	89 words — < 1%

scholar.sun.ac.za